

VALIDATING BURN SEVERITY CLASSIFICATIONS USING
LANDSAT IMAGERY ACROSS WESTERN CANADIAN
NATIONAL PARKS

by

Nicholas Osborne Soverel

B.S., University of Vermont, 2004

A THESIS SUBMITTED IN PARTIAL FULFILLMENT OF THE REQUIREMENTS
FOR THE DEGREE OF

MASTER OF SCIENCE

in

The Faculty of Graduate Studies

(Forestry)

THE UNIVERSITY OF BRITISH COLUMBIA

(Vancouver)

March 2010

© Nicholas Osborne Soverel, 2010

ABSTRACT

National parks in western Canada experience wildland fire events at differing frequencies, intensities, and burn severities. These episodic disturbances have varying implications for various biotic and abiotic processes and patterns. To predict burn severity, the differenced Normalized Burn Ratio (dNBR) algorithm, derived from Landsat imagery, has been used extensively throughout the wildland fire community. Researchers have often employed this approach to study the effects of fire across multiple contrasting landscapes. Many remote sensing scientists have concluded that incorporating pre-fire information into the current remote sensing dNBR methodology may make such models more transferable.

In the first study the main purpose was to investigate the accuracies of the absolute dNBR versus its relative form (RdNBR) to estimate burn severity, in which was hypothesized that RdNBR would outperform dNBR based on former research by Miller and Thode (2007). The secondary purpose was to examine and compare the accuracies of RdNBR and dNBR algorithms in pre-fire landscapes with low canopy closure and high heterogeneity. Results indicate that the RdNBR-derived model did not estimate burn severity more accurately than dNBR (65.2% versus 70.2% classification accuracy, respectively) nor indicate improved estimates in the more heterogeneous and low canopy cover landscapes. In addition, we concluded that RdNBR is no more effective than dNBR at the regional, individual, and fine-scale vegetation levels. The results herein support the continued use of both the dNBR and RdNBR methods and the pursuit of developing regional models.

In the second study, we compare the transferability of an overall model and those stratified by land cover and ecozone. Our second objective was to test the statistical benefit of incorporating pre- and post-fire information into standard dNBR approaches. We determined that an overall dNBR derived model successfully estimated burn severity for the majority of our study fires, which supports its transferability across multiple western Canadian landscapes. Results indicate that both pre- and post-fire remote sensing information provides a means of further understanding the different post-fire responses as well as showing minimal statistical burn severity estimates across the majority of fires, however, significant improvement was evident for three of the ten study fires.

TABLE OF CONTENTS

TABLE OF CONTENTS	ii
LIST OF TABLES	vi
LIST OF FIGURES	viii
ACKNOWLEDGEMENTS	x
DEDICATION.....	xi
CO-AUTHORSHIP STATEMENT	xii
1 INTRODUCTION.....	1
1.1 Background	1
1.2 Burn severity and fire severity	3
1.3 Remote sensing application.....	7
1.4 Research objectives.....	16
1.6 References	18
2 ESTIMATING BURN SEVERITY FROM dNBR AND RdNBR INDICES ACROSS WESTERN CANADA.....	22
2.1 Introduction	22
2.2 Data and methods	27
2.2.1 Study area and characteristics	27
2.2.2 Imagery and pre-processing	32
2.2.3 Field data	33
2.2.4 Vegetation groupings and analysis technique	35
2.2.5 Data analysis	38
2.3 Results.....	40
2.3.1 Results for individual fires.....	40
2.3.1.1 Peace Point fire	40
2.3.1.2 Southesk fire	41
2.3.1.3 Hoodoo fire	42
2.3.1.4 Boyer 01 fire	43
2.3.1.5 Split Peak fire	43
2.3.1.6 Boyer 02 fire	44

2.3.2 Results for fine scale vegetation stratification	50
2.3.3 Results for regions	51
2.3.4 Results for overall dataset.....	52
2.3.5 Results for model comparison	54
2.4 Discussion	54
2.5 Conclusions	60
2.6 References	61
3 THE TRANSFERABILITY OF A dNBR DERIVED MODEL TO PREDICT BURN SEVERITY ACROSS TEN WILDLAND FIRES IN WESTERN CANADA	66
3.1 Introduction	66
3.2 Methods	69
3.2.1 Study area	69
3.2.1.1 Montane Cordillera	71
3.2.1.2 Boreal Plains	72
3.2.2 Prescribed fire and pre-fire disturbance	73
3.2.3 Imagery and dNBR pre-processing.....	74
3.2.4 Field data and collection	77
3.2.5 Land cover analysis	79
3.2.6 Tasselled cap index.....	80
3.2.7 Analysis approach.....	81
3.3 Results.....	82
3.3.1 Comparison of overall, land cover, and stratification results.....	82
3.3.2 TCI results	84
3.3.3 TCI multiple regression results.....	88
3.4 Discussion	90
3.4.1 Ecological insights into pre- and post- fire condition	90
3.4.2 Decoupled burn severity characteristics	91
3.4.3 Discussion on overall model and TCI improvement.....	93
3.5 Conclusion	94
3.6 References	96
4 CONCLUSION	101
4.1 Key findings	101
4.2 Future work and recommendations.....	103
4.3 References	106

LIST OF TABLES

Table 1.1. Simplified version of the FIREMON Landscape Assessment CBI form (Key & Benson, 2006).	6
Table 1.2. Landsat TM and ETM+ specifications.	7
Table 1.3. A short history of remote sensing burn severity research.	15
Table 2.1. Fire name, ignition and out date, fire size (ha), elevation (m), and dominant vegetation types for study fires.	28
Table 2.2. Landsat imagery used in this study for both the IA (initial assessment) or EA (extended assessment). Fire name, Landsat path and row, and pre-fire and post-fire Landsat TM/ETM+ imagery acquisition dates, are listed.	32
Table 2.3. Fire name, overall ranking, canopy closure (CC) weight value, PLADJ (percentage of like adjacencies) metric, and CONT (contagion) metric.	37
Table 2.4. The three EOSD LC 2000 vegetation groups and associated canopy	37
Table 2.5. dNBR and RdNBR results for individual fires from Figure 2.5 (A-F). Coefficient of determination, model relationship chosen, standard error of estimate, (p^L) p-value, (p^Q) predictor p-value for quadratic if significant, AIC values for both linear and quadratic models, and total (N) for each study fire.	45
Table 2.6. Classification accuracies of the producer's, user's, and overall values along with the conditional kappa (k_i), overall kappa, and the lower and upper 95% confidence intervals (CI) for the overall kappa. The results are listed from top to bottom and include the dNBR, RdNBR, EOSD vegetation type, and Hall et al. (2008) non-linear models.	46
Table 2.7. dNBR and RdNBR EOSD vegetation type regression including coefficient of determination, model relationship chosen, standard error of estimate, (p^L) p-value, (p^Q) predictor p-value for quadratic if significant, AIC values for both linear and quadratic models, and total (N).	51
Table 2.8. dNBR and RdNBR results for regions and overall datasets from Figure 2.6 (A-C) including the coefficient of determination, model relationship chosen, standard error of estimate, (p^L) p-value, (p^Q) predictor p-value for quadratic if significant, AIC values for both linear and quadratic models, and total (N).	52
Table 2.9. Hall et al. (2008) non-linear model correlation results including coefficient of determination, model relationship chosen, standard error of estimate, (p^L) p-value, and total (N).	54
Table 3.1. Includes the date of ignition, study ecozones: Boreal Plains (BP) or Montane Cordillera (MC). Park name, fire size (ha), elevation (m), type of wildland fire: wildfire	

(W) or prescribed fire (P), and dominant tree species present within the associated park. 70

Table 3.2. Landsat imagery used to calculate the initial and extended assessment images for use within the study. The table includes the IA/EA assessment, fire name, park name, path/row, pre-fire image date acquisition (if either TM or ETM+), and post-fire image acquisition date (if either TM or ETM+). 75

Table 3.3. The five EOSD land cover groups used to build each land cover model including: non-forest, coniferous-dense, coniferous-open, coniferous-sparse, and broadleaf. 80

Table 3.4. Percentage of CBI plots per fire associated with the EOSD land cover classes. 80

Table 3.5. Cross validation table that includes the three groups used for analysis within the study along and the associated total N. 84

Table 3.6. The first three columns of the table include the overall, land cover, and ecozone groups for model analysis. The rows represent the associated cross validation derived coefficient of determination (R^2) for each fire. 84

Table 3.7. Results for pre- and post-fire TCI coefficient of determination values (R^2) derived from cross validation and forward stepwise multiple regression. The brightness (B), greenness (G), and wetness (W) are included if significant ($p < 0.05$). The fifth and sixth columns represent the % change ($\% \Delta$) from the overall model variance when using pre- and post-fire TCI in multiple regression. 90

Table 3.8. Results of overall dNBR model including the model equation, R^2 , P value, and root mean square error (RSE). 94

LIST OF FIGURES

Figure 1.1. Outline of temporal resolution of burn severity (adapted from Landscape Assessment, Key & Benson, 2006).....	4
Figure 1.2. The left scatterplot represents the digital numbers (DN) of Landsat TM bands 4 (x-axis) and 7 (y-axis) of pre-fire conditions from the Split Peak fire in Kootenay National Park. The right scatterplot depicts the same bands taken from the same burned area one year post-fire.....	8
Figure 2.1. Total study area map representing the (1) Canadian Rocky Mountain and (2) western boreal study regions. Within the western boreal study region, the wildland fires include: (A) Boyer 02, (B) Peace Point, and (C) Boyer 01.	29
Figure 2.2. The Canadian Rocky Mountain study region which includes the (A) Southesk, (B) Hoodoo, and (C) Split Peak fires.	30
Figure 2.3. 3-D scatter plot depicting each fire’s pre-fire canopy closure (CC) and landscape spatial heterogeneity. The Y-axis represents the percentage of like adjacencies (PLADJ) index value, the X-axis vegetation canopy closure (CC), and the Z axis the contagion (CONT) index value.....	38
Figure 2.4. (A-F) Figures represent: (A) Peace Point, (B) Southesk, (C) Hoodoo, (D) Boyer 01, (E) Split Peak, and (F) Boyer 02 fires. Histograms depict the percent pixel variability for the associated remote sensing values within the initial perimeter of each fire. The gray bars represent total dNBR data and the dotted black line the normal distribution fitted function. The black histogram bars and solid black line represent the former information for the RdNBR data. The table below each graph refers to that fire’s total dNBR and RdNBR burn severity class proportions extracted using each fire’s regression model.	48
Figure 2.5. (A-F). X-axis of the scatterplot represents dNBR and RdNBR index derived values while the y-axis represents weighted CBI values. (A-F) figures represent: (A) Peace Point, (B) Southesk, (C) Hoodoo, (D) Boyer 01, (E) Split Peak, and (F) Boyer 02 fires. The gray circles represent dNBR while the black squares represent RdNBR weighted CBI correlations. The dotted black line represents the dNBR fitted regression model to weighted CBI values while the solid black line represents the RdNBR fitted regression model.	50
Figure 2.6. (A-C). X-axis of the scatterplot represents dNBR and RdNBR index derived values while the y-axis represents weighted CBI values. (A-C) figures represent: (A) Rocky Mountains (B) western boreal region, and (C) overall pooled dataset. The gray circles represent dNBR while the black squares represent RdNBR weighted CBI correlations. The dotted black line represents the dNBR fitted regression model to weighted CBI values while the solid black line represents the RdNBR fitted regression model.....	53

Figure 3.1. (1) Montane Cordillera and (2) Boreal Plains ecozones with the national parks of Canada in darkest gray. 71

Figure 3.2. A histogram showing the total CBI plots used within this study. 78

Figure 3.3. The graph depicts the mean overstory CBI values in black and the mean understory values in gray for each fire. The fires are ranked in order of highest difference in mean overstory and understory values to the lowest. 79

Figure 3.4. Box and whisker plots for TCI brightness values for the pre-fire (black), post-fire (dark gray), and the differenced (light gray and connected line). The whisker represents the mean plus and minus the standard deviation and the box represents the mean plus or minus the standard error. 86

Figure 3.5. Box and whisker plots for TCI greenness values for the pre-fire (black), post-fire (dark gray), and the differenced (light gray and connected line). The whisker represents the mean plus and minus the standard deviation and the box represents the mean plus or minus the standard error. 87

Figure 3.6. Box and whisker plots for TCI wetness values for the pre-fire (black), post-fire (dark gray), and the differenced (light gray and connected line). The whisker represents the mean plus and minus the standard deviation and the box represents the mean plus or minus the standard error. 88

Figure 3.7. Photos of two CBI plots taken from the Mitchell Ridge (left) and the Hoodoo Creek (right) fires. These photos depict the decoupled burn severity characteristics with high canopy mortality in the canopy and the lower severity in the understory. 92

Figure 3.8. Scatter plot of x-axis dNBR and y-axis weighted CBI values for the Mitchell Ridge (black diamonds) and the Hoodoo Creek (hollow triangles) fires. 92

Figure 3.9. Polynomial model fitted to the overall dNBR dataset, with the x-axis representing the weighted CBI values and the y-axis the dNBR values so that thresholds could be determined. CBI thresholds were taken from Miller et al. (2009)'s study..... 93

ACKNOWLEDGEMENTS

This research project was financially supported by Parks Canada with components funded by a Natural Sciences and Engineering Research Council (NSERC) Discovery grant to Coops. Special thanks to Dr. Daniel Perrakis who helped to sponsor this project and also for his ongoing assistance over the past two and a half years. I would like to wholeheartedly thank Dr. Nicholas Coops as he was always there to provide assistance and who made this entire experience memorable. Thanks to my other committee members, Dr. Sarah Gergel and Dr. Lori Daniels, for their advice and edits to the material herein. I would like to convey my gratitude to Darrel Zell who was especially helpful in the beginning stages of the project. I would also like to thank all of the national park staff who provided logistical support while we conducted field work in the summers of 2008 and 2009. These park staff include: Rick Kubian, Bruce Sundbo, Simon Hunt, Dave Smith, Gregg Walker, and Keith Hartery. I would also like to thank Vera Lindsay from the Northwest Territories Forest Management Division for her support. I would like to acknowledge my appreciation to those Integrated Remote Sensing Studio (IRSS) members who assisted me in collecting field data, which at times required both their sweat and blood: Trevor G. Jones, Colin J. Ferster, and Andrés Varhola. Finally, thank you to the entire IRSS lab, you all provided me with a welcome distraction from work as well as technical assistance when I really needed it.

DEDICATION

I dedicate this work to my parents, Susan and James Soverel, for their support, strength,
and hope throughout my life.

CO-AUTHORSHIP STATEMENT

This manuscript thesis is a combination of two peer-reviewed scientific papers for which I am lead author on both. The project idea was first proposed by Dr. Daniel Perrakis, who provided an outline of the goals of Parks Canada. Darrel Zell provided assistance in the pre-processing of Landsat data in the first year of work. The scope of the research, the field data and image processing analysis, as well as lead authorship reflect the portion of work that I completed towards this thesis. Dr. Nicholas Coops and Dr. Daniel Perrakis provided project oversight as well as editorial assistance. Dr. Sarah Gergel and Dr. Lori Daniels offered additional editorial and scientific oversight throughout the process.

1 INTRODUCTION¹

1.1 Background

Fire is an important ecosystem process, particularly in boreal forests where burning represents a dominant form of disturbance (Wein & MacLean 1983; Goldammer & Furyaev, 1996; Kasischke & Stocks, 2000). Since the last Ice Age, Canada's foremost forest disturbance agent has been fire (Stocks et al., 2003). Fire can stimulate soil microbial processes (Wells et al., 1979; Borchers & Perry, 1990), promote seed germination, seed production, and sprouting (Lyon & Stickney, 1976; Hungerford & Babbitt, 1987; Anderson & Romme, 1991; Lamont et al., 1993), and combust vegetation, ultimately altering the structure and composition of both soils and vegetation (Ryan & Noste, 1985; Wyant et al., 1986).

Since its inception, the personnel across the Canadian national park system have had varying perspectives on wildland fire management. For instance, in the late 1800's the agency attempted to simply protect lands from human encroachment and natural disturbance (Government of Canada, 2000), which meant that fire was considered undesirable and destructive.

¹ A version of this chapter has been published. Soverel, N.O., Coops, N.C., White, J.C., & Wulder, M.A. (2009). Characterizing the forest fragmentation of Canada's national parks. *Environmental Monitoring and Assessment*. DOI: 10.1007/s10661-009-0908-7

As a result, fires were actively suppressed until the 1960's when a paradigm shift occurred and fire was accepted as a natural process in forest renewal in national parks (Government of Canada, 2000). Managing fire is now mandated under the National Parks Act's ecological integrity mandate, which states that "an ecosystem has integrity when it is deemed characteristic for its natural region, including the composition and abundance of native species and biological communities, rates of change and supporting processes" (Government of Canada, 2000).

Currently, Parks Canada actively inventories and monitors the impacts of fire to better understand and improve ecosystem management. Western Canada is frequently divided into two major regions unique for their fire regimes, which including the Rocky Mountain and the western boreal regions (Van Wagner et al., 2006; Weber & Stocks, 1998). In the Rocky Mountain region, wildland fires can occur on steep and inaccessible slopes while in the western boreal these fires frequently occur in remote areas without road access. Until recently, Parks Canada fire managers and scientists monitored the effects of fire using aerial photography, Global Positioning System (GPS) devices, and in some cases, conventional field methods. Although aerial photography is available throughout Canada, interpretation of these photographs can be time consuming and involves subjective human interpretation over limited spatial and temporal extents. Similarly, approaches that utilize field data are even more limited in their spatial extent and are expensive and time consuming, as well as potentially lack consistency. Advanced digital remote sensing methods allow scientists to perform timely and accurate assessments of wildland fire impacts while simultaneously minimizing and/or eliminating

the aforementioned limitations. These methods have also been shown to provide important information pertaining to the processes of vegetation re-growth, plant succession, and ecological processes.

1.2 Burn severity and fire severity

Fire severity is defined as the direct effects of the combustion process including tree mortality and the loss of vegetation and organic biomass (Jain et al., 2004; Lentile et al., 2006). Burn severity is defined as “the degree of ecological change to a landscape caused by fire” (Key & Benson, 2006). The difference between these two terms is temporal: fire severity refers to the immediate post-fire effects whereas burn severity relates to the environment one or more growing seasons following fire. Figure 1.1 depicts two types of severity assessments herein, the initial assessment (IA), or an analysis of the fire severity taken from the same year as fire ignition and the extended assessment (EA), or burn severity data from one year post-fire.

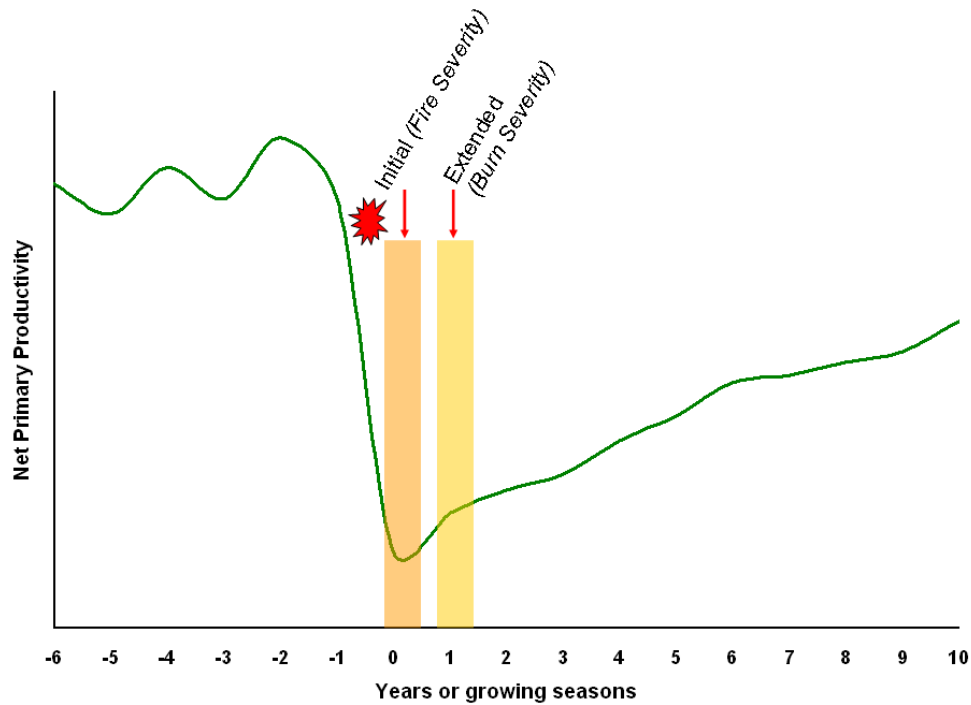


Figure 1.1. Outline of temporal resolution of burn severity (adapted from Landscape Assessment, Key & Benson, 2006).

At the landscape scale, burn severity represents fire-induced vegetation mortality that in combination with unburned islands creates a mosaic landscape consisting of distinct forest type and age class patches (Miller & Urban, 1999; Fule et al., 2003). Burned area maps impart critical information about the patterns of heterogeneity within a burned area (van Wagendonk et al., 2004), which relate directly to patch size and fragmentation (Soverel, 2009), factors which ultimately control the number of surviving individuals and distance to viable seed sources (Pickett & White, 1985; Turner et al., 1998). Accurate burn severity maps provide input data for studies that predict ecosystem recovery and succession (Epting & Verbyla, 2005), biomass burning and emission (Michalek et al.,

2000), wildlife population dynamics (Kotliar et al., 2008), and forest fragmentation (Soverel et al., 2009).

There is debate in the remote sensing community over the measuring and classifying of burn severity data. This is because characterisation of burn severity is dependent on the natural resource objective being studied. In addition, the physical and ecological effects of fire differ depending on ecosystem ecology, composition, and physical structure. For example, burn severity may be more related to canopy mortality in the Canadian Rocky Mountain region versus the western boreal where ground organic deposits hold the majority of organic-based carbon (Gorham, 1991; Harden et al., 2000). In order to develop and apply a consistent field methodology, the well known Composite Burn Index (hereafter as CBI) was employed. CBI is a field validation rating that takes into account the overall visible effects of fire as they relate to the pre-fire environment (Key & Benson, 2006). CBI has been cited as somewhat subjective since the CBI rating is determined by a researcher most often without available pre-fire data. In order to measure burn severity, the CBI form in “Landscape Assessment: Sampling and Analysis Methods” (Key & Benson, 2006) was used. CBI is divided into five strata: substrates, herbaceous vegetation, large shrubs and small trees, intermediate, and canopy trees. This method includes fire effects that include duff consumption/scorch, herbaceous vegetation mortality, shrub mortality, char height, and overstory mortality (Table 1.1). CBI scores are ranked from 0 to 3.0, zero representing a site that was unchanged from fire and 3.0 having the highest possible burn severity. The values for each of the strata are combined to an overall CBI rating which provides an average of all five strata within a plot. CBI

ratings are important in the interpretation process of remote sensing values because they can lay the groundwork for calibrating satellite observations and also set thresholds for severity class maps (Key & Benson, 2006). CBI was well suited to this study because of the large geographic range of fires and the diversity of landscapes studied.

Table 1.1. Simplified version of the FIREMON Landscape Assessment CBI form (Key & Benson, 2006).

Five Strata	Rating factor criteria- each between 0.0 - 3.0
A. Substrates	<i>Litter/Light fuel consumption Duff Medium Fuel, 3-8 in. Heavy Fuel, > 8 in. Soil & Rock Cover/Color</i>
B. Herbs, Low Shrubs & Trees (< 1 meter)	<i>% Foliage altered (blk-brn) Frequency % Living % Change in Cover Spp. Composition/Relative Abundance</i>
C. Tall Shrubs & Trees (1 to 5 m)	<i>% Foliage Altered (blk-brn) Frequency % Living % Change in Cover Spp. Comp. -Rel. Abund.</i>
D. Intermediate Trees (Subcanopy)	<i>% Green (Unaltered) % Black (Torch) % Brown (Scorch/Girdle) % Canopy Mortality Char Height</i>
E. Big Trees (Dominant/Codominant)	<i>% Green (Unaltered) % Black (Torch) % Brown (Scorch/Girdle) % Canopy Mortality Char Height</i>

1.3 Remote sensing application

The Landsat remote sensing program has been in operation since 1972 and its utility has been demonstrated in many related research fields including forestry, geography, and land resource analysis (Lillesand & Kiefer, 2008). One of the notable advantages of the Landsat program is the relatively large and complete historical archive which is freely available in North America (USGS, 2010). The two operational Landsat sensors include the Thematic Mapper (TM) and Enhanced Thematic Mapper (ETM+), onboard the Landsat 5 and 7 satellites, respectively. The TM and ETM+ sensors detect reflected radiation in the visible, near infrared (NIR), middle infrared (MIR), and thermal wavelengths of the electromagnetic spectrum. Due to its scan line error malfunction in 2003, the Landsat-7 ETM+ sensor has limited utility and therefore Landsat-5 TM imagery forms the majority of data used for spectral analysis for this research (Table 1.2).

Table 1.2. Landsat TM and ETM+ specifications.

Specifications	Landsat 5 TM	Landsat 7 ETM+
Ground Resolution	30 x 30 m	15 x15 m panchromatic
	120 x 120 m thermal	30 x 30 m 60 x 60 m thermal
Coverage	185 x 172 km swath	183 x 170 km swath
Orbital repeat	16 days	16 days
Mission length	1984 - present	1999-present
Band Number	1 0.45- 0.52 μm	0.45- 0.52 μm
	2 0.52 - 0.60 μm	0.53 - 0.60 μm
	3 0.63 - 0.69 μm	0.63 - 0.69 μm
	4 0.76 - 0.90 μm	0.75-0.9 μm
	5 1.55 - 1.75 μm	1.55-1.75 μm
	6 10.4 - 12.6 μm	10.4-12.5 μm
	7 2.08 - 2.35 μm	2.09-2.35 μm
	8 NA	0.52-0.9 μm

The combination of Landsat bands 4 and 7 has been found to be most sensitive to the effects of fire. Band 4 (B4) measures near-infrared reflectance between 0.76 μm and 0.90 μm wavelengths and is primarily sensitive to the chlorophyll content of live vegetation (Miller & Thode, 2007). Band 7 (B7) records middle infrared 2.08 μm - 2.35 μm wavelengths, which are sensitive to water content of both soils and vegetation, the lignin content of non-photosynthetic vegetation, and hydrous minerals such as clay, mica, and some oxides and sulfates (Avery & Berlin, 1992; Elvidge, 1990). A Normalized Burn Ratio (NBR) image is calculated by normalizing bands 4 and 7 in the equation:

$$NBR = (B4 - B7) / (B4 + B7)$$

NBR is particularly sensitive to changes in the amount of live green vegetation, moisture content, and some soil conditions that may occur after fire (Miller & Thode, 2007). Fire affected vegetation has decreased reflectance in Band 4 and increased reflectance in Band 7 as depicted in the spectroscopic graphs below (Figures 1.2).

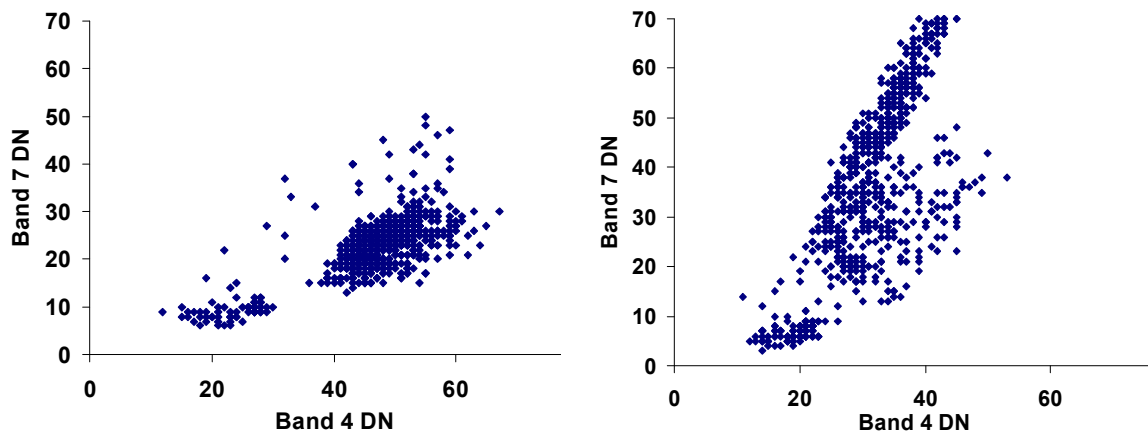


Figure 1.2. The left scatterplot represents the digital numbers (DN) of Landsat TM bands 4 (x-axis) and 7 (y-axis) of pre-fire conditions from the Split Peak fire in Kootenay National Park. The right scatterplot depicts the same bands taken from the same burned area one year post-fire.

The differenced Normalized Burn Ratio (dNBR) algorithm is a remote sensing change detection approach that has been shown to be correlative in magnitude to the environmental change caused by fire. To derive the differenced Normalized Burn Ratio (dNBR) image, the pre and post-fire images are subtracted from each other. The equation is as follows:

$$dNBR = (NBR_{pre-fire}) - (NBR_{post-fire})$$

To derive burn severity models for multiple fires that have a large range of differing vegetation types and conditions, it has been proposed that the use of the absolute change dNBR algorithm may not be the most appropriate (Miller & Thode, 2007; Miller et al., 2009). This is because the degree of severity should be dependent upon the amount of pre-fire vegetation before the fire (Miller & Thode, 2007). To address this issue, remote sensing researchers have proposed the RdNBR algorithm:

$$RdNBR = \frac{NBR_{prefire} - NBR_{postfire}}{\sqrt{|NBR_{prefire} / 1000|}}$$

Table 1.3 provides a summary of selected research that has utilized the NBR, dNBR, and RdNBR remote sensing methods to estimate burn severity within the last twenty years.

Table 1.3. A short history of remote sensing burn severity research.

Author(s)	Year	Remote Sensing Platform	Field Observations	Vegetation Type
Lopez-Garcia and Caselles	1991	Landsat TM (in-scene dNBR)	% Vegetated Cover	Mediterranean forest and scrubland
Key and Benson	1999	Landsat TM dNBR	Composite Burn Index (CBI)	Conifer forests, western USA
Bobbe et al.	2003	Landsat TM dNBR	Fire severity class (four levels), surface measures of fire severity	Conifer forests, western USA
Hidak et al.	2004	NBR and dNBR using Landsat TM and SPOT data	Field measures of aboveground and surface severity	Conifer forests, western USA
van Wagtenonk et al.	2004	dNBR derived from Landsat TM and AVIRIS data	Composite Burn Index (CBI)	Pine forests, western USA
Cocke et al.	2005	dNBR derived from Landsat ETM+ data	CBI and fire severity classes (4 levels) based on pre and post-fire measurements	Pine forests, western USA
Epting et al.	2005	dNBR and other indices derived from Landsat imagery	Composite Burn Index (CBI)	Conifer, deciduous, mixed forests and shrublands in Alaska
Lewis et al.	2007	SMA (Spectral mixture analysis), NBR, dNBR, RdNBR from airborne hyperspectral (Probe-1) and Landsat TM	Fractional cover of seven components	Shrublands and grasslands of California
Miller and Thode	2007	dNBR and RdNBR derived from Landsat TM data	Composite Burn Index (CBI)	Conifer forest, shrublands, Sierra Nevada Mountains of California and Nevada
Allen and Sorbel	2008	dNBR generated from Landsat TM data	Composite Burn Index (CBI)	Conifer, deciduous, mixed forests, tundra, Alaska
Hall et al.	2008	dNBR generated from Landsat TM data	Composite Burn Index (CBI)	Conifer, deciduous, mixed forests, western Canada
Hoy et al.	2008	dNBR generated from Landsat TM data, TC (tasseled cap transformation), PC (principal-component transformation), and other spectral indices	CBI (modified for Alaskan forests), additional field measures of burn severity	Black Spruce forests, Alaska
Murphy et al.	2008	dNBR generated from Landsat TM data	CBI (modified for Alaskan forests)	conifer, deciduous, mixed forests, shrublands, Alaska
Miller et al.	2009	RdNBR from Landsat TM and ETM+	Composite Burn Index (CBI)	Conifer forest, shrublands, Sierra Nevada Mountains of California and Nevada
Wulder et al.	2009	NBR, dNBR, RdNBR from Landsat TM and ETM+	LIDAR	Boreal plains region of Alberta, Canada

1.4 Research objectives

Parks Canada fire managers and scientists are interested in utilizing the most accurate Landsat derived index as a tool to predict burn severity across large geographic areas and varying landscapes. Previous studies have mainly occurred in the forests of the western United States and Alaska, with many of the field observations using CBI (Table 1.3). Within Canada, however, research on this topic has been undertaken by Hall et al. (2008) and Wulder et al. (2009). Hall et al. (2008) highlighted the need for continued work in three areas of burn severity research. They recommended analysis of dNBR models with additional burn severity data, an accuracy comparison of the dNBR and RdNBR indices, and the incorporation of pre-fire vegetation data into burn severity modelling. Wulder et al. (2009) found that RdNBR was no more superior than dNBR at predicting post-fire effects, and they acknowledged that burn severity modelling is a subject of ongoing research in differing ecological regions, cover types, and conditions.

Based on previous research and the operational needs of Parks Canada, a key question was proposed: How well does a commonly used remote sensing algorithm estimate field-assessed burn severity in Canadian western parks?

Two additional questions were formed:

- 1) Of the two algorithms, the dNBR and RdNBR, which one is most appropriate to estimate burn severity across the study fires in western Canadian?
- 2) How accurately can a developed burn severity model be transferred across all study fires in western Canada?

Chapter 2 investigates the estimated accuracies of burn severity derived from both dNBR and RdNBR for six study fires. In addition, we assessed the accuracy of derived models stratified by pre-fire vegetation data and an analysis of the effects of pre-fire vegetation heterogeneity and sparseness.

As a critical step towards application and model development, the objective of chapter 3 was to test the ability of an overall derived dNBR model across all fires and to test the strengths and weaknesses of this method. An assessment of the accuracy and transferability of various models across the study fires was followed by an assessment of the benefit of incorporating pre- and post-fire data into standard dNBR approaches.

Finally, chapter 4 is a discussion of the overall results, conclusions, and recommendations for future work.

1.6 References

- Anderson, J.E. & Romme, W.H. (1991). Initial floristics in lodgepole pine (*Pinus contorta*) forests following the 1988 Yellowstone fires. *International Journal of Remote Sensing*, 22, 2015-2032.
- Borchers, J.G., Perry, D.A. (1990). Effects of prescribed fire on soil organisms. In 'Natural and prescribed fire in Pacific Northwest forests'. (Eds JD Walstad, SR Radosevich, DV Sandberg) pp. 143-158. (Oregon State University Press: Corvallis)
- Epting, J., & Verbyla, D. (2005). Landscape-level interactions of prefire vegetation, burn severity, and postfire vegetation over a 16-year period in interior Alaska. *Canadian Journal of Forest Research*, 35, 1367-1377.
- Fule, P.Z., Crouse, J.E., Heinlein, T.A., Moore, M.M., Covington, W.W., & Verkamp, G. (2003). Mixed-severity fire regime in a high-elevation forest of Grand Canyon, Arizona, USA. *Landscape Ecology*, 18, 465-485.
- Goldammer, J.G., & Furyaev, V.V. (Eds). (1996). 'Fire in Ecosystems of Boreal Eurasia. (Kluwer Academic: Dordrecht, the Netherlands)
- Gorham, E. (1991). Northern peatlands: role in the carbon cycle and probable responses to climatic warming. *Ecological Applications*, 1, 182-195.
- Government of Canada, Parks Canada Agency. (2000). 'Unimpaired for future generations'? Protecting Ecological Integrity with Canada's National Parks Vol. I "A Call to Action." Vol II "Setting a New Direction for Canada's National Parks." Report of the panel on the Ecological Integrity of Canada's National Parks. (Ottawa, ON)
- Hall, R.J., Freeburn, J.T., Groot, W.J.dG., Pritchard, J.M., Lynham, T.J., & Landry, R. (2008). Remote sensing of burn severity: experience from western Canada boreal fires. *International Journal of Wildland Fire*, 17, 476-489.
- Harden, J.W., Trumbore, S.E., Stocks, B.J., Hirsch, A., Gower, S.T., O'Neill, K.P., & Kasischke, E.S. (2000). The role of fire in the boreal carbon budget. *Global Change Biology*, 6, 174-184.
- Hungerford, R.D., & Babbitt, R.E. (1987). 'Overstory removal and residue treatments affect soil surface, air, and soil temperatures: implications for seedling survival.' USDA Forest Service, Intermountain Research Station Research Paper INT-377. (Ogden, UT)
- Jain, T., Pilliod, D., & Graham, R. (2004). Tongue-tied. *Wildfire*, 4, 22-26.

- Kasischke, E.S., & Stocks, B.J.. (Eds). (2000). 'Fire, Climate Change, and Carbon Cycling in the Boreal Forest' (Springer-Verlag: New York)
- Key, C.H., & Benson, N.C. (2006). Landscape Assessment: ground measure of severity, the Composite burn index, and remote sensing of severity, the Normalized Burn Index. In 'FIREMON: Fire Effects Monitoring and Inventory System'. (Eds DC Lutes, RE Keane, JF Caratti, CH Key, NC Benson, S Sutherland, LJ Gangi) USDA Forest Service, Rocky Mountain Research Station, General Technical Report RMRS-GTR-164-CD:LA1-51. (Ogden, UT)
- Kotliar, N.B., Reynolds, E.W., & Deutschman, D.H. (2008). American Three-toed Woodpecker response to burn severity and prey availability at multiple spatial scales. *Fire Ecology Special Issue*, 4, 2.
- Lamont, B.B., Witkowski, E.T.F., & Enright, N.J. (1993). Post-fire litter microsites safe for seeds, unsafe for seedlings. *Ecology*, 74, 501-512.
- Lentile, L.B., Holden, Z.A., Smith, A.M.S., Falkowski, M.J., Hudak, A.T., Morgan, P., Lewis, S.A., Gessler, P.E., & Benson, N.C. (2006). Remote Sensing techniques to assess active fire characteristics and post-fire effects. *International Journal of Wildland Fire*. 15, 319-345.
- Lillesand, T.M., Kiefer, R.W., & Chipman J.W. (2008). Chapter 6. pp 419. Remote Sensing and Image Interpretation, 6th edition. John Wiley & Sons, Inc. USA.
- Lyon, L.J., Stickney, P.F. (1976). Early vegetal succession following large northern Rocky Mountain wildfires. In 'Proceedings of the Montana tall timbers fire ecology conference and fire and land management symposium' No.14. 8-10 October, Missoula, MT. pp. 355-375. (Tall Timbers Research Station: Tallahassee, FL)
- Michalek, J.L., French, N.H.F., Kasischke, E.S., Johnson, R.D., & Colwell, J.E. (2000). Using Landsat TM data to estimate carbon release from burned biomass in an Alaskan spruce forest complex. *International Journal of Remote Sensing*, 21, 323-338.
- Miller, C., & Urban, D.L. (1999). Interactions between forest heterogeneity and surface fire regimes in the southern Sierra Nevada. *Canadian Journal of Forest Research*, 29, 202-212.
- Miller, J.D., & Thode, A.E. (2007). Quantifying burn severity in a heterogeneous landscape a relative version of the delta Normalized Burn Ratio (dNBR). *Remote Sensing of Environment*, 109, 66-80.
- Miller, J.D., Knapp, E.E., Key, C.H., Skinner, C.N., Isbell, C.J., Creasy, R.M., & Sherlock, J.W. (2009). Calibration and validation of the relative differenced

- Normalized Burn Ratio (RdNBR) to three measures of fire severity in the Sierra Nevada and Klamath Mountains, California, USA. *Remote Sensing of the Environment*, 113, 645-656.
- Pickett, S.T.A., & White, P.S. (Eds.). (1985). The ecology of natural disturbance and patch dynamics. New York, NY. Academic Press, 472 pp.
- Ryan, K.C. & Noste, N.V. (1985). Evaluating prescribed fires. In 'Proceedings of the symposium and workshops on wilderness fire. 15-18 November 1983, Missoula, MT'. (Eds JE Lotan, BM Kilgore, WC Fischer, RW Mutch) pp. 230-238. USDA Forest Service, Intermountain Forest and Range Experiment Station General Technician Report INT-GTR-182. (Ogden, UT)
- Soverel, N.O., Coops, N.C., White, J.C., & Wulder, M.A. (2009). Characterizing the forest fragmentation of Canada's national parks. *Environmental Monitoring and Assessment*. DOI: 10.1007/s10661-009-0908-7
- Stocks, B.J., Mason, J.A., Todd, J.B., Bosch, E.M., Wotton, B.M., Amiro, B.D., Flannigan, M.D., Hirsch, K.G., Logan, K.A., Martell, D.L., & Skinner, W.R. (2003). Large forest fires in Canada, 1959-1997. *Journal of Geophysical Research*, 107, 8149.
- Turner, M.G., Baker, W.L., Peterson, C.J., & R.K. Peet. (1998). Factors influencing succession: Lessons from large, infrequent natural disturbances. *Ecosystems*, 1, 511-523.
- Van Wagtenonk, J.W., R.R. Root & C.H. Key. (2004). Comparison of AVIRIS and Landsat ETM+ detection capabilities for burn severity. *Remote Sensing of Environment*, 92, 397-408.
- USGS (United States Geologic Survey). GLOVIS website: <http://glovis.usgs.gov/>
- Van Wagtenonk, J.W., Root, R.R., & Key, C.H. (2004). Comparison of AVIRIS and Landsat ETM+ detection capabilities for burn severity. *Remote Sensing of Environment*, 92, 397-408.
- Van Wagner, C.E., Finney, M.A., & Heathcott, M. (2006). Historical Fire Cycles in the Canadian Rocky Mountain Parks. *Forest Science*, 52, 704-717.
- Weber, M.G., & Stocks, B.J. (1998). Forest fires and sustainability in the boreal forest of Canada. *Ambio*, 27, 545-550.
- Wein, R.W., & MacLean, D.A. (Eds). (1983). 'The Role of Fire in Northern Circumpolar Ecosystems' (Wiley: New York)

- Wells, C.G., Campbell, R.E., DeBano, L.F., Lewis, C.E., Fredriksen, R.L., Franklin, E.C., Froelich, R.C., & Dunn, P.H. (1979). 'Effects of fire on soil, a state-of-knowledge review.' USDA Forest Service, Washington Office General Technical Report WO-7. (Washington, DC)
- Wulder, M.A., White, J.C., Alvarez, F., Han, T., Rogan, J., & Hawkes, B. (2009) Characterizing boreal forest wildfire with multi-temporal Landsat and LIDAR data. *Remote Sensing of Environment*, 113, 1540-1555.
- Wyant, J.G., Omi, P.N., & Laven, R.D. (1986). Fire-induced tree mortality in a Colorado ponderosa pine/Douglas-fir stand. *Forest Science*, 32, 49-59.

2 ESTIMATING BURN SEVERITY FROM dNBR AND RdNBR INDICES ACROSS WESTERN CANADA²

2.1 Introduction

Since the last ice age, wildland fire is considered to be the dominant disturbance agent across much of western Canada (Stocks et al., 2003). Consequently, a multitude of fire regimes can be found in western Canada, each possessing their own characteristics and spatial patterns. Wildland fire can drive biotic changes that are observed in landscape structure, composition, and species biodiversity, as well as change the function, rate, and pathways of ecological succession and encroachment (Lentile et al., 2006). In addition, fire can impact abiotic processes including soil and atmospheric nutrient cycling, as well as have direct implications for air quality from smoke emissions (Hardy et al., 2001). Under changing climate, Canadian wildland fire management agencies are becoming increasingly concerned with changes in fire season length, size and intensity, and financial cost (Tymstra et al., 2007). Fire projection models coupled with climate change forecasts predict increases in area burned, fire season length, fire intensity and burn severity (Wotton & Flannigan, 1993; Flannigan et al., 1998, 2005). In response, scientists and fire managers require the most accurate data available regarding landscape burn severity and estimates of total burned area so that they can calculate total carbon emissions and fluctuations in burned area over time.

² A version of this chapter has been submitted for publication. Soverel, N.O., Perrakis, D.B., Coops, N.C. (2010) Estimating burn severity from Landsat dNBR and RdNBR indices across western Canada.

In addition, burn severity spatial data and the fire's perimeter can characterize fire-induced vegetation mortality along with associated unburned islands to create a mosaic landscape consisting of distinct forest type and age class patches (Miller & Urban, 1999; Fule et al., 2003).

Canadian land managers, including provincial natural resource agencies and Parks Canada, are often limited in their ability to acquire wildland fire data because many burned areas are located in roadless and remote areas. Remote sensing techniques can be inexpensive, reduce safety hazards, and provide greater accuracy when compared to traditional fire monitoring methods. This information can then be used by land managers and stakeholders for the purpose of monitoring vegetation, wildlife, soil and hydrologic changes, as well as various ecological processes.

Fire severity can be defined as the direct effects of the combustion process on vegetation such as tree mortality and the losses of biomass in the forms of vegetation and soil organic material (Jain et al., 2004; Lentile et al., 2006). Alternatively, burn severity can be defined as “the degree of ecological change to a landscape caused by fire” (Key & Benson, 2005). Inherently, field measured burn severity is not a direct measure but a subjective judgement that can change based on the context or resource being addressed (Lentile et al., 2006). Burn severity represents the majority of the research focus herein and is assessed in the field by classifying sites of similar visible burn characteristics.

The direct impacts of fire on vegetation include changes in the composition, density, and vigour of plant species as well as the overall moisture content of the vegetation, litter, and the soil of the burned area. For this reason, changes in the near and short-wave infrared regions of the electromagnetic spectrum following fire can be detected by multispectral remote sensing devices. Landsat's Thematic Mapper (TM) and Enhanced Thematic Mapper Plus (ETM+) sensors are appropriate for burn severity analysis because they record near infrared (NIR) and short-wave infrared (SWIR) reflectance in Bands 4 (B4) and 7 (B7), respectively. Band 4 is recorded in the wavelengths between 0.76 μm – 0.90 μm while Band 7 between 2.08 μm –2.35 μm . Landsat TM/ETM+ Band 4 is primarily sensitive to the chlorophyll content of live vegetation (Miller & Thode, 2007) while Landsat's TM/ETM+ Band 7 is sensitive to water content in both soils and vegetation, the lignose content of non-photosynthetic vegetation, and hydrous minerals such as clay, mica, and some oxides and sulphates (Avery & Berlin, 1992; Elvidge, 1990). In addition to the appropriate spectral bands, Landsat TM and ETM+ imagery provides moderate spatial resolution, is freely available in North America, and has an archive ranging from 1984 onwards, containing an extensive dataset covering most of Canada.

French et al. (2008), in a detailed review, documented 41 studies worldwide which utilized moderate and coarse resolution satellite data to extract the Normalized Burn Ratio (NBR) and differenced Normalized Burn Ratio (dNBR) data to detect burn severity. Of these studies, 26 of them utilized Landsat imagery to derive the normalization of near infrared and shortwave infrared wavelengths to measure burn severity. NBR and dNBR are calculated as follows:

$$NBR = (B4-B7) / (B4+B7) \quad (1)$$

$$dNBR = (NBR_{prefire} - NBR_{postfire}) \quad (2)$$

To derive either the initial assessment (IA) or extended assessment (EA) dNBR images, suitable pre- and post-fire NBR grids are acquired and the images subtracted to yield the differenced Normalized Burn Ratio (dNBR). The extended assessment (EA) is the difference between the pre-fire NBR image and an image acquired one year post-fire, and this image is most commonly used in burn severity ecological assessments. In contrast, fire perimeter delineation and immediate burn severity mapping normally utilizes the initial assessment (IA) which is the difference between the pre-fire image and an image acquired in the same year as the fire event. A recent variation of the dNBR approach is the relative differenced Normalized Burn Ratio (RdNBR). While the dNBR algorithm measures absolute change between the pre and post fire images, the RdNBR algorithm determines burn severity based on pre-fire reflectance and calculates the relative change caused by fire (Miller & Thode, 2007) as defined in equation 3:

$$RdNBR = \frac{NBR_{prefire} - NBR_{postfire}}{\sqrt{|NBR_{prefire} / 1000|}} \quad (3)$$

The evaluation of the sensitivity of the dNBR algorithm to measure field measured burn severity has been tested on a large number of fires in the USA (Zhu et al., 2006). From the studies discussed in French et al. (2008), an overall dNBR classification accuracy of 73% (range 50-90%) was determined across a range of fires. Miller and Thode (2007) compiled burn severity data from 14 fires in the Sierra Nevada region, USA, and found a

coefficient of determination (R^2) of 0.49 for dNBR while the RdNBR reported an R^2 of 0.61. Zhu et al. (2006) also found overall that the RdNBR was a better estimator than dNBR within the more sparsely vegetated Southwest region and over a pooled dataset of all fires. They also concluded that RdNBR was a better estimate in landscapes that had either sparse or non-productive pre-fire vegetation, and therefore may provide a more consistent broad scale relationship to burn severity. Miller and Thode (2007) proposed two advantages of the RdNBR algorithm over the dNBR: 1) it provided a consistent definition for comparison across space and time and 2) classification accuracies should be higher in high severity categories, especially in heterogeneous pre-fire vegetation.

Only a limited amount of published literature regarding remote sensing of burn severity exists for Canadian landscapes. A pilot study conducted by Perrakis and Zell (2008) found promising results using Landsat to estimate burn severity across three fires in national parks of western Canada. Hall et al. (2008) investigated the relationship between dNBR and ground based burn severity measurements for four fires in Canada's boreal region reporting R^2 values as high as 0.84. They also discussed the need for future research in the Canadian boreal using RdNBR to better understand the effects of pre-fire vegetation on burn severity modelling from remote sensing data.

Based on this existing research we hypothesized that the RdNBR algorithm would perform better in heterogeneous or sparsely vegetated landscapes, as well as provide a more accurate index across our total study area. The goal of this research, therefore, is to assess and compare the capacity of both the dNBR and RdNBR algorithms to estimate

burn severity. To fulfill this objective, dNBR and RdNBR data were derived from a number of Landsat scenes and compared with field estimates of burn severity across a range of fires. The difference in the capacity of the two datasets to estimate burn severity was first assessed on an individual fire basis. Fires were then stratified by both broad vegetation type (coniferous, broadleaf, and ‘other vegetation’) and region (Rocky Mountain, western boreal), and lastly all fires were pooled to assess the capacity of a generalised model to estimate burn severity across all fires. Finally, we assessed the capacity of a previously-developed model from Hall et al. (2008) to estimate burn severity over the western boreal region and the fires within that region. With this comprehensive examination of Canadian burn severity monitoring we anticipate a clearer picture of the strengths and weaknesses of these two algorithms will be realized, which in turn should provide additional insight for model applications in routine burn severity research.

2.2 Data and methods

2.2.1 Study area and characteristics

Six fires were analyzed in this study, all of which occurred in four Canadian national parks (Figure 2.1, Figure 2). Three of the fires occurred in the Canadian Rockies and the remaining three in the western boreal forest (Table 2.1). The four national parks and their associated ecoregions (Ecological Stratification Working Group, 1996) are as follows: Yoho and Kootenay National Parks within the Western Continental Ranges ecoregion, Jasper National Park in the Eastern Continental Ranges, and Wood Buffalo National Park in the Slave River Lowlands and Hay River Lowlands ecoregions. Elevations of these fire

affected landscapes ranged from 250 m on the Peace River in Wood Buffalo National Park, Alberta to 2,100 m in Yoho National Park, British Columbia. Of the six fires, four were lightning-ignited wildfires (Boyer 01, Boyer 02, Peace Point, Southesk). The Hoodoo and Split Peak fires were prescribed fires (Hoodoo, Split Peak) planned to meet various ecological objectives which included reducing canopy cover and canopy fuel continuity. The fires ranged in size from 560 to 106,772 ha and covered various vegetation types within each respective ecoregion.

Table 2.1. Fire name, ignition and out date, fire size (ha), elevation (m), and dominant vegetation types for study fires.

Fire Name	Ignition Date	Out Date	Fire Size (ha)	Elevation (m)	Vegetation Type
Hoodoo Creek	2005-05-28	2005-05-30	1,525	1400-2100	Lodgepole pine, Douglas fir, Engelmann spruce, and Trembling aspen
Southesk	2006-07-21	2006-07-26	1,168	1500 -2100	Lodgepole pine, Engelmann spruce
Split Peak	2007-09-15	2007-09-20	560	1350-2000	Lodgepole pine, Douglas fir, Englemann-White spruce
Peace Point	2005-06-07	2005-07-26	12,432	250-300	White spruce, Black spruce, Jack pine, Trembling aspen
Boyer 01	2007-05-27	2007-08-20	75,963	250-350	Black spruce, Tamarack, Jack pine, Trembling aspen, White spruce, and shrub/grass cover matrix
Boyer 02	2007-05-27	2007-08-20	106,772	250-350	Black spruce, Tamarack, Jack pine, Trembling aspen, White spruce, and shrub/grass cover matrix

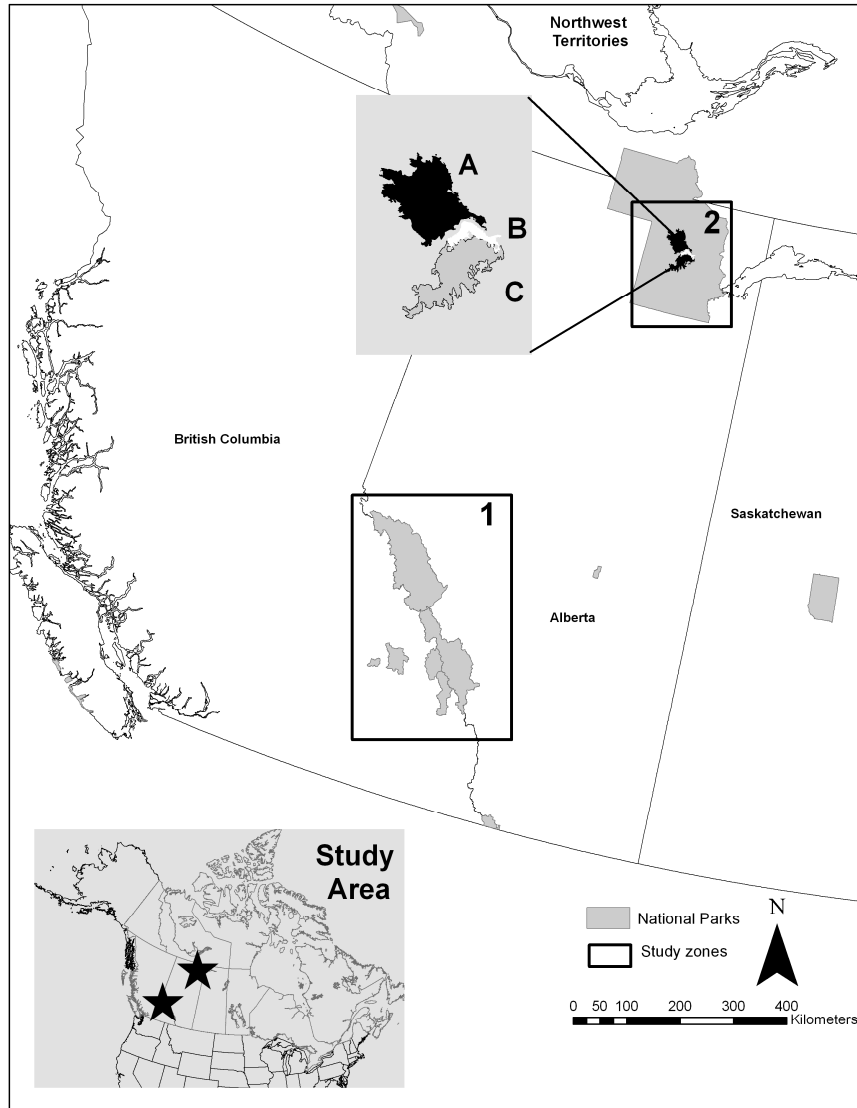


Figure 2.1. Total study area map representing the (1) Canadian Rocky Mountain and (2) western boreal study regions. Within the western boreal study region, the wildland fires include: (A) Boyer 02, (B) Peace Point, and (C) Boyer 01.

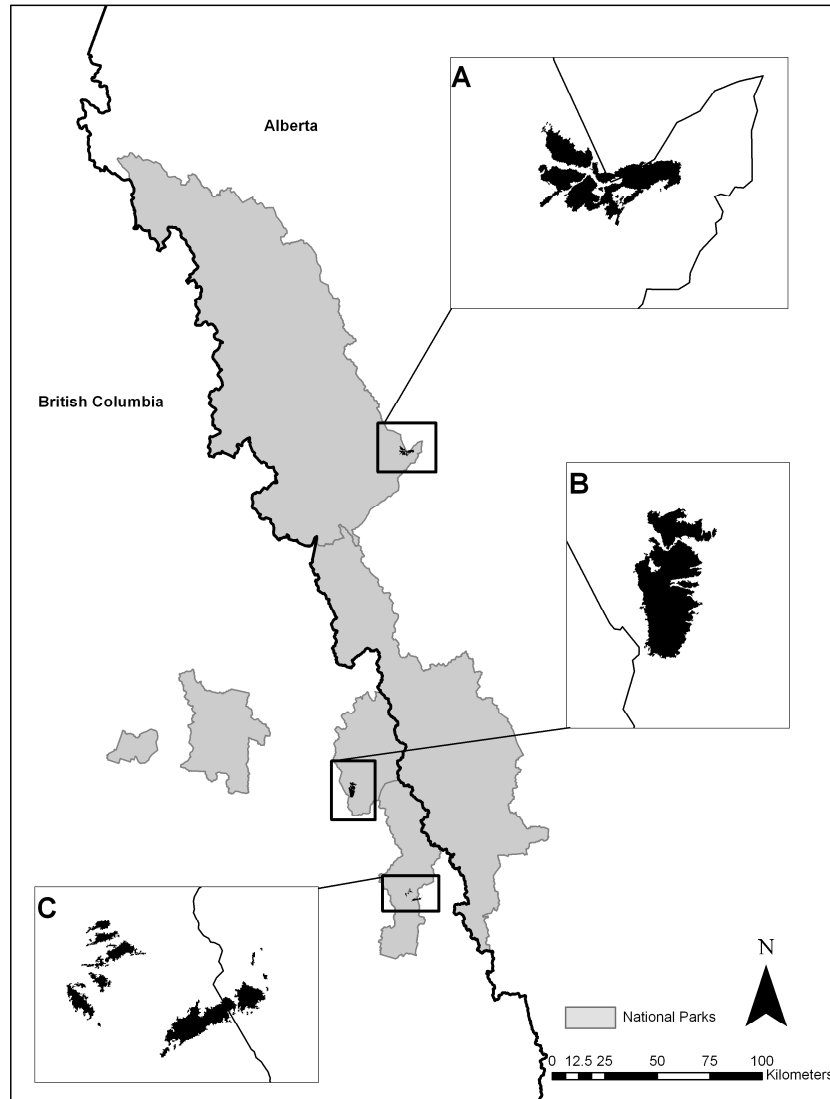


Figure 2.2. The Canadian Rocky Mountain study region which includes the (A) Southesk, (B) Hoodoo, and (C) Split Peak fires.

The historic fire regimes and dominant species composition for the Rocky Mountain and western boreal forests are described in more detail below. For the Rocky Mountain region of Canada, two major ecosystem types can be delineated with respect to fire regimes: montane and subalpine forests. Subalpine forest ecosystems in this region are composed of subalpine fir (*Abies lasiocarpa*), lodgepole pine (*Pinus contorta*), and Engelmann spruce (*Picea engelmannii*). In contrast, montane forests are dominated by fire-adapted

species such as Douglas-fir (*Pseudotsuga menziesii*), lodgepole pine (*Pinus contorta*), and trembling aspen (*Populus tremuloides*). The controlling factor for these ecosystem types is elevation, with higher elevation areas being historically characterized by subalpine forests and the lower by montane forests. Due to topographic variation and local micro-climates, the boundaries between these two ecosystem types can be intertwined. The subalpine region was historically affected by infrequent, intense, and higher severity fires (Agee, 1993). In contrast, the montane ecosystem has been characterized by more frequent fires with a broad range of fire intensities and severities (Klenner et al., 2008), but likely dominated by low severity fire effects (Fischer & Clayton, 1983; Tande, 1979).

Alternatively, the western boreal forest of Canada is composed of the following dominant tree species: jack pine (*Pinus banksiana*), black spruce (*Picea mariana*), trembling aspen (*Populus tremuloides*), tamarack (*Larix laricina*), and white spruce (*Picea glauca*). Fires are typified by large, infrequent, and stand-replacing events, with a range of fire cycles depending on local climate and tree species (Johnson, 1992; Turner et al., 2003).

However, patches of grasslands, shrublands, wet meadows, and other non-forested vegetation are also frequent and sometimes extensive in this part of the boreal plains (Schwarz & Wein, 1997); the addition of non-forested communities within the mosaic of surrounding forests makes burn severity assessment more complex in these areas.

2.2.2 Imagery and pre-processing

Landsat TM/ETM+ imagery were the sole sources of remote sensing imagery utilized in this analysis. Images were selected based on minimal cloud, fire ignition site, season, and anniversary dates (Table 2.2). Pre-fire imagery was chosen in the year of fire ignition if suitable, or else an image was obtained in the years previous to the fire. Two post fire images were selected in the growing seasons following the wildland fire, one for the IA and one for the EA. The IA burn severity map was utilized only for fire perimeter extraction and for burn severity ground plot sampling, while the EA dNBR and RdNBR indices were the primary source of data for the analysis.

Table 2.2. Landsat imagery used in this study for both the IA (initial assessment) or EA (extended assessment). Fire name, Landsat path and row, and pre-fire and post-fire Landsat TM/ETM+ imagery acquisition dates, are listed.

Fire Name	IA/EA	Path/Row	Pre-fire image date (TM/ETM+)	Post-fire image date (TM/ETM+)
Hoodoo Creek	IA	44/24	24/08/1999 (ETM+)	30/07/200 (TM)
Hoodoo Creek	EA	44/24	24/08/1999 (ETM+)	09/04/2006 (TM)
Southesk	IA	44/23	23/08/2002 (ETM+)	26/08/2006 (TM)
Southesk	EA	44/23	07/10/2003 (TM)	07/05/2007 (TM)
Split Peak	IA	43/24	15/08/2007 (TM)	16/09/2007 (TM)
Split Peak	EA	43/24	15/08/2007 (TM)	17/08/2008 (TM)
Peace Point	IA	44/19	14/09/2001 (ETM+)	28/08/2005 (TM)
Peace Point	EA	44/19	14/09/2001 (ETM+)	09/04/2006 (TM)
Boyer 01 & 02	IA	44/18/19	29/06/2005 (TM)	21/07/2007 (TM)
Boyer 01 & 02	EA	44/18/19	29/06/2005 (TM)	08/08/2008 (TM)

Each image was orthorectified to Universal Transverse Mercator (UTM) Zone 11 or 12 North, Datum WGS-84 with a root mean squared error less than 15 meters. Four of the sixteen images utilized in this research were downloaded from the GLOVIS website (USGS, 2009) and were orthorectified using Level 1 Terrain correction procedures (USGS, 2009). The remaining twelve images were orthorectified on an image by image

basis using a minimum of 12 control points and publicly available 30 m resolution digital elevation models (DEMs). After orthorectification, Landsat TM and ETM+ digital numbers were converted to at sensor reflectance using standard procedures (detailed in NASA, 1998; Chander & Markham, 2003) with additional information on current coefficients for these sensors available at Chandler et al. (2009). Atmospheric correction was undertaken by using the dark body subtraction technique where for each band the darkest pixel value within a Landsat scene is subtracted, providing a simple and effective haze correction in multispectral data (Chavez, 1989). This method has been found to have consistent and improving effects in multi-date radiometric correction analyses (Song et al., 2001; Schroeder et al., 2006). Finally, the NBR, dNBR, and RdNBR were calculated using Equations (1-3). For the IA images only, a density slice classification was undertaken with dNBR values > 100 classified as “burned” (Key & Benson, 2006), thus delineating the fire perimeters used throughout this analysis. To minimize any phenological or inter-annual differences between the pre and post fire images, methods of Zhu et al. (2006) were used to calibrate both the dNBR and RdNBR images. This was achieved by extracting a sample of unchanged pixels from outside the dNBR and RdNBR fire perimeters, followed by the calculation of the sample’s mean, and then the subtraction of the mean from the dNBR and RdNBR images.

2.2.3 Field data

Field data were collected utilizing the Composite Burn Index (hereafter as CBI) field protocol, which takes into account the visible and averaged burn severity condition found in a plot (Key & Benson, 2005). The CBI assessment is a somewhat subjective assessment of the entire averaged burn severity across multiple layers at a plot and is

heavily weighted to measuring fire effects on vegetation. This method assesses burn severity in relation to its effects on five forest strata: substrates, herbaceous vegetation, large shrubs and small trees, intermediate trees, and dominant and co-dominant canopy trees. Fire effects on these strata can include but are not limited to site characteristics such as duff and litter consumption, soil exposure, herbaceous mortality and percent cover, shrub mortality, char and scorch heights, overstory mortality, and overall site biodiversity.

CBI plot locations were positioned using the following methodology. Using the initial assessment (IA), we first stratified suitable points using homogenous patches of similar burn severity in a 3 x 3 pixel window with an initial dNBR value difference < 150 as recommended by Key and Benson (2005). Those points were then stratified into burn severity classes derived from Key and Benson (2006) and were then randomly sampled to select potential plot locations. Ideally, locally developed class breaks would have been used to help plot selection as recommended by Lentile et al. (2006), however, previously defined class breaks were not available for this region. Plot locations that were close to the fire edge < 45 m or within 90 m of a class boundary were removed from contention. All CBI plots were field validated approximately one year after the fire occurred at that location. Field protocol closely followed the directions outlined in Landscape Assessment (Key & Benson, 2005). A 30 m circular plot was laid out, an averaged GPS location acquired for the plot center, plot photographs taken, and the CBI field data form was completed. Additional information to the CBI indicators was also recorded including dominant plant species per strata, pre-fire percent cover per strata, and other notable

characteristics of the stand. A percent cover-weighted CBI value per plot was calculated, with additional weighting provided to the overstory layer. This involved weighting each stratum according to its estimated coverage within the plot, and providing a double weight for overstory trees due to the dominant role of larger trees in forest biomass and habitat attributes of forest ecosystems. To reduce any assessor bias, CBI assessments were conducted by the same two individuals.

2.2.4 Vegetation groupings and analysis technique

To provide consistent information on pre-fire vegetation type and canopy closure (hereafter referred to as CC), the Earth Observation for Sustainable Development of Forests Land Cover 2000 (hereafter referred to as EOSD) data was utilized. This Canada-wide, forest cover classification was derived from circa 2000 Landsat imagery and provides a 23 class classification at a spatial resolution of 25 m (Wulder et al., 2008a). The accuracy of the EOSD LC 2000 is estimated to be approximately 80% over all classes, with greater accuracy found for the more dominant forest classes (Wulder et al., 2007; Wulder et al., 2008b). Furthermore, class accuracy can also be expected to increase as class generalization or simplification is applied (Rommel et al., 2005).

The EOSD classification was applied at two scales of analysis. First, at the broad fire scale, the EOSD classes within each fire perimeter were utilized to determine an overall ranking of each fire's combined heterogeneity and sparseness. At the fine scale, the EOSD classification was used to class each weighted CBI plot as either coniferous, broadleaf, or 'other vegetation', allowing individual weighted CBI-NBR models to be developed for each vegetation type irrespective of its fire location.

In more detail at the broad fire scale, an EOSD land cover vegetation and CC weighting calculation was applied which assigned higher weights to the increased canopy closure EOSD classes. For example, forest classes were weighted higher than non-forest classes, and canopy weightings increased from “sparse” to “open” to “dense” canopy classes. To assess landscape heterogeneity we utilized FRAGSTATS (McGarigal & Marks, 1995) software to determine two landscape metrics: percentage of like adjacencies (PLADJ) and the Contagion Index (CONT). PLADJ is computed as the sum of the diagonal elements of the adjacency matrix divided by the total number of adjacencies (McGarigal & Marks, 1995). This landscape metric only measures dispersion, not interspersion, at the patch scale. Unlike PLADJ, CONT measures both dispersion and interspersion at the landscape level, and the output is based on the probability of finding a cell of type (i) next to a cell of type (j) (McGarigal & Marks, 1995). The two landscape metrics have similar interpretations: as the metric values increase, the aggregation or “clumpiness” of the vegetated pixels in the landscape increases. Table 2.3 and Figure 2.3 both indicate, for each fire, the PLADJ, CONT, and CC values. Included in Table 2.3 is the overall ranking of all three metrics: CC, PLADJ, and CONT. All three of the metric rankings were summed in order to provide an overall ranking that could be used to compare pre-fire vegetation across fires. The overall ranking (1-6) compares the highest overall CC and homogeneous pre-fire vegetation with the lowest rankings, or those that had less CC and more spatial heterogeneity. In order of ranking, these fires were: Peace Point, Southesk, Hoodoo, Boyer 01, Split Peak, and Boyer 02 (Table 2.3, Figure 2.3).

For the fine scale analysis, the EOSD classes were collapsed into three broad vegetation groups (Table 2.4). The conifer group consisted of the three main EOSD conifer classes of: “Coniferous – Dense (> 60% CC)”, “Coniferous – Open (26-60% CC)”, and “Coniferous – Sparse (10-25% CC)”. The broadleaf group in the study consisted of: “Broadleaf – Dense (> 60% CC)”, “Broadleaf – Open (26-60% CC)”, and “Broadleaf – Sparse (10-25% CC)”. The ‘other vegetation’ group consisted of all other possible non-forest EOSD groups: shrub (tall, short), herb, and wetland (treed, shrub, herb). The EOSD water class pixels found in the two Wood Buffalo fires were extracted and disregarded from the analysis.

Table 2.3. Fire name, overall ranking, canopy closure (CC) weight value, PLADJ (percentage of like adjacencies) metric, and CONT (contagion) metric.

Fire Name	Overall Ranking	CC Weight	PLADJ	CONT
Peace Point	1	56.1	86.9	76.8
Southesk	2	51.7	83.2	68.5
Hoodoo	3	48.1	69.3	65.2
Boyer 01	4	46.9	75.0	51.8
Split Peak	5	44.7	67.2	55.7
Boyer 02	6	40.7	72.4	45.5

Table 2.4. The three EOSD LC 2000 vegetation groups and associated canopy closure (CC) percentage for conifer, broadleaf, and ‘other vegetation’.

Conifer	Broadleaf	Other
Dense (>60% CC)	Dense (>60% CC)	Wetland (treed, shrub, herb)
Open (26-60% CC)	Open (26-60% CC)	Shrub (tall, low)
Sparse (10-25% CC)	Sparse (10-25% CC)	Herbaceous

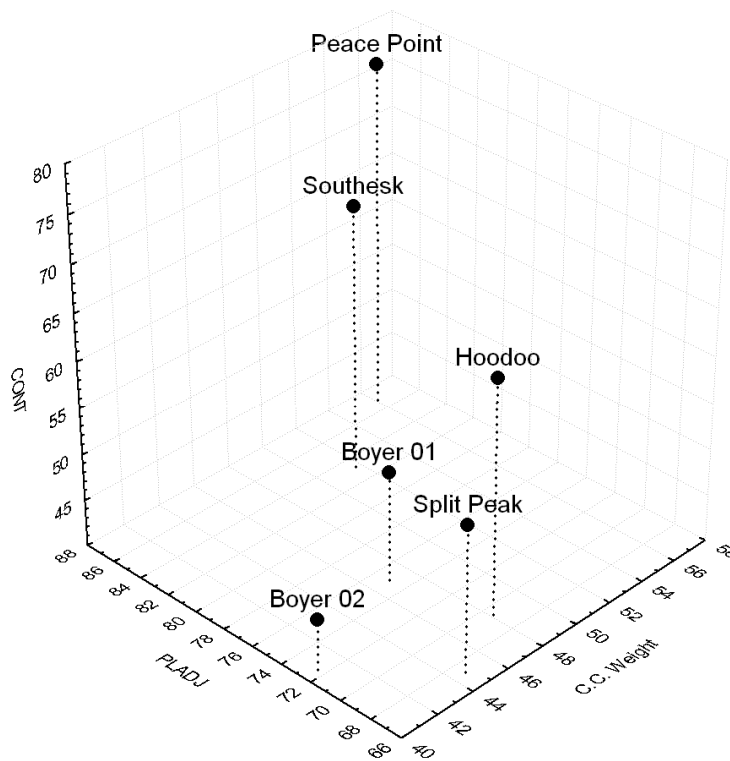


Figure 2.3. 3-D scatter plot depicting each fire’s pre-fire canopy closure (CC) and landscape spatial heterogeneity. The Y-axis represents the percentage of like adjacencies (PLADJ) index value, the X-axis vegetation canopy closure (CC), and the Z axis the contagion (CONT) index value.

2.2.5 Data analysis

The field plot GPS locations were differentially corrected to improve accuracy. Extended assessment dNBR/RdNBR values were calculated for each location using a weighted average of the surrounding pixels as described by previous authors (Cocke et al., 2005; Key & Benson, 2005). The weighted CBI locations that fell in areas of high local burn heterogeneity, defined as a difference in the surrounding pixels of 250 for dNBR or 350 for RdNBR, were removed. Weighted CBI classes were chosen with the same threshold values as Miller et al. (2009) and as outlined in Table 2 of Miller and Thode (2007), who

divided their fires into three main classes: unchanged/low (0-1.25), moderate (1.26-2.25), and high (2.26-3.0). We chose to use these generalized CBI thresholds because they allowed us to compare the two indices across multiple fires with more consistency than developing CBI thresholds on a fire by fire basis.

Prior to regression analysis, we verified that each dataset could pass the assumptions of serial correlation, homoscedasticity, and normality. It was unnecessary to test for linearity between the dependent (weighted CBI) and independent (remote sensing) variables as this has already been proven (Wagtendonk, 2004; Miller et al., 2009; Zhu et al., 2006; and many others). Serial correlation was tested using the Durbin Watson statistic and homoscedasticity was tested using the White test; in both tests each dataset passed. The normality of the residuals was tested using the Kolmogorov-Smirnov test in which each dataset was significant for normal distribution. Landsat derived dNBR or RdNBR values were fitted to weighted CBI values using linear and quadratic regression models. Models were then evaluated and chosen by comparing the coefficient of determination, standard error, model significance and Akaike Information Criterion (AIC; Hilborn & Mangel, 1997) values. AIC is founded on the principles of parsimony and attempts to utilize “the smallest possible number of parameters for adequate representation of the data” (Box & Jenkins, 1970). In addition, confusion matrices and their subsequent producer’s, user’s, and overall accuracies were extracted for each model. The confusion matrix consisted of the three classes: unchanged/low, moderate, and high, with the weighted CBI data (ground truth) in the columns versus the remote sensing (classified data) in the rows. The overall kappa and 95% CI intervals along with the conditional kappa (k_i) statistics were

computed as a means of determining the percentage correct values due to true agreement versus chance agreement. For comparison, Hall et al.'s (2008) non-linear model was used: $CBI = dNBR * (0.22 * [dNBR] + .09)^{-1}$ to compute regional and western boreal individual fire results. The Hall et al. (2008) non-linear model was chosen because it is not asymptotic, it was shown to be accurate ($R^2=0.82$), and it was derived from CBI data within the same region. To test the performance of the model, we calculated the regressed non-linear CBI values using our western boreal dNBR values. Secondly, these CBI values were compared to our total unweighted CBI values using linear regression. Finally, we created confusion matrices with the columns representing the field measured total CBI and the rows representing the Hall et al. (2008) derived CBI values.

2.3 Results

2.3.1 Results for individual fires

2.3.1.1 Peace Point fire

The overall ranking of CC and heterogeneity indicates that of all fires, the Peace Point fire ranked number one (Table 2.3, Figure 2.3). The broad scale analysis of EOSD land cover for the Peace Point fire designates that pre-fire vegetation was approximately 88% coniferous, 2% broadleaf and 10% 'other vegetation'. Of the 88% pre-fire coniferous vegetation, more than 83% was dense coniferous, and the PLADJ and CONT metrics measure a comparatively low level of heterogeneity. As compared to the other study fire histograms (Figure 2.4A), the Peace Point fire indicates a distribution that is moderate to high severity. The three severity classes depict consistent results for both the dNBR and RdNBR indices, with both estimating high severity effects over 29.0% and 30.3% of the

fire area, respectively. The moderate and unchanged/low severity proportions for these fires were also consistent with the dNBR estimating 27.3% and 43.7% and the RdNBR estimating 27.7% moderate and 42.0%, respectively. Linear models were chosen for both indices because neither showed statistical significance using a quadratic function and the AIC value was lower for the linear dNBR model and very similar for the RdNBR (Table 2.5, Figure 2.5A). The linear dNBR model estimated weighted CBI well ($R^2=0.70$, $SE=0.42$, $p<0.05$) as did RdNBR ($R^2=0.72$, $SE=0.40$, $p<0.05$) (Table 2.5). An accuracy assessment of the Peace Point fire (Table 2.6) indicates similar results for the two indices. The overall accuracies were similar with 70.3% dNBR and 70.7% RdNBR, with the producer's and user's accuracies, kappa statistics, and conditional kappa values all highly related.

2.3.1.2 Southesk fire

The Southesk fire was ranked second among the other study fires (Table 2.3, Figure 2.3). The EOSD classification defined the two largest vegetation classes as dense conifer (76.5%), and tall shrub (11.7%). The large proportion of dense coniferous canopies and high PLADJ and CONT values indicate a closed canopy and aggregated pre-fire forest landscape. A large shift in the index values occurred between the dNBR and the RdNBR models (Figure 2.4B). Additionally, the Southesk fire had the greatest area proportion in the high severity class. The RdNBR class delineated an estimated 47.4% high severity burn while the dNBR calculated 47.6% (Figure 2.4B). The quadratic model was significant for both dNBR and RdNBR (Figure 2.5B) and indicated the lowest AIC values when compared to the linear model. Field data correlated more closely with dNBR

values, ($R^2=0.81$, $SE=0.44$, $p<0.05$) (Table 2.5) than did RdNBR, ($R^2=0.79$, $SE=0.42$, $p<0.05$) (Table 2.6). Confusion matrix results indicate a higher dNBR overall accuracy (82.4%) than RdNBR (74.2%) (Table 2.6). Lowest accuracies occurred in the moderate classes for both dNBR and RdNBR; dNBR user's and producer's at 62.5%, and RdNBR user's and producer's at 0.0%.

2.3.1.3 Hoodoo fire

According to the EOSD data, the majority of pre-fire vegetation consisted of open coniferous (63.5%), and dense coniferous (26.5%) forests. The overall ranking of the pre-fire vegetation was third overall, with a moderately closed coniferous canopy with moderate landscape heterogeneity according to the PLADJ and CONT spatial metrics (Table 2.3, Figure 2.3). As compared to the other study fire histograms, Figure 2.4C indicates that this fire was fairly moderate for both the dNBR and RdNBR. The RdNBR index represents the following burn severity class distributions: 29.4% high, 19.2% moderate, and 51.4% unchanged/low. The dNBR index indicates 34.2% high, 16.0% moderate, and 49.8% unchanged/low class values. Of all the fires in this research study, the Hoodoo fire had the lowest correlations with weighted CBI field data (Table 2.5) for both dNBR and RdNBR, but also the smallest weighted CBI sample size. Based on statistical significance and AIC values (Table 2.5), a linear regression was the most significant model for both dNBR and RdNBR (Figure 2.5C). Regressions were weak for both dNBR and RdNBR, but higher for the latter index: ($R^2=0.40$, $SE=0.63$, $p<0.05$) (RdNBR: $R^2=0.55$, $SE=0.54$, $p<0.05$) (Table 2.5). The overall confusion matrix accuracy

for dNBR and RdNBR is 65.2%, with lower high severity user's (33.3%) and conversely high producer's accuracies (100.0%) (Table 2.6).

2.3.1.4 Boyer 01 fire

Pre-fire vegetation type and heterogeneity indicate that this fire was ranked fourth (Table 2.3, Figure 2.3). According to the EOSD data, the majority of pre-fire vegetation was within two main classes: non-forest wetland shrub (39.3%) and dense coniferous forest (39.8%). Figure 2.4D indicates that as compared to the other study fires, this was lower in severity, with the RdNBR index estimating 4.3% high, 10.9% moderate, and 84.7% unchanged/low, and the dNBR estimating 1.1% high 12.9% moderate, and 86.1% unchanged/low. Both indices were statistically significant for quadratic models with lower AIC values than linear (Table 2.5), results showing both the dNBR and weighted CBI field data ($R^2=0.76$ SE=0.35 $p<0.05$), and the RdNBR index ($R^2=0.77$, SE=0.35, $p<0.05$) (Table 2.5, Figure 2.5D). Equal accuracies were found for dNBR and RdNBR (69.4%) and very poor accuracies in the high severity class (0.0%) (Table 2.6).

2.3.1.5 Split Peak fire

The Split Peak pre-fire EOSD vegetation indicates a majority open coniferous (73.5%) with the remaining dense coniferous (4.5%), broadleaf (5%), and non-forest (17%). This fire was fifth overall with low CC and heterogeneous pre-fire vegetation (Table 2.3, Figure 2.3). Compared to the other study fires, the Split Peak burn severity histogram (Figure 2.4E), indicates moderately severity fire effects, and the dNBR showing a bell-shaped curve and the RdNBR a bimodal distribution. These class proportions were highly

related, the RdNBR containing 25.5% high severity, 31.5% moderate, and 43.0% unchanged/low; while dNBR had 24.9% high, 36.8% moderate, and 38.3% unchanged/low (Figure 2.4E). Quadratic models were statistically significant and showed lower AIC values than the linear models, with the dNBR ($R^2 = 0.70$, $SE = 0.50$, $p < 0.05$) and RdNBR ($R^2 = 0.69$, $SE = 0.52$, $p < 0.05$) (Table 2.5, Figure 2.5E). Overall accuracy for dNBR was 60.4% and RdNBR 59.6%, both indices was 58.5%, the lowest overall accuracy compared to all study fires (Table 2.6).

2.3.1.6 Boyer 02 fire

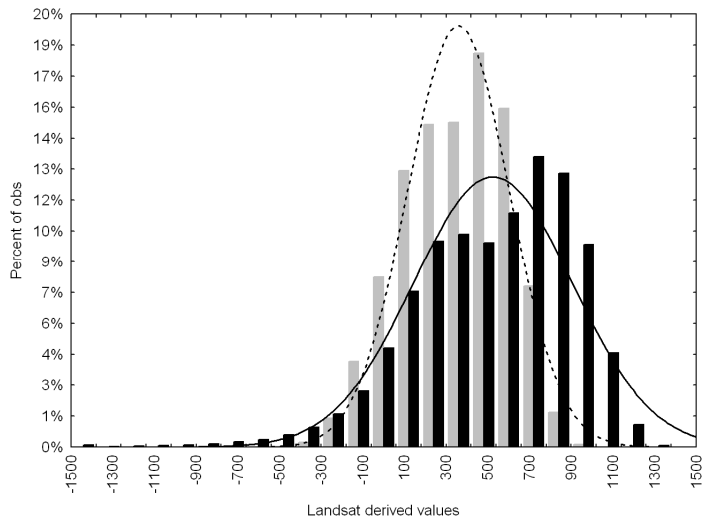
The EOSD imagery indicated that pre-fire vegetation was similar to the Boyer 01 fire, except with lower CC overall and higher spatial heterogeneity. In terms of overall ranking, the Boyer 02 fire was lowest overall compared to all fires (Table 2.3, Figure 2.3). As compared to the other study fires, Figure 2.4F indicates similar burn severity histogram as the Boyer 01 fire, although with a larger proportion in the higher severity category. The RdNBR index classified 14.4% of the fire as high, 23.6% as moderate, and 62.0% as unchanged/low. The dNBR index classified 10.2% high, 23.6% moderate, and 62.2% unchanged/low. Neither models were statistically significant for quadratic models and were therefore fitted using linear regression only. The linear dNBR model showed strong results ($R^2 = 0.72$, $SE = 0.41$, $p < 0.05$) while the RdNBR was weaker ($R^2 = 0.67$, $SE = 0.48$, $p < 0.05$) (Table 2.5, Figure 2.5F). The confusion matrix outputs give an overall accuracy of 77.1% for both indices and weaker accuracies were found in the user's high severity class for both indices, RdNBR at 50.0% and 48.6% accuracy for dNBR.

Table 2.5. dNBR and RdNBR results for individual fires from Figure 2.5 (A-F). Coefficient of determination, model relationship chosen, standard error of estimate, (p^L) p-value, (p^Q) predictor p-value for quadratic if significant, AIC values for both linear and quadratic models, and total (N) for each study fire.

	<i>Fire Name</i>	<i>R²</i>	<i>model</i>	<i>std. error of est.</i>	<i>p^L</i>	<i>p^Q</i>	<i>linear AIC</i>	<i>quad AIC</i>	<i>CBI (N)</i>
dNBR	Peace Point	0.70	linear	0.42	0.000	<i>n.s.</i>	43.82	44.31	37
	Southesk	0.81	quadratic	0.44	0.000	0.010	62.11	39.59	34
	Hoodoo	0.40	linear	0.63	0.004	<i>n.s.</i>	46.61	46.86	23
	Boyer 01	0.76	quadratic	0.35	0.000	0.044	44.49	34.27	49
	Split Peak	0.70	quadratic	0.50	0.000	0.011	95.57	87.69	53
	Boyer 02	0.72	linear	0.41	0.000	<i>n.s.</i>	57.41	43.42	38
RdNBR	Peace Point	0.72	linear	0.40	0.000	<i>n.s.</i>	44.42	43.45	41
	Southesk	0.79	quadratic	0.42	0.000	0.042	46.14	42.54	31
	Hoodoo	0.55	linear	0.54	0.000	<i>n.s.</i>	38.12	38.72	23
	Boyer 01	0.77	quadratic	0.35	0.000	0.005	57.85	42.28	50
	Split Peak	0.69	quadratic	0.52	0.000	0.012	96.24	88.64	53
	Boyer 02	0.67	linear	0.48	0.000	<i>n.s.</i>	57.76	38.28	36

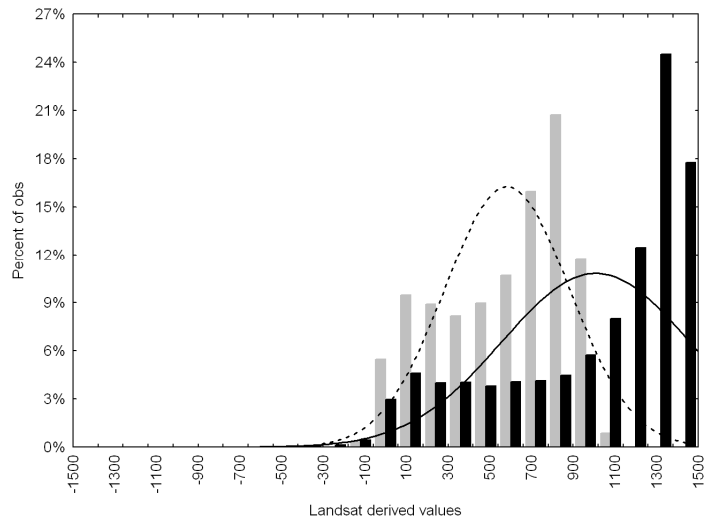
Table 2.6. Classification accuracies of the producer's, user's, and overall values along with the conditional kappa (ki), overall kappa, and the lower and upper 95% confidence intervals (CI) for the overall kappa. The results are listed from top to bottom and include the dNBR, RdNBR, EOSD vegetation type, and Hall et al. (2008) non-linear models.

Dataset	Producer's Accuracy (%)						User's Accuracy (%)							Overall Kappa	CI 95% lower	CI 95% upper
	Unchanged /Low	ki	Moderate	ki	High	ki	Unchanged /Low	ki	Moderate	ki	High	ki	Overall			
dNBR																
Overall	89.0	0.82	39.2	0.30	80.4	69.69	77.4	0.64	63.3	0.58	63.4	0.55	70.2	0.54	0.45	0.63
Rocky Mountains	75.0	0.67	51.3	0.40	88.2	0.84	69.2	0.59	60.6	0.52	81.1	0.74	70.6	0.56	0.43	0.69
western boreal	89.1	0.80	30.0	0.23	42.9	0.38	82.6	0.68	44.4	0.39	31.0	0.26	62.4	0.38	0.24	0.52
Peace	80.0	0.74	12.5	0.10	89.5	0.81	72.7	0.65	25.0	0.23	77.3	0.58	70.3	0.50	0.25	0.75
Southesk	80.0	0.77	62.5	0.56	90.5	0.78	57.1	0.51	62.5	0.56	100.0	1.00	82.4	0.69	0.46	0.92
Hoodoo	76.9	0.59	37.5	0.28	100.0	1.00	83.3	0.71	60.0	0.54	33.3	0.27	65.2	0.43	0.11	0.75
Boyer 01	77.8	0.62	59.1	0.71	0.0	0.00	84.0	0.79	72.2	0.60	0.0	0.00	69.4	0.60	0.38	0.82
Split Peak	77.8	0.70	30.4	0.20	91.7	0.89	58.3	0.43	58.3	0.52	64.7	0.55	60.4	0.41	0.22	0.61
Boyer 02	92.0	0.80	40.0	0.33	100.0	1.00	85.2	0.62	67.1	0.63	48.6	0.57	77.1	0.56	0.29	0.83
RdNBR																
Overall	90.9	0.85	28.9	0.22	69.0	0.63	76.3	0.61	47.8	0.42	58.0	0.49	65.2	0.46	0.37	0.56
Rocky Mountains	83.8	0.77	34.3	0.26	85.7	0.80	70.5	0.58	52.2	0.46	75.0	0.65	68.2	0.52	0.39	0.65
western boreal	88.7	0.80	17.1	0.12	60.9	0.56	79.7	0.64	36.8	0.33	36.8	0.29	60.3	0.37	0.23	0.50
Peace	80.0	0.75	11.1	0.09	90.9	0.82	72.7	0.66	20.0	0.18	80.0	0.61	70.7	0.50	0.26	0.74
Southesk	100.0	1.00	0.0	0.00	85.7	0.66	71.4	0.66	0.0	0.00	85.7	0.66	74.2	0.47	0.16	0.79
Hoodoo	84.6	0.71	25.0	0.18	100.0	1.00	84.6	0.83	50.0	0.45	33.3	0.27	65.2	0.42	0.09	0.74
Boyer 01	77.8	0.61	59.1	0.44	0.0	0.00	84.0	0.72	72.2	0.62	0.0	0.00	69.4	0.45	0.21	0.68
Split Peak	84.2	0.77	22.7	0.15	91.7	0.89	61.5	0.45	55.6	0.51	61.1	0.51	59.6	0.41	0.22	0.61
Boyer 02	88.0	0.69	33.3	0.27	100.0	1.00	84.6	0.83	50.0	0.45	50.0	0.47	77.1	0.45	0.13	0.76
EOSD vegetation model (dNBR)																
coniferous	89.3	0.83	36.2	0.28	70.6	0.63	77.0	0.64	52.5	0.46	63.2	0.54	67.4	0.50	0.40	0.60
broadleaf	75.0	0.69	60.0	0.36	100.0	1.00	50.0	0.38	85.7	0.77	66.7	0.62	68.8	0.49	0.11	0.86
other	90.9	0.80	72.7	0.65	33.3	0.31	100.0	1.00	66.7	0.57	25.0	0.23	80.6	0.65	0.41	0.88
EOSD vegetation model (RdNBR)																
coniferous	88.7	0.83	32.8	0.25	62.3	0.54	76.8	0.65	44.4	0.38	56.9	0.48	63.3	0.43	0.33	0.54
broadleaf	75.0	0.69	50.0	0.27	100.0	1.00	42.9	0.30	83.3	0.76	66.7	0.62	62.5	0.41	0.03	0.78
other	100.0	1.00	20.0	0.17	33.3	0.31	92.3	0.69	33.3	0.31	33.3	0.31	81.3	0.49	0.12	0.86
Hall et al. (2008) non-linear model																
western boreal	76.6	0.67	26.0	0.17	92.6	0.91	78.3	0.69	54.2	0.49	46.3	0.33	59.7	0.41	0.29	0.54
Peace	14.3	0.12	45.5	0.37	94.4	0.89	100.0	0.49	45.5	0.37	73.9	0.51	63.9	0.37	0.10	0.65
Boyer 01	83.3	0.76	11.5	0.06	83.3	0.81	71.4	0.59	60.0	0.57	20.8	0.12	46.0	0.27	0.08	0.46
Boyer 02	90.5	0.80	38.5	0.29	100.0	1.00	82.6	0.64	71.4	0.67	42.9	0.38	73.0	0.52	0.27	0.78



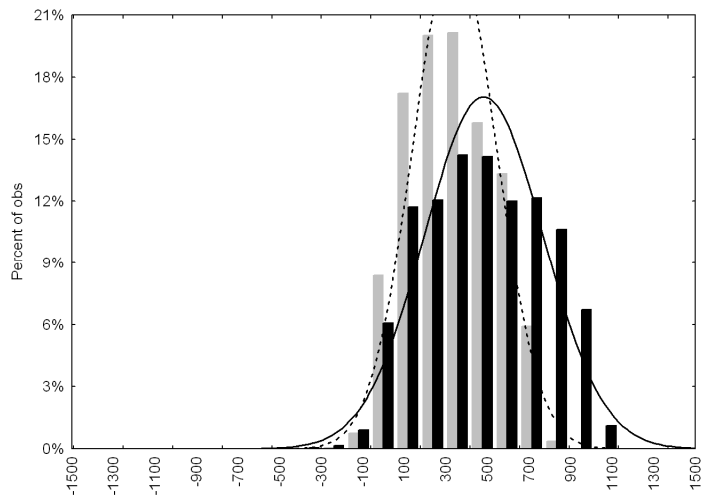
	dNBR	RdNBR
	%	%
unchanged/low	43.7	42.0
moderate	27.3	27.7
high	29.0	30.3

Figure 2.4A.



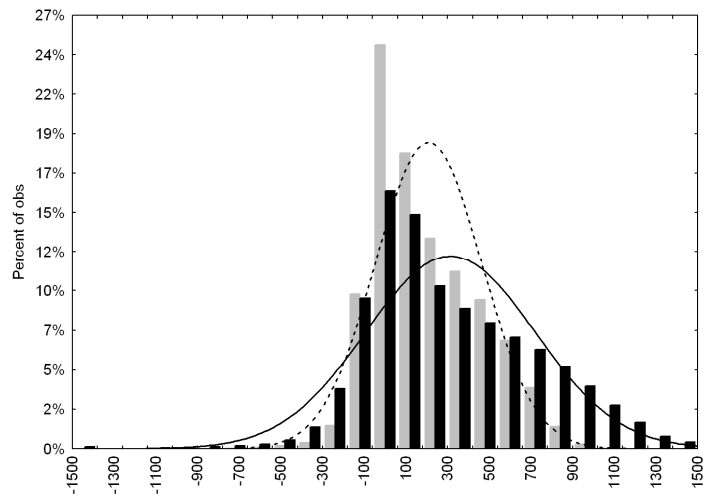
	dNBR	RdNBR
	%	%
unchanged/low	32.3	23.3
moderate	20.1	29.1
high	47.7	47.6

Figure 2.4B.



	dNBR	RdNBR
	%	%
unchanged/low	49.8	51.4
moderate	16.0	19.2
high	34.2	29.4

Figure 2.4C.



	dNBR	RdNBR
	%	%
unchanged/low	86.1	84.7
moderate	12.9	10.9
high	1.1	4.3

Figure 2.4D.

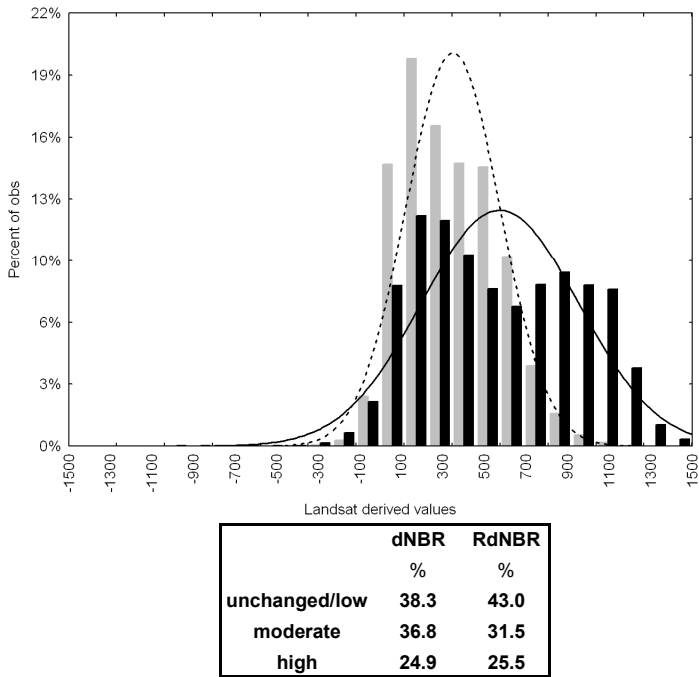


Figure 2.4E.

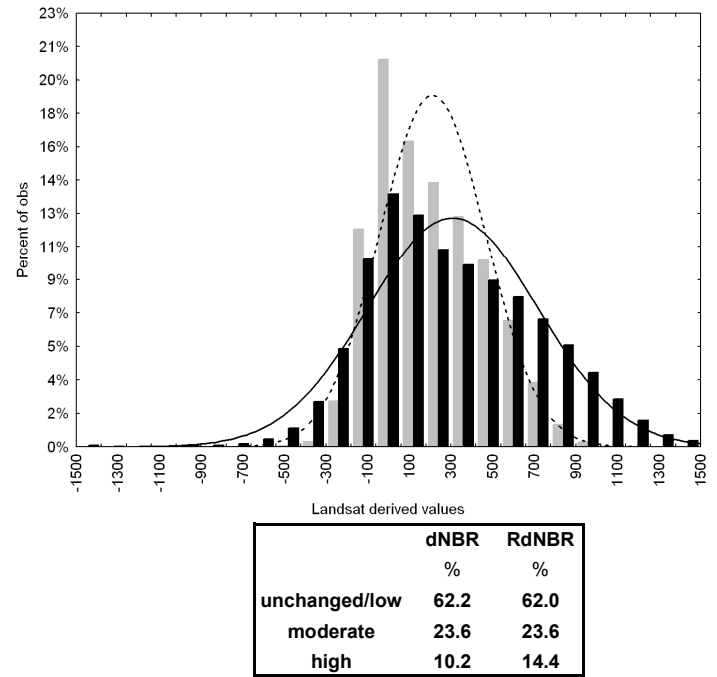


Figure 2.4F.

Figure 2.4. (A-F) Figures represent: (A) Peace Point, (B) Southesk, (C) Hoodoo, (D) Boyer 01, (E) Split Peak, and (F) Boyer 02 fires. Histograms depict the percent pixel variability for the associated remote sensing values within the initial perimeter of each fire. The gray bars represent total dNBR data and the dotted black line the normal distribution fitted function. The black histogram bars and solid black line represent the former information for the RdNBR data. The table below each graph refers to that fire's total dNBR and RdNBR burn severity class proportions extracted using each fire's regression model.

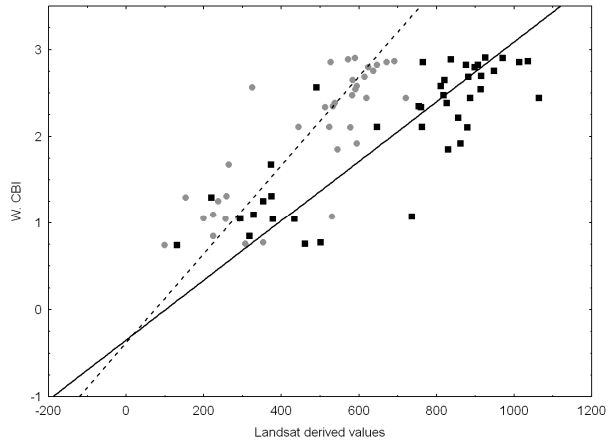


Figure 2.5A.

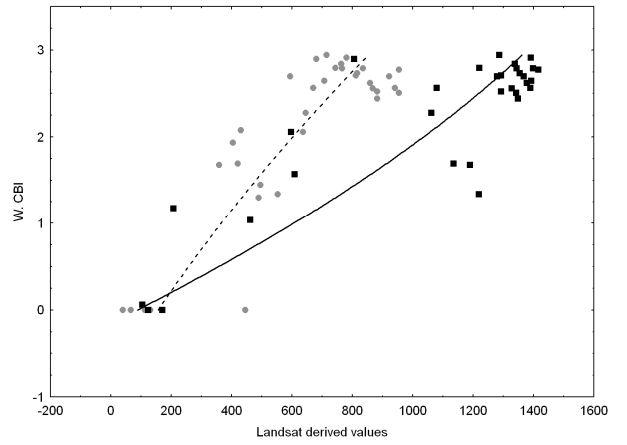


Figure 2.5B

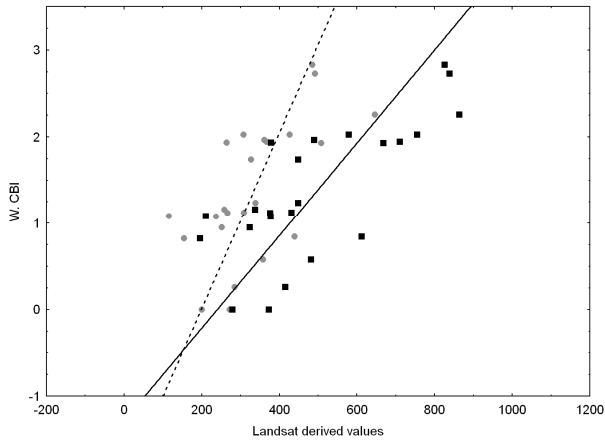


Figure 2.5C.

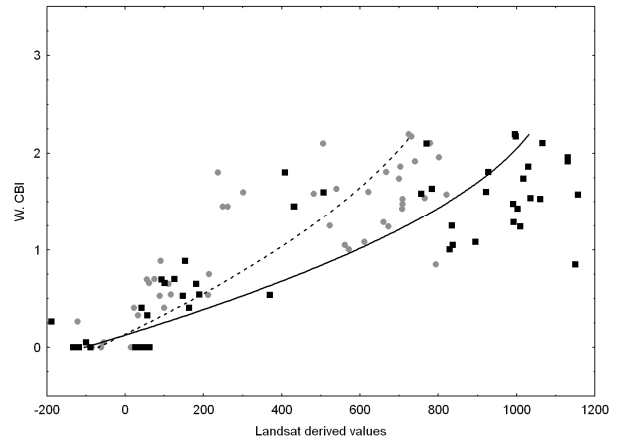


Figure 2.5D.

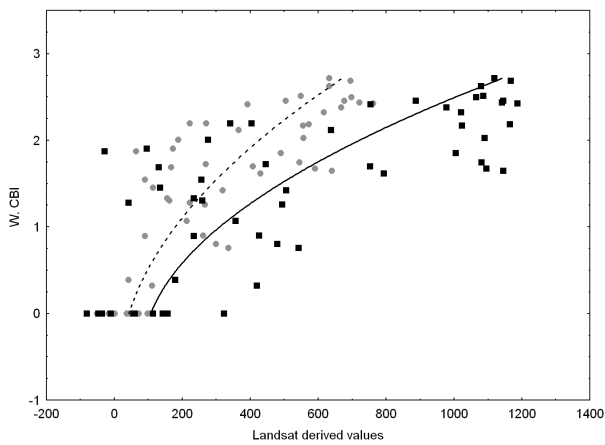


Figure 2.5E.

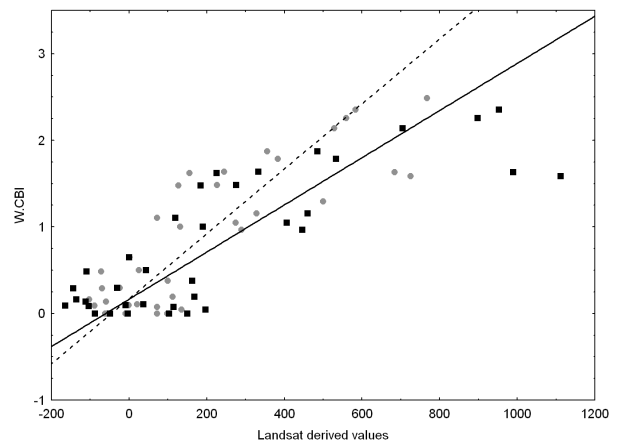


Figure 2.5F.

Figure 2.5. (A-F, above). X-axis of the scatterplot represents dNBR and RdNBR index derived values while the y-axis represents weighted CBI values. (A-F) figures represent: (A) Peace Point, (B) Southesk, (C) Hoodoo, (D) Boyer 01, (E) Split Peak, and (F) Boyer 02 fires. The gray circles represent dNBR while the black squares represent RdNBR weighted CBI correlations. The dotted black line represents the dNBR fitted regression model to weighted CBI values while the solid black line represents the RdNBR fitted regression model.

2.3.2 Results for fine scale vegetation stratification

The relationships between weighted CBI, dNBR, and the RdNBR data grouped by EOSD pre-fire vegetation are shown in Table 2.7. Weighted CBI plots occurred most often in coniferous EOSD classes, followed by ‘other vegetation’, and lastly in broadleaf. The AIC values for the RdNBR and dNBR coniferous models were lowest using quadratic models and statistically significant, the dNBR model ($R^2=0.69$, $SE=0.53$, $p<0.05$) and RdNBR ($R^2=0.71$, $SE=0.51$, $p<0.05$). The broadleaf vegetation group was well-represented by linear regression models for both dNBR ($R^2=0.69$, $SE=0.33$, $p<0.05$) and RdNBR ($R^2=0.62$, $SE=0.37$, $p<0.05$) (Table 2.7). For the ‘other vegetation’ group, the linear model was chosen for dNBR ($R^2=0.69$, $SE=0.49$, $p<0.05$) and quadratic for the RdNBR ($R^2=0.75$, $SE=0.44$, $p<0.05$) (Table 2.7). Confusion matrix results show the dNBR index having higher overall accuracies for the conifer and broadleaf groups and higher kappa values for all three groups (Table 2.6).

Table 2.7. dNBR and RdNBR EOSD vegetation type regression including coefficient of determination, model relationship chosen, standard error of estimate, (p^L) p-value, (p^Q) predictor p-value for quadratic if significant, AIC values for both linear and quadratic models, and total (N).

	<i>Vegetation</i>	<i>R²</i>	<i>model</i>	<i>std. error of est.</i>	<i>p^L</i>	<i>p^Q</i>	<i>linear AIC</i>	<i>quad AIC</i>	<i>CBI (N)</i>
dNBR	Coniferous	0.69	quadratic	0.53	0.000	0.000	341.63	296.19	183
	Broadleaf	0.69	linear	0.33	0.004	<i>n.s.</i>	14.64	14.45	16
	Other	0.69	linear	0.49	0.000	<i>n.s.</i>	61.47	47.96	36
RdNBR	Coniferous	0.71	quadratic	0.51	0.000	0.000	337.41	295.95	185
	Broadleaf	0.62	linear	0.37	0.000	<i>n.s.</i>	17.26	16.79	16
	Other	0.75	quadratic	0.44	0.000	0.028	56.11	32.02	32

2.3.3 Results for regions

When the data was stratified by geographic region (Rocky Mountain, western boreal) both indices appear to estimate burn severity equally well. AIC values suggest that a quadratic relationship was most appropriate for all four models (Figure 2.6B, 2.6C). Approximately 70.0% of the model variability was explained by using either the dNBR or RdNBR in the Rocky Mountains and in the western boreal region. The Rocky Mountain region data was estimated with similar results for dNBR ($R^2=0.69$, $SE=0.53$, $p<0.05$) and the RdNBR ($R^2=0.71$, $SE=0.51$, $p<0.05$) (Table 2.8, Figure 2.6A). Estimates were also similar for the western boreal region for dNBR ($R^2=0.70$, $SE=0.49$, $p<0.05$) and RdNBR ($R^2=0.70$, $SE=0.50$, $p<0.05$) (Table 2.8, Figure 2.6B). Confusion matrices indicate that overall dNBR model accuracies were higher than RdNBR in both regions (Table 2.6). The Rocky Mountain results denote dNBR (70.6%) and RdNBR (68.2%) accuracies while the western boreal overall accuracy was dNBR (62.4%) and RdNBR (60.3%).

2.3.4 Results for overall dataset

The best AIC relationships between the weighted CBI data and dNBR and RdNBR across all fires were quadratic models (Figure 2.6C). The RdNBR model had a slightly better fit ($R^2=0.71$, $SE=0.51$, $p<0.05$) than the dNBR ($R^2=0.69$, $SE=0.52$, $p<0.05$) (Table 2.8), with the confusion matrix indicating a better overall dataset accuracy result using dNBR (70.2%) than RdNBR (65.2%). Of the three classes, the moderate severity class produced most often the lowest user's and producer's accuracies, as indicated by the conditional kappa (κ) values (Table 2.6).

Table 2.8. dNBR and RdNBR results for regions and overall datasets from Figure 2.6 (A-C) including the coefficient of determination, model relationship chosen, standard error of estimate, (p^L) p-value, (p^Q) predictor p-value for quadratic if significant, AIC values for both linear and quadratic models, and total (N).

	<i>Fire Area</i>	<i>R²</i>	<i>model</i>	<i>std. error of est.</i>	<i>p^L</i>	<i>p^Q</i>	<i>linear AIC</i>	<i>quad AIC</i>	<i>CBI (N)</i>
dNBR	R. Mountains	0.69	quadratic	0.53	0.000	0.005	204.87	180.75	110
	western boreal	0.70	quadratic	0.49	0.000	0.000	221.29	167.44	125
	Overall	0.69	quadratic	0.52	0.000	0.000	428.13	375.06	235
RdNBR	R. Mountains	0.71	quadratic	0.51	0.000	0.003	186.28	168.81	107
	western boreal	0.70	quadratic	0.50	0.000	0.000	226.48	167.55	126
	Overall	0.71	quadratic	0.51	0.000	0.000	418.36	364.07	233

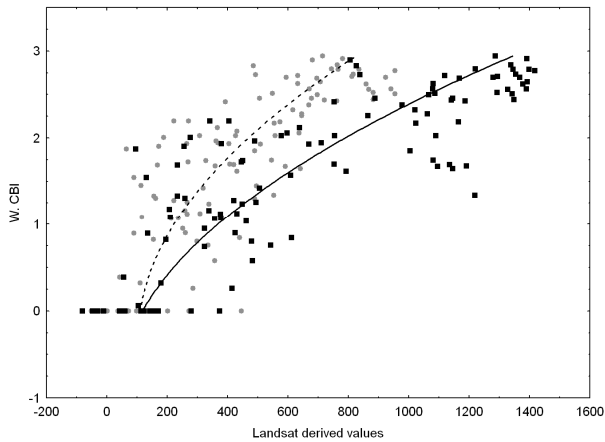


Figure 2.6A.

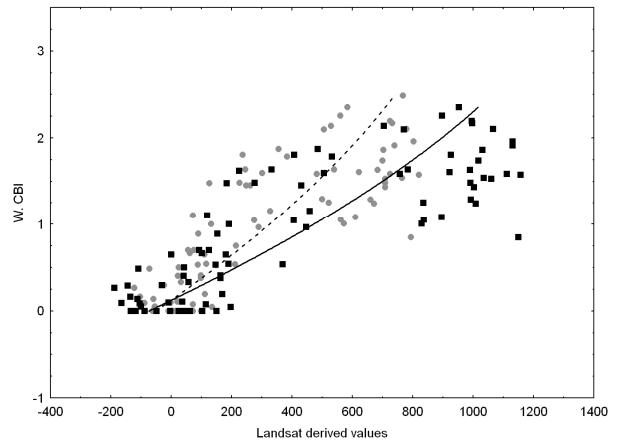


Figure 2.6B.

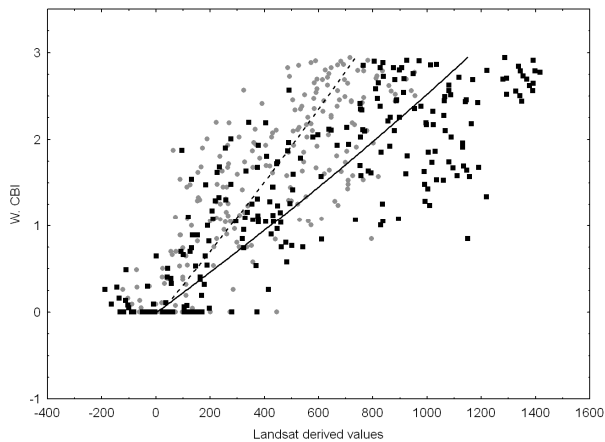


Figure 2.6C.

Figure 2.6 (A-C). X-axis of the scatterplot represents dNBR and RdNBR index derived values while the y-axis represents weighted CBI values. (A-C) figures represent: (A) Rocky Mountains (B) western boreal region, and (C) overall pooled dataset. The gray circles represent dNBR while the black squares represent RdNBR weighted CBI correlations. The dotted black line represents the dNBR fitted regression model to weighted CBI values while the solid black line represents the RdNBR fitted regression model.

2.3.5 Results for model comparison

To assess the comparability of previously developed models to our own data, the Hall et al. (2008) non-linear model was fit using linear regression and total CBI for the western boreal regional dataset and the Peace, Boyer 01, and Boyer 02 fires. The regional dataset showed moderate regression ($R^2=0.66$, $SE=0.51$, $p<0.05$), while the Peace fire the strongest ($R^2=0.68$, $SE=0.41$, $p<0.05$), and the Boyer 01 fire ($R^2=0.44$, $SE=0.51$, $p<0.05$), and the Boyer 02 fires the weakest ($R^2=0.58$, $SE=0.54$, $p<0.05$) (Table 2.9). Table 2.6 incorporates data from the Hall et al. (2008) confusion matrix, with overall accuracies lower than those found within this study. Listed respectively 59.7%, 63.9%, 46.0%, and 73.0%, they were for the western boreal region, Peace, Boyer 01, and Boyer 02 datasets. The high severity class accuracy for the user's and producer's values were higher for the western boreal region than both the dNBR and RdNBR models, respectively at 46.3% and 92.6%.

Table 2.9. Hall et al. (2008) non-linear model correlation results including coefficient of determination, model relationship chosen, standard error of estimate, (p^L) p-value, and total (N).

	<i>Hall et al. (2008)</i> <i>non-linear</i> <i>model</i>	R^2	<i>model</i>	<i>std.</i> <i>error of</i> <i>est.</i>	p^L	CBI (N)
dNBR	western boreal	0.66	linear	0.51	0.000	125
	Peace	0.68	linear	0.41	0.000	49
	Boyer 01	0.70	linear	0.44	0.000	50
	Boyer 02	0.58	linear	0.54	0.000	36

2.4 Discussion

The main objective of this study was to establish whether the RdNBR or the dNBR would be able to more accurately estimate burn severity across a range of fires in western

Canada. The dNBR method, or the absolute change of Landsat's band 4 and 7, contrasts with the RdNBR index which measures the proportional change occurring in the same bands. As an initial step, model development and statistical comparison of these two indices were applied to each fire's burn severity data. These results show similar accuracies being obtained using either the dNBR or RdNBR, with the AIC and confusion matrices indicating slightly higher accuracy for the dNBR across all study fires. The severity class with the highest accuracy across all fire, and indices, was in the unchanged/low severity class. Lower and inconsistent results occurred in the moderate and high severity categories, with the lowest accuracies in the moderate class. We can therefore infer that both indices measure similar effects of fire in our study areas.

We hypothesized that RdNBR would be a better estimator of burn severity in landscapes that consisted of lower CC and those that also had higher spatial heterogeneity. Our results indicate that this was not the case, with no significant improvement in model accuracy using the RdNBR in the Split Peak, Boyer 02, and Boyer 01 fires. The results show that the dNBR is capable of estimating more accurately weighted CBI points in our vegetation groupings as indicated by the overall accuracy and kappa statistic results (Table 2.6). Miller and Thode (2007) stated that in homogeneous vegetation, the dNBR and RdNBR indices would produce similar estimated accuracies. This may indicate that, in this study, the landscapes are relatively homogeneous with moderate to dense canopy vegetation. Moreover, the study areas of both Miller and Thode (2007) and Miller et al. (2009) were located in conifer dominated vegetation types in California, whose pre-fire vegetation and fire severity may not correspond well to our sites. Since previous research

has established the higher accuracy of RdNBR in the high severity class, our study's negative results may be due to the smaller number of high severity burns examined. However, we did not see an improvement in the classification of high severity classes using RdNBR nor in our sparsely vegetated and heterogeneous burned areas.

Overall, the regional models developed in this study were as accurate and showed similar results to other researchers in the western boreal and the Northern Rocky Mountains regions. In the western boreal region of Canada, Wulder et al. (2009) found that RdNBR was unable to estimate changes in forest structure or post-fire effects any better than dNBR or NBR. They concluded that their results supported key findings by Hudak et al. (2007), that RdNBR is not more appropriate than dNBR or NBR for broad-scale burn severity assessment. Hall et al. (2008) found higher overall correlations between dNBR and CBI data than our own. When classification accuracy was conducted on the Hall et al.'s (2008) dNBR non-linear model, results showed a higher overall kappa statistic and smaller confidence intervals than our dNBR and RdNBR derived models (Table 2.6). Within the Rocky Mountain region, Zhu et al.'s (2006) Northern Rocky Mountain study found burn severity correlations of $R^2=0.72$ for dNBR while the RdNBR had a lower correlation value of $R^2=0.69$. These results correspond well to our regional results with the Rocky Mountain regional dataset having an $R^2=0.69$ for dNBR and an $R^2=0.71$ for RdNBR. These results largely indicate the value in formulating regional models for burn severity monitoring within western Canada.

Numerous researchers have determined that the highest correlations for dNBR and RdNBR exhibit nonlinear relationships to CBI data (van Wagendonk et al., 2004; Zhu et al., 2006; Miller & Thode, 2007; Miller et al., 2009). These studies have attributed this non-linearity to Landsat's SWIR reflectance saturation at CBI values above ~2.0-2.5, and the simultaneous NIR decrease consistent with increasing burn severity (Chuvieco et al., 2006). In respect to this finding, a majority of our derived dNBR and RdNBR models were non-linear across the fire, vegetation type, regional, and overall dataset scales. Both index models at the regional and overall levels had a majority of the lowest user's, producer's, and conditional kappa values for the moderate severity class. Miller et al. (2009) found that in the majority of cases, the moderate class also had the lowest classification accuracies. These increased errors in the moderate class are most likely due to the difficulty of a passive sensor to observe the more complex fire effects that can be recorded during a CBI assessment (De Santis & Chuvieco, 2007). For the high severity classes at the regional and overall model scales, the lowest confusion matrix accuracies existed in the western boreal region. The western boreal models for dNBR and RdNBR had conditional kappa values for the user's accuracies at 0.26 and 0.29 respectively. Difficulty in correctly classifying moderate and high severity classes in the boreal was also recorded by Murphy et al. (2008) who found dNBR had limited ability to discern moderate and high severity classes. There are three likely compounding reasons for this in the western boreal. The first is the aforementioned SWIR saturation effect which has been cited by numerous authors in boreal burn severity mapping. The second factor, as discussed by Hoy et al. (2008), is that in Alaskan boreal sites the highest correlations with remote sensing dNBR were with canopy vegetation consumption and much lower in the

organic layer. This underlying evidence poses greater significance in the boreal region where the role of high severity fire and its effects to the substrate layer is of high ecological importance (Kasischke et al., 2008). Lastly, error in the high severity classes for the western boreal models is likely related to solar elevation influences which make temporal comparisons of fires across multiple years more difficult (Verbyla et al., 2008). Although image acquisition was chosen with these factors in mind, ideal imagery is limited in this region due to cloud cover and phenology. Therefore, developing burn severity models across multiple years and months can inherently have lower accuracies than southern latitudes.

Our original hypothesis stated that the RdNBR algorithm may provide a higher level of accuracy in a pooled dataset of all fires that occurred in those landscapes of lower CC and higher heterogeneity. Nevertheless, our results indicate that this hypothesis cannot be accepted for our western Canadian fire study for the following reasons. The overall dataset accuracy indicated a higher overall classification accuracy for dNBR than RdNBR and those fires with the lowest CC and heterogeneity ranking showed no improvement with RdNBR or differences in burn severity class proportions when using RdNBR.

Moreover, the RdNBR did not appear to outperform the dNBR index at the individual, vegetative, and regional dataset levels. In the case of the individual and vegetation dataset levels, we acknowledge the limitation of our smaller sample sizes which cannot be interpreted with as high a degree of certainty as the regional or overall models.

In addition to these findings the Canadian fires studied offered some additional insights. First, the ecological process of blow down after fire was a considerable factor in both

regions of our western Canadian sites, especially in the western boreal region. For this region, blow down is common in high burn severity black spruce stands (Kasischke et al., 2008), where there has been a very large consumption of the organic layer causing serious root damage and making trees more prone to blow down. This impacts overall correlations with remote sensing values as Landsat can over or under estimate higher burn severities than weighted CBI estimates at these sites. The second issue in CBI assessment was the issue of pre-fire stress or mortality caused by mountain pine beetle and its detection by the CBI assessor. This effect was seen in the Rocky Mountain region most notably at the Split Peak fire where there was a high degree of pre-fire mortality due to mountain pine beetle. At this fire it was much easier to detect those trees that were dead approximately two years or more pre-fire (gray attack), as these lodgepole pine snags had visible and deep charring characteristics. Those that had died during the two years immediately before the fire (red attack) were very difficult to detect as living or dead pre-fire. CBI assessments in these types of stands can then likely overestimate burn severity as the assessor cannot measure the level of mountain pine beetle disturbance without a pre-fire evaluation. It is important then for remote sensing researchers to be aware of pre-fire disturbances such as insect attack so that they can be able to choose appropriate imagery. The third issue was the interpretation of RdNBR values when pre-fire vegetation was extremely low or nearly lacking. These areas were located in the subalpine zone where little shrub and virtually no vegetation could survive, or in areas with large proportions of soil and rock. This observation was seen especially in the high elevation plots of the Southesk and Split Peak fires, where CBI plots were in areas without trees and were primarily composed of small shrub, grass, and exposed soil or

rock cover. These areas indicate good correlations when using dNBR, however, CBI tended to be overestimated when employing the RdNBR index. Miller and Thode (2007) observed a similar but accurate measurement of burn severity in sagebrush vegetation with RdNBR values greater than 2000.

2.5 Conclusions

Parks Canada is mandated to monitor fire disturbance across large expanses of land and time. Such an agency would be best served to use the most comprehensive and applicable remote sensing methods available. Reducing the number of models to a broad regional level is a desirable goal for agencies tasked to manage large geographic areas. The results presented within this paper indicate this goal of future regional model development may be possible. However, it is the discretion of the regional park managers to determine the level of accuracy required to utilize such models as routine monitoring tools. Research projects, and application development needs to occur to resolve the influences of pre-fire vegetation type and heterogeneity on remote sensing accuracy measurements and ecological processes within these ecosystems. This research, along with field data from a greater number of field plots within Canada, will help to improve the local, regional, and national-scale monitoring and its interpretation.

2.6 References

- Agee, J.K. (1993). *Fire Ecology of Pacific Northwest Forests*. Island Press, Covelo, CA.
- Avery, T.E., & Berlin, G.L. (1992). *Fundamentals of remote sensing and airphoto interpretation.*: Prentice e. 472 pp. (Upper Saddle River, N.J)
- Box, G.E.P., & Jenkins, G.M. (1970). *Time series analysis: forecasting and control*. Holden-Day (London, UK)
- Chander, G., & Markham, B. (2003). Revised Landsat-5 TM Radiometric Calibration Procedures and Postcalibration Dynamic Ranges. *IEEE Transactions on Geoscience and Remote Sensing*, 41, 11.
- Chavez, P.S. Jr. (1989). Radiometric calibration of Landsat Thematic Mapper multispectral images. *Photogrammetric Engineering and Remote Sensing*, 9, 1285-1294.
- Chuvieco, E., Riano, D., Danson, F.M., & Martin, M.P. (2006). Use of radiative transfer model to simulate the post-fire spectral response to burn severity. *Journal of Geophysical Research*, 111, G04S09.
- Cocke, E.A., Fulé, P.Z., & Crouse, J.E. (2005). Comparison of burn severity assessments using the Differenced Normalized Burn Ratio and ground data. *International Journal of Wildland Fire*, 14, 189-198.
- De Santis, A., & Chuvieco, E. (2007). Burn severity estimation from remotely sensed data: Performance of simulation versus empirical models. *Remote Sensing of Environment*, 108, 422-435.
- Ecological Stratification Working Group (1996). *A national ecological framework for Canada* (125 pp). Ottawa/ Hull: Agriculture and Agri-Food Canada, Research Branch, Centre for Land and Biological Resources Research and Environment Canada, State of Environment Directorate. Available online: <http://sis.agr.gc.ca/cansis/publications/ecostrat/intro.html>.
- Elvidge, C.D. (1990). Visible and near infrared reflectance characteristics of dry plant materials. *International journal of Remote Sensing*, 11(10), 1775-1795.
- Fischer, W. C., & B. D. Clayton. (1983). *Fire ecology of Montana forest habitat types east of the continental divide*. General Technical Report INT-GTR-141, USDA Forest Service Intermountain Forest and Range Experiment Station, Ogden, UT.
- Flannigan, M.D., Bergeron, Y., Engelmark, O., & Wotton, B.M. (1998). Future wildfire in circumboreal forests in relation to global warming. *Journal of Vegetation Science*, 9, 469-475.

- Flannigan, M.D., Logan, K.A., Amiro, B.D., Skinner, W.R., & Stocks B.J. (2005). Future area burned in Canada. *Climatic Change*, 72, 1-16.
- French, N.H.F., Kasischke, E.S., Hall, R.J., Murphy, K.A., Verbyla, D.L., Hoy, E.E., & Allen, J.L. (2008). Using Landsat data to assess fire and burn severity in North American boreal forest region: an overview and summary of results. *International Journal of Wildland Fire*, 17, 443-462.
- Fule, P.Z., Crouse, J.E., Heinlein, T.A., Moore, M.M., Covington, W.W., & Verkamp, G. (2003). Mixed-severity fire regime in a high-elevation forest of Grand Canyon, Arizona, USA. *Landscape Ecology*, 18, 465-485.
- Hall, R.J., Freeburn, J.T., Groot, W.J.dG., Pritchard, J.M., Lynham, T.J., & Landry, R. (2008). Remote sensing of burn severity: experience from western Canada boreal fires. *International Journal of Wildland Fire*, 17, 476-489.
- Hardy, CC, Ottmar, R.D., Peterson, J.L., Core, J.E., & Seamon, P. (2001). 'Smoke management guide for prescribed and wildland fire.' USDA National Wildfire Coordination Group Publication PMS 420-2. (Ogden, UT)
- Hilborn, R., & Mangel, M. (1997). *The ecological detective: confronting models with data*. Princeton University Press. (Princeton, New Jersey)
- Hoy, E.E., French, N.H.F., Turetsky, M.R., Trigg, S.N., & Kasischke, E.S. (2008). Evaluating the potential of Landsat TM/ETM+ imagery for assessing fire severity in Alaskan black spruce forests. *International Journal of Wildland Fire*, 17, 500-514.
- Hudak, A.T., Morgan, P., Bobbitt, M.J., Smith, A.M.S., Lewis, S.A., Lentile, L.B. et al. (2007). The relationship of multispectral satellite imagery to immediate fire effects. *Fire Ecology*, 3, 64-90.
- Jain, T., Pilliod, D., & Graham, R. (2004). Tongue-tied. *Wildfire*, 4, 22-26.
- Johnson, E.A. (1992). *Fire and Vegetation Dynamics: Studies from the North American Boreal Forest*. (New York, Cambridge University Press)
- Kasischke, E.S., Turetsky, M.R., Ottmar, R.D., French, N.H.F., Hoy, E.H., & Kane E.S. (2008). Evaluation of the composite burn index for assessing fire severity in Alaskan black spruce forests. *International Journal of Wildland Fire*, 17, 515-526.
- Key, C.H., & Benson, N.C. (2005). Landscape assessment – sampling and analysis methods. Pp. LA1-LA51 in D. Lutes (ed.), *FIREMON: Fire effects and Inventory*

- Monitoring System*. Gen Tech Rep. RMRS-GTR-164-CD, USDA Forest Service, Rocky Mountain Research Station, Ogden, UT.
- Key, C.H., & Benson, N.C. (2006). Landscape Assessment: ground measure of severity, the Composite burn index, and remote sensing of severity, the Normalized Burn Index. In *'FIREMON: Fire Effects Monitoring and Inventory System'*. (Eds DC Lutes, RE Keane, JF Caratti, CH Key, NC Benson, S Sutherland, LJ Gangi) USDA Forest Service, Rocky Mountain Research Station, General Technical Report RMRS-GTR-164-CD: LA1-51. (Ogden, UT).
- Klenner, W., Walton, R., Arsenault, A., & Kremsater, L. (2008). Dry forests in the Southern Interior of British Columbia: Historic disturbances and implications for restoration and management. *Forest Ecology and Management*, 256, 1711-1722.
- Lentile, L.B., Holden, Z.A., Smith, A.M.S., Falkowski, M.J., Hudak, A.T., Morgan, P., Lewis, S.A., Gessler, P.E., & Benson, N.C. (2006). Remote sensing techniques to assess active fire characteristics and post-fire effects. *International Journal of Wildland Fire*, 15, 319-345.
- McGarigal, K., & Marks, B. J. (1995). *FRAGSTATS: Spatial pattern analysis program for quantifying landscape structure*. Corvallis, OR: USDA Forest Service General Technical Report PNW-GTR-351.
- Miller, C., & Urban, D.L. (1999). Interactions between forest heterogeneity and surface fire regimes in the southern Sierra Nevada. *Canadian Journal of Forest Research*, 29, 202-212.
- Miller, J.D., & Thode, A.E. (2007). Quantifying burn severity in a heterogeneous landscape a relative version of the delta Normalized Burn Ratio (dNBR). *Remote Sensing of Environment*, 109, 66-80.
- Miller, J.D., Knapp, E.E., Key, C.H., Skinner, C.N., Isbell, C.J., Creasy, R.M., & Sherlock, J.W. (2009). Calibration and validation of the relative differenced Normalized Burn Ratio (RdNBR) to three measures of fire severity in the Sierra Nevada and Klamath Mountains, California, USA. *Remote Sensing of the Environment*, 113, 645-656.
- Murphy, K. A., Reynolds, J.H., & Koltun, J.M. (2008). Evaluating the ability of the differenced Normalized Burn Ratio (dNBR) to predict ecologically significant burn severity in Alaskan boreal forests. *International Journal of Wildland Fire*, 17, 490-499.
- NASA, (1998). *Landsat 7 Science Data Users Handbook. Greenbelt, Maryland: Landsat Project Science Office, NASA's Goddard Space Flight Center.*
<http://landsathandbook.gsfc.nasa.gov/handbook.html>

- Perrakis, D. & Zell, D. (2008). *Remote assessment of burn severity: A pilot study in landscape monitoring*. Western and Northern Service Centre and National Fire Centre, Parks Canada Agency.
- Rommel, T.K., Csillag, F., Mitchell, S., & Wulder, M.A. (2005). Integration of forest inventory and satellite imagery: a Canadian status assessment and research issues. *Forest Ecology and Management*, 207, 405-428.
- Schwarz, A. G., & Wein, R. W. (1997). Threatened dry grasslands in the continental boreal forests of Wood Buffalo National Park. *Canadian Journal of Botany*, 75, 1363-1370.
- Schroeder, T.A., Cohen, W.B., Song, C., Canty, M.J., & Yang, Z. (2006). Radiometric correction of multi-temporal Landsat data for characterization of early successional forest patterns in western Oregon. *Remote Sensing of Environment*, 103, 16-26.
- Song, C., Woodcock, C.E., Seto, K.C., Lenney, M.P., & Macomber, S.A. (2001). Classification and Change Detection Using Landsat TM data: When and How to Correct Atmospheric Effects? *Remote Sensing of Environment*, 75, 230-244.
- Stocks, B.J., Mason, J.A., Todd, J.B., Bosch, E.M., Wotton, B.M., Amiro, B.D., Flannigan, M.D., Hirsch, K.G., Logan, K.A., Martell, D.L. & Skinner, W.R. (2003). Large forest fires in Canada, 1959-1997. *Journal of Geophysical Research*, 108, (5-1) to (5-12).
- Tande, G. F. (1979). Fire history and vegetation pattern of coniferous forest in Jasper national park, Alberta. *Canadian Journal of Botany*, 57, 1912-1930.
- Turner, M.G., Romme, W.H., & Tinker, D.B. (2003). Surprises and Lessons from the 1988 Yellowstone Fires. *Frontiers in Ecology and the Environment*, Vol 1, No 7, pp. 351-358,
- Tymstra, C., Flannigan, M.D., Armitage, O.B., & Logan, K. (2007). Impact of climate change on area burned in Alberta's boreal forest. *International Journal of Wildland Fire*, 16, 153-160.
- USGS (United States Geologic Survey). GLOVIS website: <http://glovis.usgs.gov/>
Accessed between October, 2008 and February, 2009
- Van Wagtendonk, J.W., Root, R.R., & Key, C.H. (2004). Comparison of AVIRIS and Landsat ETM+ detection capabilities for burn severity. *Remote Sensing of Environment*, 92, 397-408.

- Verbyla, D.L., Kasischke, E.S., & Hoy, E.E. (2008). Seasonal and topographic effects on estimating fire severity from Landsat TM/ETM+ data. *International Journal of Wildland Fire*, 17, 527-534.
- Wotton, B.M., & Flannigan, M.D. (1993). Length of fire season in a changing climate. *The Forestry Chronicle*, 69, 187-192.
- Wulder, M. A., White, J. C., Magnussen, S., & McDonald, S. (2007). Validation of a large area land cover product using purpose-acquired airborne video. *Remote Sensing of Environment*, 106, 480-491.
- Wulder, M.A., White, J.C., Cranny, M., Hall, R.J., Luther, J.E., Beaudoin, A., Goodenough, D.G., & Dechka J.A. (2008a). Monitoring Canada's forests. Part 1: Completion of the EOSD land cover project. *Canadian Journal of Remote Sensing*, 34, 549-548.
- Wulder, M.A., White, J.C., Han, T., Coops, N.C., Cardille, J.A., Holland, T., & Grills, D. (2008b). Monitoring Canada's forests. Part 2: National forest fragmentation and pattern. *Canadian Journal of Remote Sensing*, 34, 563-584.
- Wulder, M.A., White, J.C., Alvarez, F., Han, T., Rogan, J., & Hawkes, B. (2009) Characterizing boreal forest wildfire with multi-temporal Landsat and LIDAR data. *Remote Sensing of Environment*, 113, 1540-1555.
- Zhu, Z., Key, C. H., Ohlen, D., & Benson, N.C. (2006). Evaluate Sensitivities of Burn-Severity Mapping Algorithms for Different Ecosystems and Fire Histories in the United States. Available at http://jfsp.nifc.gov/projects/01-1-4-12/01-1-4-12_Final_Report.pdf [Accessed October 2008]

3 THE TRANSFERABILITY OF A dNBR DERIVED MODEL TO PREDICT BURN SEVERITY ACROSS TEN WILDLAND FIRES IN WESTERN CANADA³

3.1 Introduction

The historical and ecological importance of wildland fire as a disturbance agent to Canadian ecosystems is well established (Larsen, 1997; Stocks et al., 2003; Van Wagner et al., 2006). Wildland fire is a dynamic process that impacts ecosystems in various ways, by its injury and mortality of vegetative plant species, its rate of re-establishment of re-sprouting species (Lyon & Stickney, 1976; Ryan & Noste, 1985; Morgan & Neuenschwander, 1988; DeBano et al., 1998) and can alter ecosystem composition, functioning, and plant encroachment (Lentile et al., 2006). The Boreal Plains ecozone of Canada (Ecological Stratification Working Group, 1996), is a geographic area that has been shaped and influenced dramatically by the effects of wildland fire (Weir et al., 2000; Burton et al., 2008). Similarly, the Montane Cordillera ecozone of Canada has a long history of fire occurrence with forests in a constant state of renewal by random periodic fire (Van Wagner et al., 2006). Over the past four decades there has been an increase in the area burned in Canada compared to historical times (Podur et al., 2002; Gillett et al., 2004). This increase is projected to continue as climate change models forecast an increase in length of fire seasons coupled with larger and more intense fires (Balshi et al., 2009; Flannigan et al., 2009). Canadian land management agencies, therefore, have

³ A similar version of this chapter has been submitted for publication. Soverel, N.O., Coops, N.C., Perrakis, D.B., Daniels, L., & Gergel, S. In review. The transferability of a dNBR derived model to predict burn severity across ten wildland fires in Western Canada.

become increasingly interested in studying the effects of fire. Parks Canada is a land management agency that is responsible for the accurate monitoring, inventory, and management of federal parks in Canada. Particularly in western Canada, where both wildland and prescribed fires burn an average of 75,000-80,000 hectares per year (Parks Canada, unpublished files), the study and monitoring of fire disturbance has become a major objective.

Fire scientists define three important variables that can be used to measure wildland fire: fire intensity, fire severity, and burn severity; however, the main focus here is burn severity. Lentile et al. (2006) define burn severity as the degree to which an ecosystem has changed owing to fire. In our field studies, burn severity was characterized using the Composite Burn Index (Key & Benson, 2006), which incorporates a range of post-fire physical aspects that are measured using the visual evidence remaining a year after fire occurrence. The method provides little information regarding pre-fire condition; however, it provides a consistent, repeatable, and interpretable method that is ideal for broad scale comparisons.

In contrast, remote sensing has two major advantages over traditional methods of field assessment for determining burn severity: cost effectiveness and seamless global coverage in extremely remote areas. Landsat imagery, in particular is well suited to study burn severity due to its ability to acquire data in the spectral bands sensitive to map fire disturbance, its global coverage, and availability as it is freely downloadable in Canada (USGS, 2009). The extensive history of Landsat burn severity mapping includes applying

the normalized ratio of this sensor's near infrared and shortwave infrared bands.

Originally, Lopez-Garcia and Caselles (1991) developed a method to detect burn severity using a Normalized Burn Ratio (hereafter as NBR). A more recent adaptation of the NBR is the differenced NBR (dNBR), a post-fire NBR subtracted from a pre-fire NBR (Key & Benson, 2006), which is useful for ecological research and for land management projects across various ecosystems (Key & Benson, 2006; van Wagtenonk, 2004; Cocke et al., 2005; Zhu et al., 2006). In a literature review, French et al. (2008) compiled results from 41 worldwide NBR approach-based studies and calculated an overall 73% classification accuracy with an overall range between 50% to 90%. Investigations using remote sensing to predict burn severity across Canada are more limited. Hall et al. (2008) used Landsat derived dNBR to predict Composite Burn Index data for four western boreal fires and found strong correlations using a single non-linear model ($R^2=0.82$). Using Light Detection and Ranging (LIDAR) data and Landsat TM imagery, Wulder et al. (2009) correlated dNBR to the LIDAR calculated absolute change canopy closure with an R^2 of 0.71. Hall et al. (2008) found that burn severity was influenced by pre-fire land cover type while Wulder et al. (2009) found that denser pre-fire stands had stronger relationships to both post-fire NBR and dNBR.

One criticism of the Landsat derived dNBR approach is that linear models developed for individual fires cannot be easily extrapolated to different ecosystems due to their individual specific land cover types and conditions (De Santis & Chuvieco, 2007). However, based on the results from Hall et al. (2008), the potential to create broad scale models that have the potential to cover large geographic areas appears to be feasible.

Therefore, our first objective was to assess the relative transferability and accuracy of an overall dNBR model, as well as make a comparison of the overall model to one stratified by land cover groups and the two ecozones across a range of fires in western Canada. Based on their findings, Wulder et al. (2009) and Hall et al. (2008) concluded that pre-fire specific land cover and vegetation condition data may have the capacity to improve burn severity predictions. Therefore, developing models that incorporate alternative sources of pre- and post-fire remote sensing data appears to be a promising endeavour. The second objective of this paper was to assess the benefit of incorporating pre- and post-fire data into the standard Composite Burn Index and dNBR approaches. To accomplish this objective we chose to employ the tasselled cap index transformation (Crist & Cicone, 1984) as a means of extracting additional Landsat pre- and post-fire data. The tasselled cap index (hereafter referred to as TCI) was chosen because it has been found previously by other authors to be responsive to the impacts of fire (Kushla & Ripple, 1998; Rogan & Yool, 2001).

3.2 Methods

3.2.1 Study area

This research focuses on a total of ten fire events that occurred between 2005 and 2008 in the Montane Cordillera and Boreal Plains ecozones. These fires occurred in the following five national parks in western Canada: Glacier, Jasper, Kootenay, Wood Buffalo, and Yoho (Figure 3.1). The Montane Cordillera ecozone encompassed six fires, two of which took place in Kootenay National Park (Split Peak and Mitchell Ridge), the Hoodoo Creek fire occurred in Yoho National Park, the Southesk and Henry House II fires both occurred in Jasper National Park, and the Grizzly Ridge fire in Glacier National

Park. Six of these total ten fires were classified as wildfire events and four were prescribed fires, these include: the Hoodoo Creek, Mitchell Ridge, Split Peak and Henry House II. The Boreal Plains ecozone contained Wood Buffalo National Park and its environs where four fires occurred: the Boyer 01, Boyer 02, Peace Point, and Sandy. Burned areas ranged from 203 to 106,772 hectares, with the largest events taking place in this ecozone (Table 3.1).

Table 3.1. Includes the date of ignition, study ecozones: Boreal Plains (BP) or Montane Cordillera (MC). Park name, fire size (ha), elevation (m), type of wildland fire: wildfire (W) or prescribed fire (P), and dominant tree species present within the associated park.

Date of Ignition	Study Region	Province	Fire Name	Park Name	Fire Size (ha)	Elevation (m)	W/P	Dominant Tree Species
05/27/07	BP	AB	Boyer 01	Wood Buffalo	75,963	250-350	W	Black spruce, Tamarack, Jack pine, trembling aspen, White spruce, and shrub/grass cover matrix
05/27/07	BP	AB	Boyer 02	Wood Buffalo	106,772	250-350	W	Black spruce, Tamarack, Jack pine, trembling aspen, White spruce, and shrub/grass cover matrix
08/03/08	MC	BC	Grizzly Ridge	Glacier	203	1,500-2,150	W	Subalpine fir, Engelmann spruce, Western white pine, Lodgepole pine, Douglas fir
05/19/08	MC	AB	Henry House II	Jasper	330	1,020	P	Lodgepole pine, Douglas fir, Englemann spruce
05/28/05	MC	BC	Hoodoo Creek	Yoho	1,525	1,400-2,100	P	Lodgepole pine, Douglas fir, Engelmann spruce, and Trembling aspen
05/30/08	MC	BC	Mitchell Ridge	Kootenay	1,574	1,100-1,500	P	Lodgepole pine, Trembling aspen, Englemann spruce, Douglas fir
06/07/05	BP	AB	Peace Point	Wood Buffalo	12,432	250-300	W	White spruce, Black spruce, Jack pine, Trembling aspen
07/19/08	BP	NT	Sandy	near Wood Buffalo	41,194	250-300	W	Jack pine, Trembling aspen, Black Spruce, White spruce, shrub/grass cover matrix
07/21/06	MC	AB	Southesk	Jasper	1,168	1,500-2,100	W	Lodgepole pine, Engelmann spruce
09/15/07	MC	BC	Split Peak	Kootenay	560	1,350-2,000	P	Lodgepole pine, Douglas fir, Englemann spruce



Figure 3.1. (1) Montane Cordillera and (2) Boreal Plains ecozones with the national parks of Canada in darkest gray.

3.2.1.1 Montane Cordillera

One of the most defining features of the Montane Cordillera (hereafter referred to as MC) ecozone is its rugged and highly variable topography. The six MC fires had elevations that ranged between 1020 to 2000 m and encompassed two forest ecosystem types. The first type, the montane forest, generally ranges between 1,000 and 1,650 m, and the

second, or subalpine forest, ranges between 1,500 and 2,300 m. The dominant tree species in the montane forests of our study area consist of lodgepole pine (*Pinus contorta*), Engelmann spruce (*Picea engelmannii*), Douglas-fir (*Pseudotsuga manziesii*), and trembling aspen (*Populus tremuloides*). The fire regime of the montane ecosystem is characterized by more frequent, less severe, and more heterogeneous fire effects than the subalpine zone (Klenner et al. 2008; Fischer & Clayton 1983; Tande 1979). The subalpine zone consists mainly of lodgepole pine, Engelmann spruce, subalpine fir (*Abies lasiocarpa*), which is typified by infrequent fire events that are generally intense and result in stand-replacing disturbances (Agee, 1993). The Hoodoo Creek, Southesk, Split Peak, Mitchell Ridge, and Henry House II occurred in the area situated on the eastern and western slopes of the Rocky Mountains. In contrast, the Grizzly Ridge fire took place in the Columbia Mountains range; a Biogeoclimatic Ecosystem Classification (BEC) zone (Meidinger & Pojar, 1991) that is west of the Rocky Mountains called the Interior Cedar-Hemlock forest, known for its higher annual rainfall than the parks to the east.

3.2.1.2 Boreal Plains

The Boreal Plains ecozone (hereafter referred to as BP) has less relief than the MC ecozone with fires that ranged between 200 to 300 m in elevation. Forests are typically complex, dominated by the following tree species: Jack pine (*Pinus banksiana*), black spruce (*Picea mariana*), trembling aspen (*Populus tremuloides*), white spruce (*Picea glauca*), and tamarack (*Larix laricina*). These forests are also intermixed with grassland, shrubland, and wetland vegetation types. Fire regimes in this ecozone tend to be dominated by very large, infrequent, and stand-replacing events with a range of fire

cycles depending on local climate and tree species (Johnson 1992; Turner et al. 2003). Wood Buffalo National park alone recorded 1011 fires between 1950 and 1989, with 8% of fires exceeding 10 km² in size, accounting for 99% of the total burned area (Larsen, 1997).

3.2.2 Prescribed fire and pre-fire disturbance

Each of the four prescribed fires achieved their general burn objectives. The Hoodoo Creek prescribed burn was implemented to create fuelbreaks, to reintroduce mixed severity fire, and as a mitigation tool against the mountain pine beetle (*Dendroctonus ponderosae*). The Henry House II prescribed burn was implemented to maintain a thinned overstory and herbaceous understory while providing a fuelbreak for the nearby town of Jasper. Two objectives of the Split Peak and Mitchell Ridge fires were to return wildfire to a fire-suppressed landscape and to mitigate the progress of the mountain pine beetle. In order to research the long-term impacts of mountain pine beetle presence on fire behaviour at the Mitchell Ridge fire, park managers used a unique fire ignition technique which consisted of helitorch ignition from the valley floor left alone to run up to treeline (Kubian, 2009). Due to the varying weather and fuel moisture conditions at the time of burning, post-fire characteristics were unique among fires. In the case of the Mitchell Ridge, Hoodoo Creek, and Split Peak fires, higher intensity fire behaviour resulted in greater canopy mortality while the Henry House II achieved relatively lower canopy mortality.

3.2.3 Imagery and dNBR pre-processing

Landsat imagery was the main source of remote sensing data utilized in this study. Images were chosen based on minimal cloud content, ignition site, phenology, and anniversary date (Table 3.2). Pre-fire imagery was chosen in the year of fire, if available, or else an optimum image selected in previous years. Thirty-two images were analyzed which were orthorectified to Universal Transverse Mercator (UTM) Zone 11 or 12 North, Datum WGS-84 with a root mean squared error of less than 15 m with at least 30 ground control points. After orthorectification, the raw digital numbers of each image were converted to reflectance values using standard approaches (detailed in NASA 1998; Chander & Markham, 2003). Since multiple images from differing geographic and time periods were used, an atmospheric correction was undertaken using the dark body subtraction approach (Chavez, 1989).

Table 3.2. Landsat imagery used to calculate the initial and extended assessment images for use within the study. The table includes the IA/EA assessment, fire name, park name, path/row, pre-fire image date acquisition (if either TM or ETM+), and post-fire image acquisition date (if either TM or ETM+).

IA/EA	Fire name	Park Name	Path/Row	Pre-fire image date (TM/ETM+)	Post-fire image date (TM/ETM+)
EA	Boyer 01	Wood Buffalo	44_18/19	06/29/2005-TM	08/08/2008-TM
IA			44_18/19	06/29/2005-TM	07/21/2007-TM
EA	Boyer 02	Wood Buffalo	44_18/19	06/29/2005-TM	08/08/2008-TM
IA			44_18/19	06/29/2005-TM	07/21/2007-TM
EA	Grizzly Ridge	Glacier	44_24	08/19/2006-TM	08/27/2009-TM
IA			44_24	09/14/2001-ETM+	08/24/2008-TM
EA	Henry House II	Jasper	45_23	07/12/2007-TM	08/02/2009-TM
IA			45_23	09/14/2007-TM	09/16/2008-TM
EA	Hoodoo Creek	Yoho	44_24	08/24/1999-ETM+	09/04/2006-TM-
IA			44_24	08/24/1999-ETM+	07/31/2005-TM-
EA	Mitchell Ridge	Kootenay	43_25	07/14/2007-TM	07/03/2009-TM
IA			43_24	06/17/2003-TM	06/30/2008-TM
EA	Peace Point	Wood Buffalo	44_19	09/14/2001-ETM+	09/04/2006-TM-
IA			44_19	09/14/2001-ETM+	08/28/2005-TM-
EA	Sandy	near Wood Buffalo	45_18	06/23/2006-TM	07/17/2009-TM
IA			46_18	09/2/2006-TM	08/22/2008-TM
EA	Southesk	Jasper	44_23	07/10/2003-TM-	07/05/2007-TM-
IA			44_23	08/23/2002-ETM+	08/26/2006-TM-
EA	Split Peak	Kootenay	43_24	08/15/2007-TM-	08/17/2008-TM-
IA			43_24	08/15/2007-TM-	09/16/2007-TM-

The spectral bands from Landsat TM and ETM+ imagery that were used to create the NBR and dNBR images were bands 4 (B4) and 7 (B7). Landsat's band 4 records spectral data in the near infrared (NIR) between the wavelengths 0.76 μ m – 0.90 μ m, while band 7 records in the shortwave infrared (SWIR) between 2.08 μ m – 2.35 μ m. Band 4 provides information about living plant cell structure and chlorophyll content (Rogan & Yool, 2001; Miller & Thode, 2007), while band 7 is sensitive to water content in plants and substrate, the content of lignin in non-photosynthetic vegetation, and hydrous minerals

such as clay, mica, and some oxide and sulphates (Elvidge, 1990; Avery & Berlin, 1992).

These bands are used as follows in the equations:

$$(1) \text{NBR} = (B4 - B7) / (B4 + B7)$$

$$(2) \text{dNBR} = (\text{NBR}_{\text{prefire}} - \text{NBR}_{\text{postfire}})$$

The relative dNBR, or RdNBR (Miller & Thode, 2007), was not calculated because it has not been found to better estimate burn severity over dNBR outside the southwestern United States and parts of California (Hudak et al., 2007; Wulder et al., 2009). Two dNBR analyses are commonly identified, the first being the initial assessment (IA) which is a dNBR image consisting of a post-fire image from the same year as the fire ignition (Key & Benson, 2006). The second, or the extended assessment (EA), uses a post-fire image from the year following the fire (Key & Benson, 2006). For this study, the IA image was used for extraction of suitable field plots and for fire perimeter delineation, while the EA represented the primary source of burn severity data within the analysis. Calibration of the EA dNBR images was undertaken using the methods of Zhu et al. (2006), whereby the mean of an unburned area outside the fire perimeter of a dNBR image is calculated and subtracted from the dNBR image. To extract the fire perimeter, a dNBR IA image was created and a density slice classification was performed; this effectively classified all dNBR values greater than 100 as burned pixels (Key & Benson, 2006). To extract values from the EA dNBR image, a weighted average of the pixels surrounding the field plots were calculated (Cocke et al., 2005). Those plots that had one or more surrounding pixels exceeding a 250 dNBR value were removed as these were considered geo-referenced errors.

3.2.4 Field data and collection

Burn severity herein is defined as the combined ecological and physical impacts from fire as it relates to its pre-fire environment (Key & Benson, 2006; Lentile et al., 2006; Hall et al., 2008). Ground based burn severity data was measured by using the Composite Burn Index (hereafter as CBI), following the methods of Key and Benson (2006). The CBI is a continuous index between 0.0 and 3.0 that effectively measures the impact of fire one year following the event, with 0.0 representing an unchanged condition and 3.0 representing the maximum impact from fire. To calculate the CBI value for each plot in the field, the CBI datasheet was utilized (Key & Benson, 2006) which divides a 30 meter circular plot into five vertical strata: substrate, herbaceous, shrub and small tree, intermediate tree, and big tree layers. CBI burn severity values are measured by using some of the following characteristics: litter and duff consumption, soil and rock percent cover change, herbaceous plant mortality and re-colonization, shrub and small tree foliage altered, overstory tree mortality, char height, and percentage torched or scorched.

Before conducting the CBI assessments, we produced the IA image, identified homogenous patches of 3 x 3 pixels, and then randomly sampled points from the class breaks outlined by Key and Benson (2006). We used these pre-determined class breaks since no other thresholds had been quantified prior to this analysis. As a means of avoiding additional georeferencing errors, plots that arose near the fire edge (<45 m) or were within 90 m of a class boundary were removed from further analysis. At each CBI plot a GPS location was recorded at plot centre, photographs taken, and the CBI data was recorded. Additional information regarding each stratum's percent pre-fire cover was

recorded, along with dominant plant species and other notable characteristics. CBI points were differentially corrected to improve their geographic accuracy. To combine all strata into one CBI plot value, a weighted CBI value was calculated based on the estimated pre-fire percent cover of each stratum. The weight of the ‘big tree’ stratum was doubled to roughly account for the biomass and additional importance of overstory trees. A histogram of total CBI values used within this study is displayed in Figure 3.2, while the means for both overstory and understory CBI values per fire are displayed in Figure 3.3. To reduce bias error, two primary researchers recorded CBI data throughout the four year study.

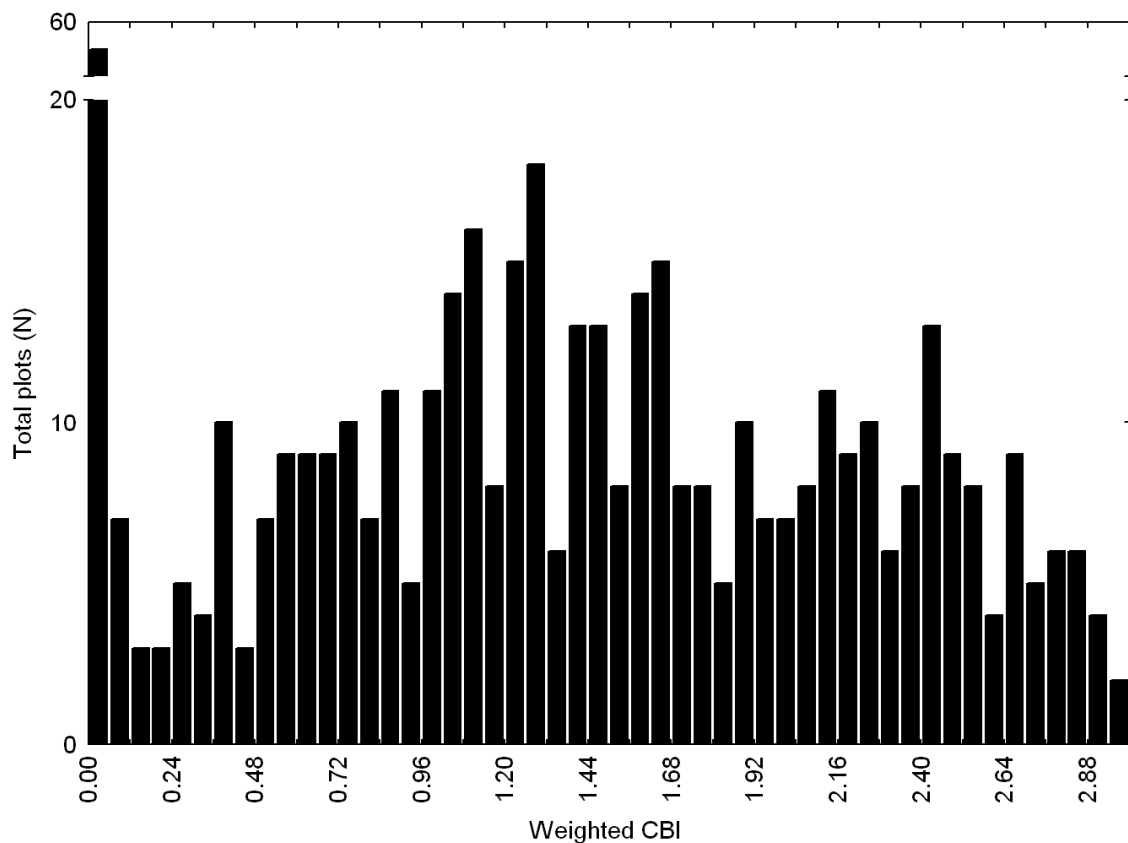


Figure 3.2. A histogram showing the total CBI plots used within this study.

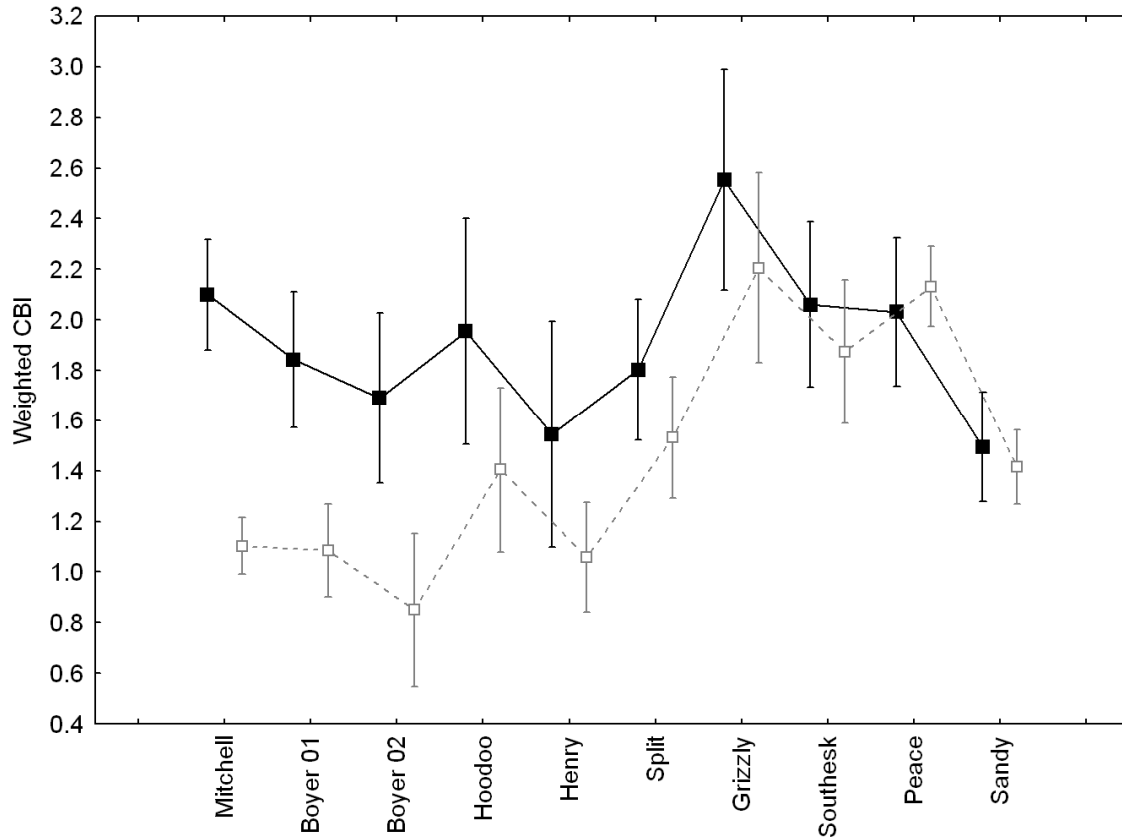


Figure 3.3. The graph depicts the mean overstory CBI values in black and the mean understory values in gray for each fire. The fires are ranked in order of highest difference in mean overstory and understory values to the lowest.

3.2.5 Land cover analysis

In order to classify field plots by pre-fire land cover, the Earth Observation for Sustainable Development of Forests Lands Cover 2000 (hereafter referred to as EOSD) was utilized. This dataset covers all of the forested land area of Canada and was derived from circa 2000 Landsat imagery, providing 23 classes with a spatial resolution of 25 m (Wulder et al., 2008a). Studies have shown that EOSD classifies vegetation with about 80% accuracy overall, with greater accuracy for the more dominant forest classes (Wulder et al., 2007; Wulder et al., 2008b). To reduce the number of EOSD classes for

model development, we grouped the EOSD classes into five land cover groups: non-forest, dense-coniferous, open-coniferous, sparse-coniferous, and broadleaf forests (Table 3.3). Table 3.4 shows the percentage of land cover groups for each of the fire’s CBI plots.

Table 3.3. The five EOSD land cover groups used to build each land cover model including: non-forest, coniferous-dense, coniferous-open, coniferous-sparse, and broadleaf.

	Non-forest	Coniferous-dense	Coniferous-open	Coniferous-sparse	Broadleaf
EOSD Classes	Shrub-Tall	Coniferous-dense	Coniferous-open	Coniferous-sparse	Broadleaf-dense
	Shrub-Low				Broadleaf-open
	Wetland-Treed				Mixed Wood-dense
	Wetland-Shrub				Mixed Wood-open
	Wetland-Herb				Mixed Wood-sparse
	Herb				

Table 3.4. Percentage of CBI plots per fire associated with the EOSD land cover classes.

EOSD Class (%)	Boyer 01	Boyer 02	Grizzly Ridge	Henry House II	Hoodoo Creek	Mitchell Ridge	Peace Point	Sandy	Southesk	Split Peak
Shadow						1.0				
Shrub-Tall				4.8					20.5	
Shrub-Low			5.0		4.3			13.1		
Wetland-Treed								4.0		
Wetland-Shrub	30.0	23.7			4.3					
Wetland-Herb				14.3						
Herb					4.3				6.0	
Coniferous-dense	64.0	52.6		81.0	13.0	2.0	100.0		73.5	
Coniferous-open	6.0	2.6	75.0		69.6	86.1		31.3		85.0
Coniferous-sparse			20.0		4.3			44.4		
Broadleaf-dense		18.4								
Broadleaf-open						10.9				15.0
Mixed Wood-dense		2.6								
Mixed Wood-open								4.0		
Mixed Wood-sparse								3.0		
Total (%)	100.0	100.0	100.0	100.0	100.0	100.0	100.0	100.0	100.0	100.0

3.2.6 Tasselled cap index

We used the three TCI indices which have also been utilized in other studies to characterize vegetation pre- and post-fire and is a linear combination of Landsat bands

and includes three indices: brightness, greenness and wetness. Tasseled cap brightness is responsive to the physical processes responsible for total reflectance (Crist & Cicone, 1984) and has been used in forest disturbance studies to relate spectral reflectance values to substrate conditions such as soil exposure, dryness and increased reflectance (Chuvieco & Congleton, 1988; Rogan & Yool, 2001; Kuzera et al., 2005). Greenness, on the other hand, has been found to be highly correlated to total vegetative cover (Kuzera et al., 2005) and has been used as an indicator of photosynthetic processes and plant/leaf structure post-fire (Rogan & Yool, 2001). Tasseled cap wetness has been found to be responsive to the water content and structure of the forest in closed canopy stands (Cohen et al., 1995) and to have strong relationships to forest changes caused by insects, fire, or harvesting (Wulder, 2004; Jin & Sader, 2005). To transform Landsat imagery to the TCI of brightness, greenness, and wetness, the calculations of Crist and Cicone (1984) were used. The TCI transformation was applied to the two EA images per fire and the TCI values were extracted at the CBI locations.

3.2.7 Analysis approach

As part of objective one, we assessed the transferability of the dNBR derived models while using a cross validation “leave-one-out” approach. Cross validation approaches are appropriate for datasets that cover a range of conditions and multiple years (Snee, 1977). Cross validation iterations involved the *learning sample*, or the dataset that we used to build each model, which was each fire’s CBI points subtracted from the total ten-fire dataset. The *test sample*, which in this case was each fire, was used to test the accuracy of the learning sample model. The dataset was cross validated in two manners: first, the overall dataset was analyzed without stratification and secondly, the dataset was stratified

by its pre-fire land cover group and ecozone. The three model cross validation iterations were fitted to the CBI data using linear, quadratic, or cubic regression models, and evaluated by choosing the best model based on the lowest value of the Akaike Information Criterion (AIC) (Box & Jenkins, 1970).

Objective two was conducted in order to evaluate the relative improvement of using the multiple TCI pre- and post-fire predictor variables. Using the same overall model as above, we utilized the addition of pre- and post-fire TCI in cross validation and forward stepwise multiple regression. In addition to regression, we tested differences between the pre- and post-fire TCI values using two statistical analyses. The first was a one-way Analysis of variance (ANOVA) followed by a post-hoc Scheffé test. This was conducted to determine if significant variation existed among fires in the pre- and post-fire TCI means. The second was a Levene's t-test which was conducted to test for the homogeneity of variances between the pre- and post-fire TCI values. Statistical significance for the ANOVA and the t-test were determined at the $p < 0.05$ level.

3.3 Results

3.3.1 Comparison of overall, land cover, and stratification results

To calculate the cross validation statistics, each fire's CBI data points were removed so that the learning sample model could be built and then assessed for its prediction strength (Table 3.5). The overall model analysis used no stratification and showed most accurate correlation for the Grizzly Ridge fire ($R^2=0.89$) while the Hoodoo Creek ($R^2=0.40$) and Mitchell Ridge fires ($R^2=0.50$) were found to be the poorest (Table 3.6). The land cover stratification results indicate that the Grizzly Ridge fire was predicted the most accurately ($R^2=0.89$) (Table 3.6) with land cover pre-fire vegetation classified as either open-

coniferous, sparse-coniferous, or non-forest (Table 3.5). The lowest accuracies were found at the Hoodoo Creek ($R^2=0.33$) and Sandy fires ($R^2=0.40$) (Table 3.6). The ecozone stratification of the CBI plots resulted in 252 CBI plots being classified as MC and the remaining 224 as BP (Table 3.5). Results show a similar trend to the land cover stratification, with the Grizzly Ridge fire being predicted the most accurately ($R^2=0.89$) and the Hoodoo Creek and Mitchell Ridge fires remained weak ($R^2=0.39$ and $R^2=0.52$, respectively) (Table 3.6). Overall, fires occurring in the MC ecozone had greater variation in accuracy (R^2 between 0.39 and 0.89) when compared to the BP ecozone, which had more consistent predictions across its fires (R^2 between 0.69 and 0.74). Comparing the overall results to the land cover and ecozone stratifications from Table 3.6, it is apparent that the analyses compute very similar accuracies. Some exceptions were apparent, for example the land cover models for the Sandy fire had very low correlation ($R^2=0.40$), and the overall model predicted CBI values for the Southesk fire more poorly than the land cover and ecozone stratifications ($R^2=0.63$ versus $R^2=0.77$ and $R^2=0.76$, respectively).

Table 3.5. Cross validation table that includes the three groups used for analysis within the study along and the associated total N.

Overall	(N)	Land cover	(N)	Ecozone	(N)
<i>Boyer 01</i>	50	<i>non-forest</i>	58	<i>Montane Cordillera</i>	252
<i>Boyer 02</i>	38	<i>coniferous-dense</i>	136	<i>Boreal Plains</i>	224
<i>Grizzly Ridge</i>	20	<i>coniferous-open</i>	198		
<i>Henry House II</i>	21	<i>coniferous-sparse</i>	49		
<i>Hoodoo Creek</i>	23	<i>broadleaf</i>	34		
<i>Mitchell Ridge</i>	101				
<i>Peace Point</i>	37				
<i>Sandy</i>	99				
<i>Southesk</i>	34				
<i>Split Peak</i>	53				
Total	476	Total	475	Total	476

Table 3.6. The first three columns of the table include the overall, land cover, and ecozone groups for model analysis. The rows represent the associated cross validation derived coefficient of determination (R^2) for each fire.

Fire Name	Overall model R^2	Land cover model R^2	Ecozone model R^2
<i>Boyer 01</i>	0.74	0.70	0.72
<i>Boyer 02</i>	0.74	0.76	0.74
<i>Grizzly Ridge</i>	0.89	0.89	0.89
<i>Henry House II</i>	0.80	0.79	0.80
<i>Hoodoo Creek</i>	0.40	0.33	0.39
<i>Mitchell Ridge</i>	0.50	0.51	0.52
<i>Peace Point</i>	0.69	0.70	0.69
<i>Sandy</i>	0.77	0.40	0.74
<i>Southesk</i>	0.63	0.77	0.76
<i>Split Peak</i>	0.68	0.71	0.69

3.3.2 TCI results

The TCI provides detailed information on pre- and post-fire conditions and were interpreted as such: brightness the degree of soil and substrate exposure, greenness the overall vegetation biomass content or density, and wetness the moisture content of both vegetation and soil attributes. There was no significant difference across fires in pre-fire

brightness (Figure 3.4). The analysis of pre-fire greenness showed significant differences between fires, however an ANOVA for pre-fire greenness mean values showed significant differences, with the Boyer 02 and Mitchell Ridge fires having higher means overall and the Southesk the lowest (Figure 3.5). Overall, pre-fire wetness was highest for the Peace and Hoodoo Creek fires and lowest for the Southesk and Sandy fires (Figure 3.6). It was apparent that the pre-fire TCI data taken from the Split Peak fire was unreasonably high based on a comparison to all other fire events; this was believed to be due to atmospheric scattering, a factor well known to affect vegetation indices (Kaufman & Sendra, 1988; Qi et al., 1991). To mitigate errors from this fire, we decided to remove it from only the TCI analysis portion of the study.

Post-fire mean brightness was significantly higher for the Hoodoo Creek and Southesk fires, and lowest for the Peace Point and Boyer fires (Figure 3.4). Post-fire greenness was highest overall for the Boyer 02 fire with the Grizzly Ridge and Southesk the lowest (Figure 3.5). The moisture index results showed that the highest mean values were from the Henry House II fire while the lowest were respectively the Southesk and Grizzly Ridge fires (Figure 3.6).

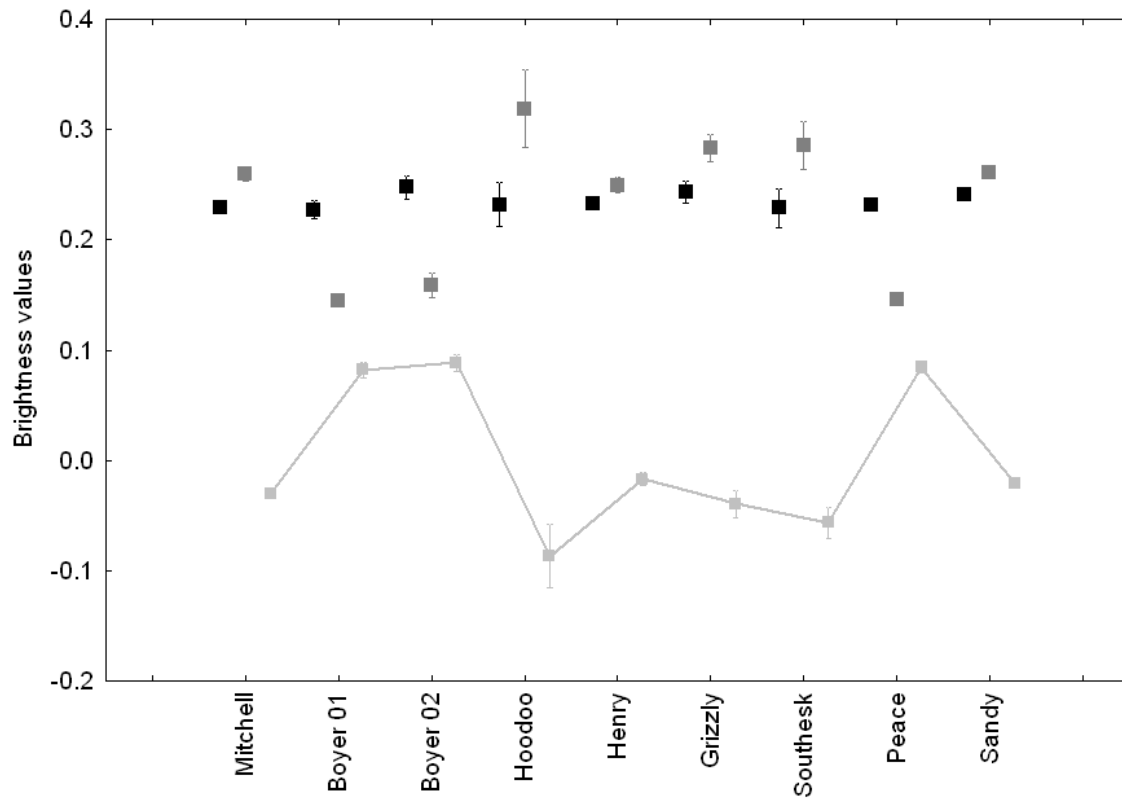


Figure 3.4. Box and whisker plots for TCI brightness values for the pre-fire (black), post-fire (dark gray), and the differenced (light gray and connected line). The whisker represents the mean plus and minus the standard deviation and the box represents the mean plus or minus the standard error.

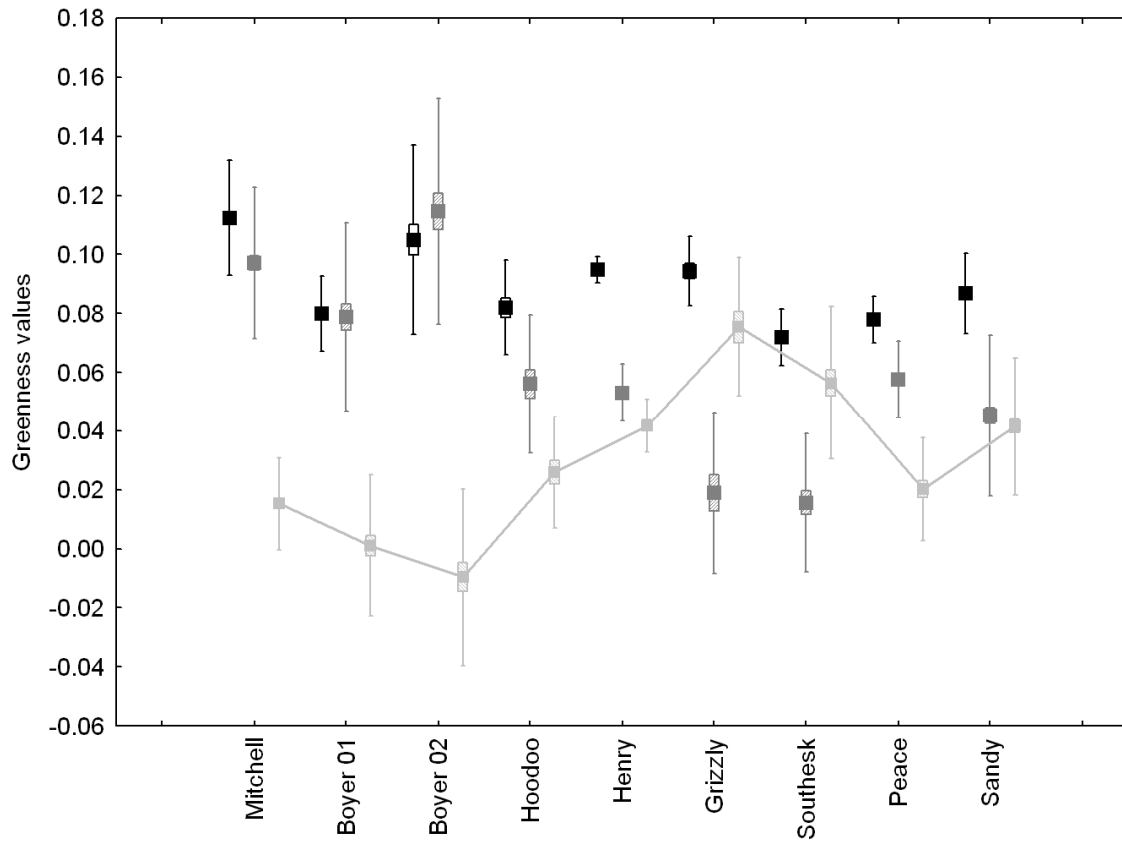


Figure 3.5. Box and whisker plots for TCI greenness values for the pre-fire (black), post-fire (dark gray), and the differenced (light gray and connected line). The whisker represents the mean plus and minus the standard deviation and the box represents the mean plus or minus the standard error.

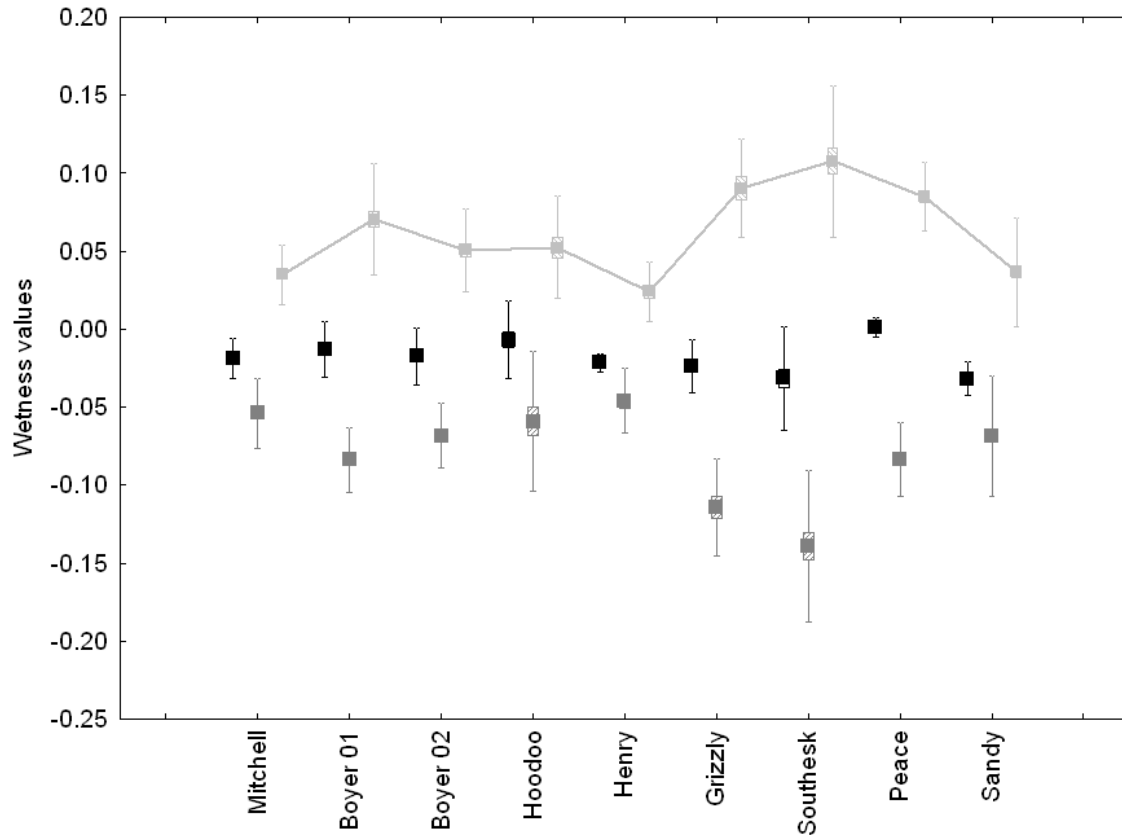


Figure 3.6. Box and whisker plots for TCI wetness values for the pre-fire (black), post-fire (dark gray), and the differenced (light gray and connected line). The whisker represents the mean plus and minus the standard deviation and the box represents the mean plus or minus the standard error.

To assess differences in the variability of pre- and post-fire TCI values, the Levene's test showed that all fires, excluding the Boyer 02 and Grizzly Ridge fires, had increased post-fire spectral variability for at least one of the three indices, with the greenness and wetness TCI having the greatest increases in variability.

3.3.3 TCI multiple regression results

Overall, the Grizzly fire had the highest correlation in multiple regression between pre- and post-fire TCI, (pre- $R^2=0.92$, post- $R^2=0.94$) while the Hoodoo Creek (pre- $R^2=0.61$, post- $R^2=0.57$) and Mitchell Ridge fires (pre- $R^2=0.62$, post- $R^2=0.66$) were the least well

predicted (Table 3.7). Of the pre-fire variables, TCI wetness showed the most commonly significant variable with five of the ten fires indicating statistical significance. The results for the post-fire TCI wetness were not as consistent, with each fire indicating its own unique significance. It appears that both the pre- and post-fire TCI achieved similar multiple regression results. In order to test the improvement of using the pre- and post-fire TCI, we calculated the pre- and post-fire TCI percent difference in explained variability ($\% \Delta$) for each fire (Table 3.7). This was a simple subtraction of the overall cross validation R^2 results per fire (Table 3.6) from the R^2 TCI results in Table 3.7. Excluding results from the Hoodoo Creek, Mitchell Ridge, and Southesk fires, the TCI percent difference in explained variability ($\% \Delta$) across the fires was in the general range of a few percent points (Table 3.7). More significant improvements were seen for the Hoodoo Creek, Mitchell Ridge, and Southesk fires using either pre- or post-fire TCI values, and always when using pre-fire wetness. Of the various TCI covariates for these three fires, pre- and post-fire wetness were the most consistently significant.

Table 3.7. Results for pre- and post-fire TCI coefficient of determination values (R^2) derived from cross validation and forward stepwise multiple regression. The brightness (B), greenness (G), and wetness (W) are included if significant ($p < 0.05$). The fifth and sixth columns represent the % change ($\% \Delta$) from the overall model variance when using pre- and post-fire TCI in multiple regression.

<i>Fire Name</i>	<i>pre-fire R^2</i>	<i>TCI</i>	<i>post-fire R^2</i>	<i>TCI</i>	<i>pre-fire $\% \Delta$</i>	<i>post-fire $\% \Delta$</i>
<i>Boyer 01</i>	0.74	B, G	0.75	B,G,W	0.01	0.01
<i>Boyer 02</i>	0.81	G	0.80	G	0.06	0.06
<i>Grizzly Ridge</i>	0.92	W	0.94	B	0.03	0.05
<i>Henry House II</i>	0.80	none	0.80	none	0.00	0.00
<i>Hoodoo Creek</i>	0.61	W	0.57	W	0.21	0.17
<i>Mitchell Ridge</i>	0.62	W	0.66	G, W	0.12	0.16
<i>Peace Point</i>	0.71	none	0.70	none	0.01	0.01
<i>Sandy</i>	0.81	W	0.77	none	0.04	0.00
<i>Southesk</i>	0.85	W	0.90	B	0.23	0.27

3.4 Discussion

3.4.1 Ecological insights into pre- and post- fire condition

The pre- and post-fire conditions measured using TCI highlight three key findings: the contrast in post-fire ecozone brightness values, the effect of season of burn on TCI greenness values, and the overall increase in heterogeneity across all fires' TCI. All MC fires showed an increase in brightness regardless of season of burn, whereas three of the four BP fires exhibited significant post-fire brightness decreases. This post-fire variation in soil reflectance is likely due to the generally deeper levels of organic content found in the BP which insulates the substrate layer from soil exposure (Ryan, 2002). The greenness results suggest a strong relationship to season of burn, with higher post-fire reflectance for those events occurring earlier in the season (Figure 3.5). For example, the spring season timing of the Hoodoo Creek and Mitchell Ridge fires had higher duff moisture conditions than the mid-summer Grizzly Ridge and Southesk wildfires, subsequently causing higher post-fire green up. In general, we found that the TCI

greenness and wetness reflectance values closely resemble those taken from CBI measurements (Figure 3.3) a result that is not surprising as the CBI is heavily weighted to vegetation (Miller & Thode, 2007). The third finding of the TCI analysis indicated that an increase in spectral heterogeneity occurred across all fires, with a statistically significant increase across 60% of all TCI that was independent of land cover or ecozone. The significance of this finding supports earlier research that fire imparts heterogeneity across a majority of landscapes regardless of the pre-fire environment (Turner et al., 2003).

3.4.2 Decoupled burn severity characteristics

Across the overall, land cover, and ecozone analyses, the Hoodoo Creek and Mitchell Ridge fires were the most often poorly estimated. The likely reason for this weak result is the high incidence of these fires' CBI plots in a decoupled moderate severity class (Figure 3.7). This decoupling effect was likely caused by high soil moisture levels during their springtime burning (Halofsky & Hibbs, 2009) in addition to the high intensity fire in the canopy that caused increased canopy mortality. This decoupling is not truly captured in a weighted averaged CBI assessment, and more importantly, correlating dNBR with these CBI values becomes much more difficult due to the competing responses of the forest strata (Figure 3.8). These more complex interactions were also reported to be the cause of low accuracies in the moderate severity class by Miller et al. (2009).



Figure 3.7. Photos of two CBI plots taken from the Mitchell Ridge (left) and the Hoodoo Creek (right) fires. These photos depict the decoupled burn severity characteristics with high canopy mortality in the canopy and the lower severity in the understory.

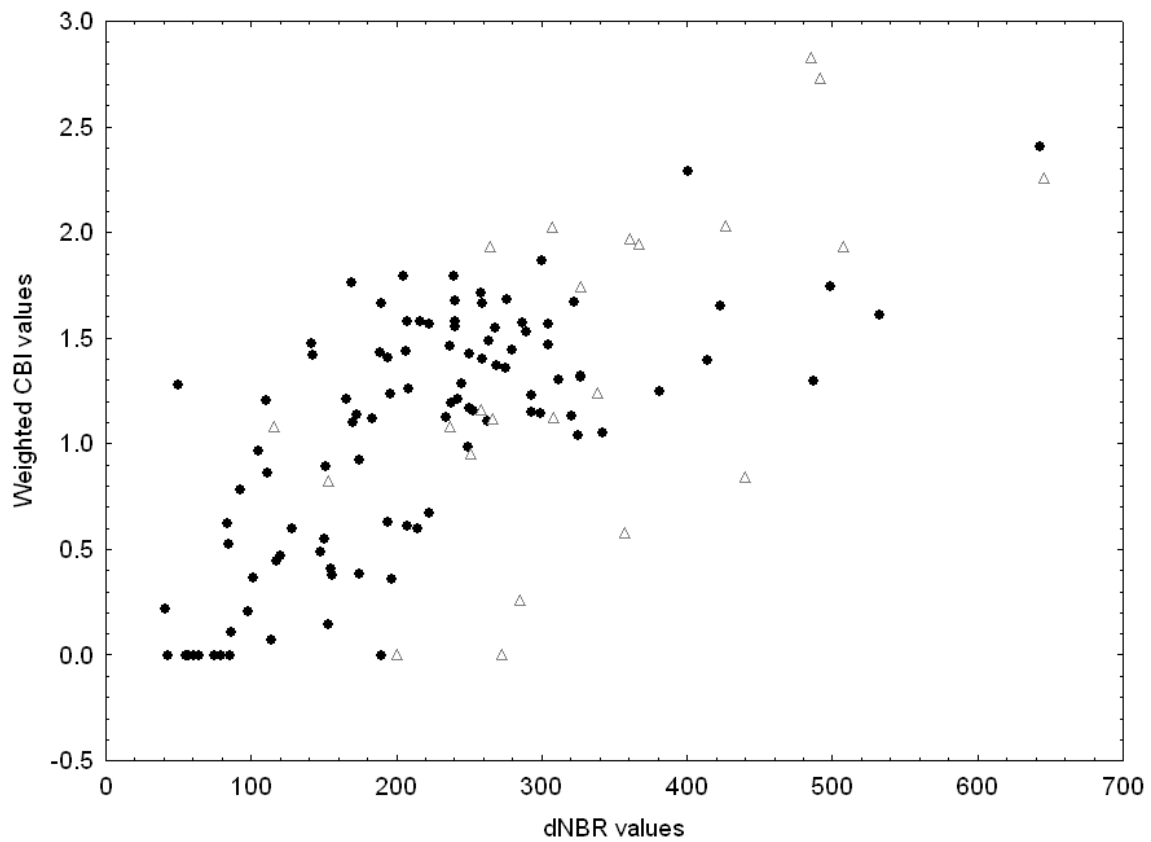


Figure 3.8. Scatter plot of x-axis dNBR and y-axis weighted CBI values for the Mitchell Ridge (black circles) and the Hoodoo Creek (hollow triangles) fires.

3.4.3 Discussion on overall model and TCI improvement

Building models that are applicable and transferable over large expanses of land is clearly a desirable goal for land management agencies such as Parks Canada. As part of objective one, we tested various dNBR derived models and confirmed that eight of the ten fires cross validated well, and there wasn't large improvement in accuracy when stratifying the fires by land cover or ecozone. Therefore, our overall dNBR derived model for western Canada appears broadly transferable across the study area (Figure 3.9 & Table 3.8).

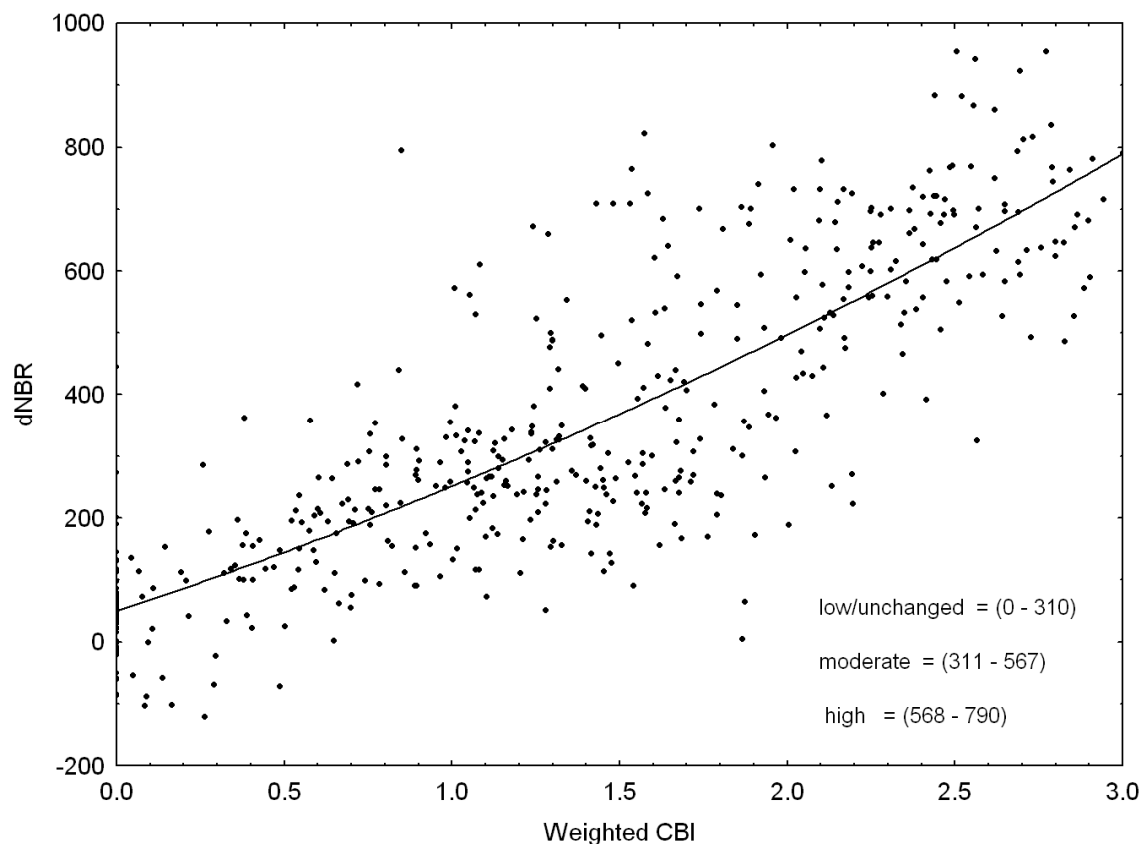


Figure 3.9. Polynomial model fitted to the overall dNBR dataset, with the x-axis representing the weighted CBI values and the y-axis the dNBR values so that thresholds could be determined. CBI thresholds were taken from Miller et al. (2009)'s study.

Table 3.8. Results of overall dNBR model including the model equation, R², P value, and root mean square error (RSE).

<i>Model</i>	<i>R²</i>	<i>P</i>	<i>RSE</i>
dNBR = 49.8323+178.9546*CBI+22.4924*CBI^2	0.69	<.0001	136.91

Our research results for objective two support the use of pre- and post-fire TCI data in order to improve the modelling accuracy of dNBR. Pre-fire TCI wetness appears to be the most consistently improving variable in multiple regression with dNBR. Post-fire TCI variables also indicate an additive but lesser capacity to the model accuracies.

Importantly, the correlations of the Hoodoo Creek and Mitchell Ridge fires (the least well predicted using cross validation) had increased accuracy after pre- or post-fire TCI wetness is used. We acknowledge, however, due to the complex nature of wildland fire, broad geographic based models that use dNBR may require additional data to improve their accuracy. In particular, fires of the moderate/mixed severity class are poorly represented by this type of monitoring, and may require further investigation. To this end, many researchers have attempted to analyze, incorporate, or study the effects of the pre-fire environment and its relationship to burn severity (Hall et al., 2008; Miller et al., 2009; Wulder, 2009).

3.5 Conclusion

Although new imagery is becoming available, the cost-effective and heavily researched Landsat TM/ETM+ archive will have a significant ongoing role in burn severity mapping. The modelling accuracies of both dNBR and the TCI hold promising results for Parks Canada and other agencies that manage large areas of fire affected landscapes. It appears that the dNBR remains to be a robust predictor of burn severity across multiple

western Canadian landscapes. However, the evidence provided herein indicates that this model does not predict all fire events with equal accuracy. We recommend that future fires that resemble the Hoodoo Creek and Mitchell Ridge fires, i.e. those ignited in springtime and exhibit moderate severity effects, may need further investigation. It will be up to the discretion of fire managers and scientists alike to determine the acceptability of error for their various project needs.

3.6 References

- Agee, J.K. (1993). 'Fire Ecology of Pacific Northwest Forests'. (Island Press: Covelo, CA).
- Avery, T.E., & Berlin, G.L. (1992). 'Fundamentals of remote sensing and airphoto interpretation'. (Prentice Hall: Upper Saddle River, N.J.)
- Balshi, M.S., McGuire, A.D., Duffy, P., Flannigan, M.D., Walsh, J., & Melillo, J. (2009). Assessing the response of area burned to changing climate in western boreal North America using Multivariate Adaptive Regression Splines (MARS) approach. *Global Change Biology*, 15, 578-600.
- Box GEP, & Jenkins, G.M. (1970). 'Time series analysis: forecasting and control'. (Holden-Day: London, UK).
- Burton, P.J., Parisien, M., Hicke, J.A., Hall, R.J., & Freeburn, J.T. (2008). Large fires as agents of ecological diversity in the North American boreal forest. *International Journal of Wildland Fire*, 17, 754-767.
- Chander, G., & Markham, B. (2003). Revised Landsat-5 TM Radiometric Calibration Procedures and Postcalibration Dynamic Ranges. *IEEE Transactions on Geoscience and Remote Sensing*, 41, 11.
- Chavez, PS Jr. (1989). Radiometric calibration of Landsat Thematic Mapper multispectral images. *Photogrammetric Engineering and Remote Sensing*, 9, 1285-1294.
- Chuvieco, E., & Congleton, R.G. (1988). Mapping and inventory of forest fires from digital processing of TM data. *Geocarto International*, 4, 41-53.
- Cocke, E.A., Fulé, P.Z., & Crouse, J.E. (2005). Comparison of burn severity assessments using the Differenced Normalized Burn Ratio and ground data. *International Journal of Wildland Fire*, 14, 189-198.
- Cohen, W.B., Spies, T.A., & Fiorella, M. (1995). Estimating the age and structure of forests in a multi-ownership landscape of Western Oregon, U.S.A. *International Journal of Remote Sensing*, 16, 721-746.
- Crist, E.P., & Cicone, R.C. (1984). A Physically-Based Transformation of Thematic Mapper Data—The TM Tasseled Cap. *IEEE Transactions on Geoscience and Remote Sensing*, GE-22, 3.
- DeBano, L.F., Neary, D.G., & Ffolliott, P.F. (1998). 'Fire's Effects on Ecosystems'. (John Wiley and Sons: New York, NY)

- DeSantis, A., & Chuvieco, E. (2007). Burn severity estimation from remotely sensed data: Performance of simulation versus empirical models. *Remote Sensing of Environment*, 108, 422-435.
- Elvidge, C.D. (1990). Visible and near infrared reflectance characteristics of dry plant materials. *International Journal of Remote Sensing*, 11 (10), 1775-1795.
- Epting, J., & Verbyla, D. (2005). Landscape-level interactions of prefire vegetation, burn severity, and postfire vegetation over a 16-year period in interior Alaska. *Canadian Journal of Forest Research*, 35, 1367-1377.
- Fischer, W.C., & Clayton, B.D. (1983). 'Fire ecology of Montana forest habitat types east of the continental divide'. USDA Forest Service Intermountain Forest and Range Experiment Station, General Technical Report INT-GTR-141. (Ogden, UT)
- Flannigan, M.D., Stocks, B.J., Turetsky, M., & Wotton, M. (2009). Impacts of climate change on fire activity and fire management in the circumboreal forest. *Global Change Biology*, 15, 549-560.
- French, N.H.F., Kasischke, E.S., Hall, R.J., Murphy, K.A., Verbyla, D.L., Hoy, E.E., & Allen, J.L. (2008). Using Landsat data to assess fire and burn severity in North American boreal forest region: an overview and summary of results. *International Journal of Wildland Fire*, 17, 443-462.
- Gillet, N.P., & Weaver, A.J. (2004). Detecting the effect of climate change on Canadian forest fires. *Geophysical Research Letters* 31, L18211.
- Hall, R.J., Freeburn, J.T., de Groot, W.J., Pritchard, J.M., Lynham, T.J., & Landry, R. (2008). Remote sensing of burn severity: Experience from western Canada boreal fires. *International Journal of Wildland Fire*, 17, 476-489.
- Halofsky, J.E., & Hibbs, D.E. (2009). Relationships among indices of fire severity in riparian zones. *International Journal of Wildland Fire*, 18, 584-593.
- Hudak, A.T., Morgan, P., Bobbitt, M.J., Smith, A.M.S., Lewis, S.A., Lentile, L.B., Robichaud, P.R., Clark, J.T., & McKinley, R.A. (2007). The relationship of multispectral satellite imagery to immediate fire effects. *Fire Ecology Special Issue*, 3, 1.
- Jin, S., & Sader, S.A. (2005). Comparison of time series tasseled cap wetness and the normalized difference moisture index in detecting forest disturbances. *Remote Sensing of Environment*, 94, 364-372.
- Johnson, E.A. (1992). 'Fire and Vegetation Dynamics: Studies from the North American Boreal Forest'. (Cambridge University Press: New York)

- Kaufman, Y.J., & Sendra, C. (1988). Algorithm for automatic atmospheric corrections to visible and near-IR satellite imagery. *International Journal of Remote Sensing*, 9, 1357-1381.
- Key, C.H., & Benson, N.C. (2006). 'Landscape Assessment: ground measure of severity, the Composite burn index, and remote sensing of severity, the Normalized Burn Index'. In 'FIREMON: Fire Effects Monitoring and Inventory System'. (Eds DC Lutes, RE Keane, JF Caratti, CH Key, NC Benson, S Sutherland, LJ Gangi) USDA Forest Service, Rocky Mountain Research Station, General Technical Report RMRS-GTR-164-CD: LA1-51 (Ogden, UT)
- Klenner, W., Walton, R., Arsenault, A., & Kremsater, L. (2008). Dry forests in the Southern Interior of British Columbia: Historic disturbances and implications for restoration and management. *Forest Ecology and Management*, 256, 1711-1722.
- Kushla, J.D., & Ripple, W.J. (1998). Assessing wildfire effects with Landsat thematic mapper data. *International Journal of Remote Sensing*, 19, 2493-2507.
- Kuzera, K., Rogan, J., & Eastman, J.R. (2005). 'Monitoring vegetation regeneration and deforestation using change vector analysis: Mt. St. Helens area'. (ASPRS Annual Conference, Baltimore, Maryland, USA)
- Larsen, C.P.S. (1997). Spatial and temporal variations in boreal forest fire frequency in northern Alberta. *Journal of Biogeography*, 24, 663-673.
- Lentile, L.B., Holden, Z.A., Smith, A.M.S., Falkowski, M.J., Hudak, A.T., Morgan, P., Lewis, S.A., Gessler, P.E., & Benson, N.C. (2006). Remote sensing techniques to assess active fire characteristics and post-fire effects. *International Journal of Wildland Fire*, 15, 319-345.
- Lopez Garcia, M.J., & Caselles, V. (1991). Mapping burns and natural reforestation using Thematic Mapper data. *Geocarto Int.*, 1, 31-37.
- Lyon, L.J., & Stickney, P.F. (1976). 'Early vegetal succession following large northern Rocky Mountain wildfires'. Proceedings of the Tall Timbers Fire Ecology Conference, 14, 355-375.
- Meidinger, D.V., & Pojar, J. (1991). Ecosystems of British Columbia. Special Report Series 06, BC Ministry of Forests Research Branch. (Victoria, BC)
- Miller, J.D., & Thode, A.E. (2007). Quantifying burn severity in a heterogeneous landscape a relative version of the delta Normalized Burn Ratio (dNBR). *Remote Sensing of Environment*, 109, 66-80.
- Miller, J.D., Knapp, E.E., Key, C.H., Skinner, C.N., Isbell, C.J., Creasy, R.M., & Sherlock, J.W. (2009). Calibration and validation of the relative differenced

- Normalized Burn Ratio (RdNBR) to three measures of fire severity in the Sierra Nevada and Klamath Mountains, California, USA. *Remote Sensing of the Environment*, 113, 645-656.
- Morgan, P., & Neuenschwander, L.F. (1988). Shrub response to high and low severity burns. *Western Journal of Applied Forestry*, 3(1), 5-9.
- NASA. (1998). Landsat 7 Science Data Users Handbook. Landsat Project Science Office, NASA's Goddard Space Flight Center. (Greenbelt, Maryland)
<http://landsathandbook.gsfc.nasa.gov/handbook.html>
- Podur, J., Martell, D.L., & Knight, K. (2002). Statistical quality control analysis of forest fire activity in Canada. *Canadian Journal of Forest Research*, 32, 195-205.
- Qi, J., Moran, M.S., Huete, A.R., Jackson, R.D., & Chehbouni, A. (1991). 'View-atmosphere soil effect on vegetation indices derived from SPOT images'. In Proceedings of the 5th International Symposium on Physical Measurements and Signatures in Remote Sensing pp. 785-790. (Courchevel, France)
- Rogan, J., & Yool, S.R. (2001). Mapping fire-induced vegetation depletion in the Peloncillo Mountains, Arizona and New Mexico. *International Journal of Remote Sensing*, 22, 3101-3121.
- Ryan, K.C. (2002). Dynamic interactions between forest structure and fire behaviour in boreal ecosystems. *Silva Fennica*, 36, 13-39.
- Ryan, K.C., & Noste, N.V. (1985). 'Evaluating prescribed fires'. In Proceedings-symposium and workshop on wilderness fire, pp 230-238. (JE Lotan, BM Kilgore, WC Fischer, RW Mutch technical coordinators). USDA Forest Service General Technical Report INT-182.
- Snee, R.D. (1977). Validation of Regression Models: Methods and Examples. *Technometrics*, 19, 415-428.
- Stocks, B.J., Mason, J.A., Todd, J.B., Bosch, E.M., Wotton, B.M., & Amiro, B.D. et al. (2003). Large forest fires in Canada 1959-1997. *Journal of Geophysical Research*, 107, 1-12.
- Tande, G.F. (1979). Fire history and vegetation pattern of coniferous forests in Jasper national park, Alberta. *Canadian Journal of Botany*, 57, 1912-1930.
- Turner, M.G., Romme, W.H., & Tinker, D.B. (2003). Surprises and Lessons from the 1988 Yellowstone Fires. *Frontiers in Ecology and the Environment*, 1, 351-358.
- USGS (United States Geologic Survey) GLOVIS website: <http://glovis.usgs.gov/>
 Accessed between October, 2008 and October, 2009

- Van Wagner, C.E., Finney, M.A., & Heathcott, M. (2006). Historical Fire Cycles in the Canadian Rocky Mountain Parks. *Forest Science*, 52, 704-717.
- Van Wagtendonk, J.W., Root, R.R., & Key, C.H. (2004). Comparison of AVIRIS and Landsat ETM+ detection capabilities for burn severity. *Remote Sensing of Environment*, 92, 397-408.
- Weir, J.M.H., Johnson, E.A., & Miyanishi, K. (2000). Fire frequency and the spatial age mosaic of the mixed-wood boreal forest in western Canada. *Ecological Applications*, 10, 1162-1177.
- Wulder, M.A., Kakun, R.S., Kurz, W.A., & White, J.C. (2004). Estimating time since forest harvest using segmented Landsat ETM+ imagery. *Remote Sensing of Environment*, 93, 179-187.
- Wulder, M.A., White, J.C., Magnussen, S., & McDonald, S. (2007). Validation of a large area land cover product using purpose-acquired airborne video. *Remote Sensing of Environment*, 106, 480-491.
- Wulder, M.A., White, J.C., Cranny, M., Hall, R.J., Luther, J.E., Beaudoin, A., Goodenough, D.G., & Dechka, J.A. (2008a). Monitoring Canada's forests. Part 1: Completion of the EOSD land cover project. *Canadian Journal of Remote Sensing*, 34, 549-548.
- Wulder, M.A., White, J.C., Han, T., Coops, N.C., Cardille, J.A., Holland, T., & Grills, D. (2008b). Monitoring Canada's forests. Part 2: National forest fragmentation and pattern. *Canadian Journal of Remote Sensing* 34, 563-584.
- Wulder, M.A., White, J.C., Alvarez, F., Han, T., Rogan, J., & Hawkes, B. (2009). Characterizing boreal forest wildfire with multi-temporal Landsat and LIDAR data. *Remote Sensing of Environment*, 113, 1540-1555.
- Zhu, Z., Key, C.H., Ohlen, D., & Benson, N.C. (2006). Evaluate Sensitivities of Burn-Severity Mapping Algorithms for Different Ecosystems and Fire Histories in the United States. Available at http://jfsp.nifc.gov/projects/01-1-4-12/01-1-4-12_Final_Report.pdf [Accessed October 2008]

4 CONCLUSION

The overall objective of the research was to answer two key questions, the first related to a comparison of the accuracy of dNBR versus RdNBR, and the second an assessment of the transferability of a dNBR derived model. In addition to these two key questions, insights were gained about the ecological patterns of burn severity, the unique nature of each fire event, the strengths and weaknesses of burn severity modelling, while at the same time calibrating and validating the derived dNBR and RdNBR models. These models provide information about the efficacy of a future Parks Canada burn severity management project that is relevant to both fire scientists and managers alike working on a wide range of projects. For example, fire managers may be able to assess the success of their prescribed burn objectives, more easily compare the effects of fire on vegetation dynamics and wildlife populations, and detect burn severity trends due to changes in climate. Information derived from these burn severity approaches may also be useful to help measure broad scale impacts of fire and for predictive modelling of future fires.

4.1 Key findings

The results from Chapter 2 indicate that both dNBR and RdNBR indices were well suited to estimate burn severity across the study areas. It was determined that dNBR and RdNBR measured burned severity similarly, however, it was found that the dNBR index was a slightly better estimator (70.2% versus 65.2% overall classification accuracy). This last finding was also determined by both Wulder et al. (2009) and Hudak et al. (2008) who reported that the use of RdNBR did not improve estimates of post-fire effects. It was hypothesized that the fires ranked with high pre-fire vegetation heterogeneity and

sparseness would be better estimated by RdNBR than dNBR, however, this was not the case. The fire rankings by pre-fire vegetation appeared to have no relation to post-fire effects, another similarity to Wulder et al. (2009). It was postulated that this lack of relationship was due to the relatively more homogenous and higher canopy closures across these sites as compared to the California conifer study region of Miller and Thode (2007). As has been found by other researchers (Miller et al., 2009), this study's overall model had the lowest class accuracy for the moderate severity class when compared to the other classes. When the data were stratified by region, the western boreal model for both indices indicated that the high severity class had the lowest classification accuracies, also confirmed in other studies (Murphy et al., 2008). The implementation of the Hall et al. (2008) non-linear model resulted in similar accuracies for the western boreal classification (59.7%) as compared to the dNBR (62.4%) and RdNBR (60.3%). This model had higher conditional kappa values for the high severity class (user's $k_1 = 0.91$, producer's $k_1 = 0.33$) as compared to the dNBR (user's $k_1 = 0.38$, producer's $k_1 = 0.26$) and RdNBR (user's $k_1 = 0.56$, producer's $k_1 = 0.29$). Based on the results of Hall et al.'s (2008) non-linear model, it can be inferred that the development of regional models for western Canada is a feasible goal.

Results for Chapter 3 showed differing responses in tasselled cap index (TCI) soil brightness after fire for the two regions. Fires in the Rocky Mountain region indicated increases in soil brightness post-fire while the western boreal showed a reduction in brightness for a majority of the fires. The time of year of the burn was also found to have a strong effect on TCI greenness, with early season fires showing either increases or a

reduction in greenness reflectance. After comparing changes in spectral variability using pre- to post-fire TCI, statistically significant results were found in 60% of the cases which implies that fire increased the heterogeneity across the CBI plots. The most pertinent finding within this chapter was that an overall dNBR model is transferable across eight of the ten fires. Two of the study fires that did not cross validate well, the Hoodoo Creek and Mitchell Ridge fires, had decoupled burn severity in their overstory and understory. This decoupling, paired with the associated confusion of the moderate severity class, were some of the reasons behind this weak result. As a way to test the improvement of additional pre- and post-fire data, the three TCI were included in multiple regression with the overall dNBR model. The results indicated that of the three indices, either pre- or post-fire TCI wetness resulted in the highest improvement, especially evident in the large improvements for the Hoodoo Creek and Mitchell Ridge fires. As was concluded from Chapter 2, dNBR appears to be transferable across western Canada but may require the addition of multiple datasets to improve its predictive accuracies.

4.2 Future work and recommendations

Landsat derived indices of burn severity have become critical operational tools for assessment. Landsat provides imagery that is publicly accessible, free, and offers data that is moderate in spatial resolution which is well suited for landscape studies. Currently, there are two Landsat satellites in operation. Landsat 5 has been in operation since 1984 and is well passed its lifespan while Landsat 7's scan line error has made most of its available imagery unsuitable for burn severity studies. The Landsat Data Continuity Mission (LDCM), planned for launch in December 2012, will produce data consistent

with the Landsat 5 and 7 specifications. This means that a gap in image availability for up to a year may be likely. It will be up to agencies such as Parks Canada to decide their plan of action should this occur.

The conclusions of this research raise two additional issues that should be addressed by operational users before implementation. First, the overall dNBR model in Chapter 3 shows high transferability using cross validation, with an overall range of R^2 values between 0.40-0.89. These results are significant, however; it demonstrates to users the need to be aware of the variability in accuracies among fires. In situations where a fire event appears to exhibit a majority of moderate severity characteristics, whether through CBI sampling or the distribution of remote sensing indices, one should expect lower classification accuracies. Secondly, it is important that CBI thresholds between the classes be set in a way that reflects the specific nature of local burn severity. Generalized class breaks used in chapter 2 and taken Miller et al. (2009), were used as a means of comparing the dNBR and RdNBR indices. However, it was recommended by Lentile et al. (2006) that the users of burn severity models develop their own locally meaningful dNBR ranges based on field measured CBI. It is therefore recommended that CBI thresholds or class breaks be developed at a finer geographic scale than those of Miller et al. (2009). A summarization of these two recommendations follows:

- 1) An assessment of the project accuracy requirements should be considered before using these or other derived burn severity models.

2) CBI thresholds should be set that exhibit locally meaningful burn severity characteristics.

The modelling accuracies determined from this research have the potential to be improved with the development of future sensor technologies. As Lentile et al. (2006) points out, fire research needs a better understanding of the role of pre-fire vegetation and topography, climate and active fire weather, vegetation structure and composition, and land use on the prediction of burn severity. The incorporation of additional datasets such as pre-fire condition, vegetation type, topography, and others should increase the accuracies of burn severity prediction while simultaneously linking these remote sensing measurements to the ecological processes of fire.

4.3 References

- Hall, R.J., Freeburn, J.T., Groot, W.J.dG., Pritchard, J.M., Lynham, T.J., & Landry, R. (2008). Remote sensing of burn severity: experience from western Canada boreal fires. *International Journal of Wildland Fire*, 17, 476-489.
- Lentile, L.B., Holden, Z.A., Smith, A.M.S., Falkowski, M.J., Hudak, A.T., Morgan, P., Lewis, S.A., Gessler, P.E., Benson, N.C. (2006). Remote sensing techniques to assess active fire characteristics and post-fire effects. *International Journal of Wildland Fire*, 15, 319-345.
- Miller, J.D., & Thode, A.E. (2007). Quantifying burn severity in a heterogeneous landscape a relative version of the delta Normalized Burn Ration (dNBR). *Remote Sensing of Environment*, 109, 66-80.
- Miller, J.D., Knapp, E.E., Key, C.H., Skinner, C.N., Isbell, C.J., Creasy, R.M., & Sherlock, J.W. (2009). Calibration and validation of the relative differenced Normalized Burn Ratio (RdNBR) to three measures of fire severity in the Sierra Nevada and Klamath Mountains, California, USA. *Remote Sensing of the Environment*, 113, 645-656.
- Wulder, M.A., White, J.C., Alvarez, F., Han, T., Rogan, J., & Hawkes, B. (2009). Characterizing boreal forest wildfire with multi-temporal Landsat and LIDAR data. *Remote Sensing of Environment*, 113, 1540-1555.